PHYSICOCHEMICAL STUDIES OF ROOM TEMPERATURE MOLTEN SALT SYSTEMS CONTAINING HYDRATED INORGANIC SALTS AND ORGANIC COMPOUNDS

ABSTRACT

SONTOSH DEV

DEPARTMENT OF CHEMISTRY
SCHOOL OF PHYSICAL SCIENCES
N E H U

A THESIS
SUBMITTED
IN FULFILMENT OF THE REQUIREMENT
FOR
THE DEGREE OF
DOCTOR OF PHILOSOPHY

To

THE NORTH-EASTERN HILL UNIVERSITY
SHILLONG-793 022, INDIA
APRIL, 1998

ABSTRACT

The thesis entitled, ' Physicochemical Studies of Room Temperature Molten Salt Systems Containing Hydrated Inorganic Salts and Organic Compounds', consists of seven chapters.

In Chapter 1 a general introduction to the subject of study has been given along with the scope and scheme of the work. In Chapter 2 a general description of the experimental techniques used has been given.

In Chapter 3 visible absorption spectra of molten systems containing calcium nitrate tetrahydrate melt (CNTH) and various organic indicators were recorded at 25°C. The indicators used are methyl red, p-nitrophenol, bromophenol blue, methyl orange, and p-nitroaniline. It has been demonstrated that spectroscopic technique using organic indicators can be employed for the determination of acidity function of hydrate melts even if the indicators undergo reaction in the acidic melt and the melt has no UV transparency. For obtaining meaningful value of acidity function, it has been shown that the indicator to be used must have low pK_a value preferably $\leq \sim 1$. Indicators having high pK_a value in the range ~ 4 are also found to be useful for the determination of acidity function if such indicators have well-separated absorption

bands for their basic and acidic forms in neat hydrate melt. The average value of the acidity function of CNTH is estimated to be ca. 2.2 ± 0.4.

In Chapter 4 the kinetics of the reaction of methyl red in acidic CNTH melt has been studied by recording the time-dependent absorption spectra. The reaction follows a pseudo-first-order kinetics up to a particular time duration. The time limit of applicability of pseudo-first-order rate expression is found to be dependent on the amount of acid (acetic acid) present in CNTH. The value of the rate constant is also found to be dependent on the acid concentration. The reaction which methyl red undergoes in acidic CNTH is shown to be nitration and it has been proposed that nitration takes place at the azo nitrogen of methyl red.

In Chapter 5 density and electrical conductance measurements of a room temperature molten salt system containing CNTH and acetamide were carried out with a view to understanding the volumetric and transport behaviour of this melt. The molar volume of this molten mixture exhibits additivity and thus provides a method to estimate the molar volume or density of acetamide at ambient temperature. This type of molten mixture behaves as an ideal mixture of hydrate melt (CNTH) and hypothetical supercooled liquid solute (acetamide). The temperature dependence of specific conductance of the molten mixture is found to be non-Arrhenius and is explained in the light of the Vogel-Tammann-Fulcher (VTF) equation. Using the VTF equation ideal glass transition temperatures of the molten mixture were estimated. The decrease in specific conductance caused by

the addition of acetamide to CNTH seems to be due to the ion-acetamide interactions.

In Chapter 6 micellization behaviour of sodium dodecyl sulfate (SDS) in CNTH + acetamide molten mixture has been investigated using conductance method. In order to ascertain occurrence of micellization of SDS in CNTH + acetamide molten mixture, electrical conductances of SDS, cetylpyridinium chloride (CPC), and $NaNO_3$ in pure acetamide melt were also measured. In pure acetamide melt both SDS and CPC are found to form micelles. The electrical conductance behaviour of SDS and CPC in pure acetamide melt at higher concentration is shown to be similar to that of a normal electrolyte like $NaNO_3$. SDS and CPC even exhibit conductance maxima in acetamide melt. SDS is also shown to form micelles in CNTH + acetamide melt. The critical micelle concentrations were estimated. The size of the micelles formed in molten media seems to be smaller than those formed in aqueous medium. In CNTH +acetamide melt the nature of the conductance behaviour of SDS is controlled either by acetamide or by CNTH depending upon their relative amounts in the mixture. It has been highlighted that, while employing conductance method to study the micellization behaviour, making distinction between interionic interactions and interactions reponsible for micelle formation is necessary in order to avoid possibility of estimating erroneous values for the critical micelle concentration.

In Chapter 7 electrical conductances of CNTH +Methanol, CNTH + Ethanol, and CNTH + Propanol binary mixtures were measured in the entire concentration range and in the temperature range from 45 to - 75°C. The non-Arrhenius type of temperature dependence of specific conductance of these three binary mixtures is explainable satisfactorily by the VTF, Adam-Gibbs (AG), and power-law (PL) equations. However, conceptually the VTF and AG equations do not seem to be applicable to these binary mixtures since the ideal glass transition temperatures obtained for the three alcohols from these equations are found to be higher than their respective calorimetric glass transition temperatures. The critical tempe-rature obtained from the PL equation does not seem to correspond to the ideal glass transition temperature and may probably refers, on the other hand, to the temperature at which α- and β- relaxations merge. The shape of the specific conductance versus concentration isotherms of the three binary systems differs from each other particularly above 20°C. The concentration at which conductance maximum occurs shifts towards alcohol side as the temperature is decreased. The concentration dependence of specific conductance seems to have a correlation with the dielectric constant and viscosity of the alcohol.

PHYSICOCHEMICAL STUDIES OF ROOM TEMPERATURE MOLTEN SALT SYSTEMS CONTAINING HYDRATED INORGANIC SALTS AND ORGANIC COMPOUNDS

SONTOSH DEV

DEPARTMENT OF CHEMISTRY
SCHOOL OF PHYSICAL SCIENCES
N E H U

A THESIS
SUBMITTED
IN FULFILMENT OF THE REQUIREMENT
FOR
THE DEGREE OF
DOCTOR OF PHILOSOPHY

To

THE NORTH-EASTERN HILL UNIVERSITY
SHILLONG-793 022, INDIA
APRIL, 1998

OM SRI GURUBAH NAMAHA

Dedicated to
SRI GURUJEE
SRI SRI 108 SWAMI DHANANJOY DAS
KATHIA BABAJEE MAHARAJ

पूर्वोत्तर पर्वतीय विश्वविद्यालय
बिजनी परिसर, शिलांग-७९३००३ (मेघालय)

Phone :
Grams: NEHU

North-Eastern Hill University
Bijni Complex, Shillong-793 003 (Meghalaya)

Dr.K. Ismail, Reader

Department of Chemistry

CERTIFICATE

I certify that the thesis entitled " **Physicochemical Studies of Room Temperature Molten Salt Systems Containing Hydrated Inorganic Salts and Organic Compounds**" submitted by Mr. Sontosh Dev for the Degree of Doctor of Philosophy of the North-Eastern Hill University, embodies the record of original investigation carried out by him under my supervision. He has been duly registered and the thesis presented is worthy of being considered for the Ph. D Degree. This work has not been submitted for any degree of any other University.

Place : Shillong

Date : 17/4/98

(Dr. K. ISMAIL)

Supervisor

ACKNOWLEDGEMENTS

With immense pleasure and great satisfaction I express my deep sense of gratitude to my Supervisor, ***Dr. KOCHI ISMAIL*** for his valuable guidance, constant encouragement and advice throughout my Ph.D programme. His liberal and pragmatic approach to any problems has only helped me complete this work.

I am thankful to the former and the present Heads of the Department of Chemistry for providing me the necessary research facilities.

I sincerely express my gratefulness to Prof. J. Subramaniam for his valuable suggestions. I am also indebted to the faculty members of the Department of Chemistry for their help, encouragement and advices. My special thanks are due to Prof. M. K. Mahanti, Prof. S.N. Bhatt , Prof. H. Junjappa, Prof. T.S.B. Narasaraju, Prof. H. Ila, Prof. M.K. Choudhuri, Dr. S. Aravamudhan , Dr. B. Myrboh.

I also wish to acknowledge the cooperation and help rendered by my senior colleagues, Dr. S. Mahiuddin, Dr. (Mrs) S. Islam, Dr. R.L. Gupta.

My special thanks goes to Babul, Abhijit whose total involvement made this work complete.

I find myself very poor in using the appropriate word for having a person like Gunaseelan in our laboratory .

My thanks are due to all the previous and present project students of our Laboratory.

My special thanks go to Prasanta and Sejuti for their immense help, cooperation.

I wish to appreciate the very presence of Mondal even in his difficult days.

Thanks are due to Deepak for his help and suggestions.

My special thanks go to Ullen and Debora for their great help and cooperation. I further acknowledge the immense help and cooperation rendered by my dear colleagues Raja, Bipul, Ankshuman, Arun, Jayashree , 'appa'Suresh, Sriram, Suchandra, Amrita, Sanchita, Paramita, Reddy, Nadeem, Akhilesh, Tomba, Pradip, Subhasish, Ashish, Wancy, Subrato, Robin, Ashim, and all others whose name my memory is failing me to recollect.

I express my sincere gratefulness to the present and former Directors, Sr. Geologist and Chief Chemists of the Directorate of Mineral Resources (DMR), Meghalaya for their cooperation and help.

I also express gratefulness to Partha and Subhojit of computer centre for their immense help and cooperation throughout my Ph.D programme. I am also grateful to Dr. S.N. Rai, Director of Computer Centre for allowing me to do computational work.

I express my special thanks to Dear Biswajit whose constant presence and company made me feel the life in its proper perspective.

The list of acknowledgements would be incomplete were I not to mention the help given to me over the years by my parents, my brother and in more recent times by my sister-in-law. This Ph.D work owes a great deal to them.

Finally, I like to express my gratitude to everybody who are directly or indirectly related to the completion of this thesis.

Shillong, Dated
17th April '98

SONTOSH DEV

CONTENTS

		PAGE NO.
ABSTRACT		i
CHAPTER 1	GENERAL INTRODUCTION	1
CHAPTER 2	EXPERIMENTAL TECHNIQUES AND DATA ANALYSIS	32
CHAPTER 3	ELECTRONIC SPECTRA OF MELTS CONTAINING CALCIUM NITRATE TETRAHYDRATE AND ORGANIC INDICATORS	40
CHAPTER 4	A SPECTRAL STUDY OF THE BEHAVIOUR OF METHYL RED IN ACIDIC CALCIUM NITRATE TETRA HYDRATE MELT	73
CHAPTER 5	VOLUMETRIC AND ELECTRICAL CONDUCTANCE BEHAVIOUR OF CALCIUM NITRATE TETRAHYDRATE + ACETAMIDE MELT : A ROOM TEMPERATURE MOLTEN SALT SYSTEM	94
CHAPTER 6	A STUDY ON THE MICELLIZATION OF SURFACTANTS IN CALCIUM NITRATE TETRAHYDRATE + ACETAMIDE AND PURE ACETAMIDE MELTS USING CONDUCTANCE METHOD	118
CHAPTER 7	ELECTRICAL CONDUCTANCE BEHAVIOUR OF CALCIUM NITRATE TETRAHYDRATE + METHANOL / ETHANOL / PROPANOL BINARY SYSTEMS FROM PURE MELT TO INFINITE DILUTION IN THE TEMPERATURE RANGE FROM 45 TO - 75°C	148

ABSTRACT

The thesis entitled, ' Physicochemical Studies of Room Temperature Molten Salt Systems Containing Hydrated Inorganic Salts and Organic Compounds', consists of seven chapters.

In Chapter 1 a general introduction to the subject of study has been given along with the scope and scheme of the work. In Chapter 2 a general description of the experimental techniques used has been given.

In Chapter 3 visible absorption spectra of molten systems containing calcium nitrate tetrahydrate melt (CNTH) and various organic indicators were recorded at 25°C. The indicators used are methyl red, p-nitrophenol, bromophenol blue, methyl orange, and p-nitroaniline. It has been demonstrated that spectroscopic technique using organic indicators can be employed for the determination of acidity function of hydrate melts even if the indicators undergo reaction in the acidic melt and the melt has no UV transparency. For obtaining meaningful value of acidity function, it has been shown that the indicator to be used must have low pK_a value preferably $\leq \sim 1$. Indicators having high pK_a value in the range ~ 4 are also found to be useful for the determination of acidity function if such indicators have well-separated absorption

bands for their basic and acidic forms in neat hydrate melt. The average value of the acidity function of CNTH is estimated to be ca. 2.2 ± 0.4.

In Chapter 4 the kinetics of the reaction of methyl red in acidic CNTH melt has been studied by recording the time-dependent absorption spectra. The reaction follows a pseudo-first-order kinetics up to a particular time duration. The time limit of applicability of pseudo-first-order rate expression is found to be dependent on the amount of acid (acetic acid) present in CNTH. The value of the rate constant is also found to be dependent on the acid concentration. The reaction which methyl red undergoes in acidic CNTH is shown to be nitration and it has been proposed that nitration takes place at the azo nitrogen of methyl red.

In Chapter 5 density and electrical conductance measurements of a room temperature molten salt system containing CNTH and acetamide were carried out with a view to understanding the volumetric and transport behaviour of this melt. The molar volume of this molten mixture exhibits additivity and thus provides a method to estimate the molar volume or density of acetamide at ambient temperature. This type of molten mixture behaves as an ideal mixture of hydrate melt (CNTH) and hypothetical supercooled liquid solute (acetamide). The temperature dependence of specific conductance of the molten mixture is found to be non-Arrhenius and is explained in the light of the Vogel-Tammann-Fulcher (VTF) equation. Using the VTF equation ideal glass transition temperatures of the molten mixture were estimated. The decrease in specific conductance caused by

the addition of acetamide to CNTH seems to be due to the ion-acetamide interactions.

In Chapter 6 micellization behaviour of sodium dodecyl sulfate (SDS) in CNTH + acetamide molten mixture has been investigated using conductance method. In order to ascertain occurrence of micellization of SDS in CNTH + acetamide molten mixture, electrical conductances of SDS, cetylpyridinium chloride (CPC), and $NaNO_3$ in pure acetamide melt were also measured. In pure acetamide melt both SDS and CPC are found to form micelles. The electrical conductance behaviour of SDS and CPC in pure acetamide melt at higher concentration is shown to be similar to that of a normal electrolyte like $NaNO_3$. SDS and CPC even exhibit conductance maxima in acetamide melt. SDS is also shown to form micelles in CNTH + acetamide melt. The critical micelle concentrations were estimated. The size of the micelles formed in molten media seems to be smaller than those formed in aqueous medium. In CNTH +acetamide melt the nature of the conductance behaviour of SDS is controlled either by acetamide or by CNTH depending upon their relative amounts in the mixture. It has been highlighted that, while employing conductance method to study the micellization behaviour, making distinction between interionic interactions and interactions reponsible for micelle formation is necessary in order to avoid possibility of estimating erroneous values for the critical micelle concentration.

In Chapter 7 electrical conductances of CNTH +Methanol, CNTH + Ethanol, and CNTH + Propanol binary mixtures were measured in the entire concentration range and in the temperature range from 45 to - 75°C. The non-Arrhenius type of temperature dependence of specific conductance of these three binary mixtures is explainable satisfactorily by the VTF, Adam-Gibbs (AG), and power-law (PL) equations. However, conceptually the VTF and AG equations do not seem to be applicable to these binary mixtures since the ideal glass transition temperatures obtained for the three alcohols from these equations are found to be higher than their respective calorimetric glass transition temperatures. The critical tempe-rature obtained from the PL equation does not seem to correspond to the ideal glass transition temperature and may probably refers, on the other hand, to the temperature at which α- and β- relaxations merge. The shape of the specific conductance versus concentration isotherms of the three binary systems differs from each other particularly above 20°C. The concentration at which conductance maximum occurs shifts towards alcohol side as the temperature is decreased. The concentration dependence of specific conductance seems to have a correlation with the dielectric constant and viscosity of the alcohol.

CHAPTER 1

GENERAL INTRODUCTION

1.1 Molten Salts

Although water is a most successful, useful and plentiful solvent it is often not an ideal solvent. This can be realized by considering the example of the electrolytic production of sodium metal. In an electrolytic cell if an aqueous solution of a sodium salt is taken, on passing current between two electrodes only liberation of hydrogen gas will take place at the cathode and there will be no electrodeposition of sodium. Sodium cannot be therefore electrowon from aqueous solutions. This is why the electrolytic extraction of sodium is done from molten sodium hydroxide, a medium free from hydrogen. This argument is valid for many other metals. Another well known example is that of aluminium production by the electrolysis of bauxite in molten cryolite. It is therefore sometimes necessary to use solvents other than water or electrolytic media other than aqueous electrolytes. Molten salts which are also known as fused salts or ionic liquids[1] form one such alternative electrolytic media as explained in the above example. Conventionally, molten salts are pure salts or a mixture of salts in the molten state which exist in the solid state at ambient conditions. It is remarkable to see that water and molten salts have some comparable properties. Most molten salts look like water and near their melting points have viscosities, thermal conductivities and surface tensions of the same orders of magnitude as those of water. For example, water at 25°C and molten NaCl at 850°C have viscosities equal to 0.895 and 1.25 cP, respectively and molten iron around 1400°C (viscosity $\approx$ 2.2 cP) flows like water.[2,3] The important difference

between water and molten salts lies in their specific conductivity values. Fused inorganic salts near the melting points have about 10^8 times better specific conductivity than water[2,3] which make them better media in batteries and electrochemical cells.

1.2 Room Temperature Molten Salts

Molten salts, in spite of having excellent electrical conductivity and other solvent properties, are associated with serious practical problems. The high liquidus temperatures of most of the inorganic salts often limit their utilization as solvents for many applications. The high temperatures involved in molten salt experiments necessitate exceptional requirements on the design of apparatus rendering these experiments extraordinarily expensive. In addition, the high working temperatures of molten salts mostly lie above the temperature ranges of thermal stability of many dissolved salts, especially organic compounds, restricting the utility of molten salts. Molten salt systems consisting of eutectic mixtures of two or more salts although reduce the working temperatures considerably, even those temperatures still lie much above the ambient temperature.

Due to the practical difficulties associated with the use of molten salts, considerable interest has arisen concerning molten salts that are liquid proximate to room temperature. Such molten salts are identified as room temperature molten salts. A considerable amount of research in the field of molten salt chemistry therefore deals with the development and study of room temperature molten

electrolytes which are important for use as electrolytes for high- voltage batteries and as media for carrying out chemical reactions. As a result, study on room temperature molten salt systems has emerged as a separate section in molten salt chemistry.[4-6]

The room temperature molten salts developed hitherto may be classified into three categories as (1) pure organic melts,[1,4,7] (2) a mixture of inorganic salt with organic compound[4,8,9] and (3) molten hydrated inorganic salts.[5,6,10]

1.2.1 Organic Melts

These molten salts include melts of ionized organic salts only and exclude the melts of molecular crystals. These organic salts may contain either organic cation or organic anion or both organic cation and anion (e.g., tetraalkylammonium tetraalkylborides). The most commonly used organic salts are quaternary ammonium salts and pyridinium salts.[1,4,7] Molten organic salts except a few are, however, not strictly room temperature molten salts and are rather low temperature molten salts since their melting points lie in the range ~100 to ~200°C.[7] Moreover, organic melts have limited application since very frequently the liquid state exists over a small temperature range only.

1.2.2 Molten Mixture of Inorganic Salts and Organic Compounds

The most widely studied classes of anhydrous room temperature molten salts are those based on mixtures of aluminium chloride with various n-alkylpyridinium

halides or with dialkylimidazolium chlorides.[4,8,9] These room temperature molten salts are employed extensively for electrochemical, spectroscopic and photochemical studies of a variety of organic, organometallic and inorganic solutes.[4,9,11-16] These ionic liquids are used as electrolytes in molten salt batteries, electrochemical cells and also in photoeletrochemical cells. The adjustable acid - base properties of these type of melts make them attractive solvents for studying acid - base dependent chemical phenomena.

Room temperature molten salt systems which are less studied include combination of copper (I) chloride with a variety of alkylammonium hydrochlorides and certain alkylphosphonium chlorides[4] and zinc chloride + pyridinium chloride melts.[17]

In recent years much interest has been shown on amide melts and on molten acetamide in particular.[18-29] Molten acetamide is a polar non-aqueous solvent and resembles water in its physical properties and chemical behaviour. It has a good ability to dissolve organic compounds and a large number of inorganic salts causing extensive freezing point depression. Room temperature molten salts are therefore prepared by mixing acetamide with inorganic salts, especially nitrates and thiocyanates.[21-29] These room temperature molten mixtures are found to have a high tendency to supercool and a reasonably high electrical conductivity. Acetamide containing room temperature melts have lately attracted considerable attention because of their possible applications in energy storage and energy conversion systems.

1.2.3 Molten Hydrated Inorganic Salts

These molten salts which are commonly known as hydrate melts form the third category of room temperature molten salts.[6,10] Hydrated salts occupy a unique position on the salt- water composition scale and basically they are highly concentrated aqueous electrolytes. These highly concentrated aqueous electrolytes with water/salt mole ratio in the range ca. 4 to 8 have characteristic low melting points and the study of their structural, transport and thermodynamic properties indicated that in the molten state they behave as analogues of corresponding anhydrous molten salts consisting of anions and hydrated cations.[30, 31] Properties of neat hydrate melts,[30-63] mixtures of hydrate melts,[64-74] and of mixtures containing hydrate melts and anhydrous inorganic salts[30, 75-107] were studied extensively. Hydrate melts were also employed as solvent media for carrying out reactions,[108] spectral studies,[84,86,87] and electrochemical studies.[75, 76, 78-83, 94-98, 107]

1.3 Supercooled Liquids

Upon cooling from high temperatures, a liquid or melt may crystallize at the freezing point, T_m. This first order phase transition usually results in a decrease in specific volume, water is an important exception. A liquid or melt that manages to bypass T_m without crystallization is called a supercooled liquid. Some of the systems have an inherent tendency to supercool. Most of the room temperature molten salts have the tendency to supercool. A few specific examples of this type of systems are calcium nitrate tetrahydrate melt, zinc chloride hexahydrate melt,

glycerol, O- terphenyl, eutectic mixture of acetamide and sodium thiocyanate (0.2 mole fraction). In those systems which do not supercool directly, supercooling can be induced by suddenly cooling (or quenching) the high temperature liquid or melt so that crystallization is averted kinetically. According to homogeneous nucleation theory crystallization process is controlled by the free energy barriers to the nucleation and to the growth of crystal nucleus (crystallite).[109] In general, the likelihood that a liquid remains in the supercooled state rather than crystallizing during cooling depends upon cooling rate, the cleanliness (absence of foreign nucleating agents like dust particle) of the liquid, the viscosity at T_m, the similarity of the liquid packing to that of the crystal, and other factors.

Conventionally, the crystal is regarded as the equilibrium state below the temperature T_m and the supercooled liquid state is considered as metastable. Nevertheless, the supercooled liquid may be regarded as the equilibrium state as long as no crystallization takes place. Supercooled liquids may be stable for very long times. For example, a pure sample of liquid O- terphenyl will not crystallize for years in a test tube at room temperature even though this is 35K below its melting point. Some of the hydrate melts also remain in the supercooled state for very long times if left undisturbed.

1.3.1 Strong and Fragile Liquids

Relaxation processes like viscosity or conductance of supercooled liquids may have Arrhenius or non-Arrhenius type of temperature dependence. On the basis of

mainly this property, supercooled liquids have been classified as strong or fragile.[110-111] Strong liquids (e.g., SiO_2) show Arrhenius relaxation processes and typically have three-dimensional network structures of covalent bonds. Fragile liquids(e.g.,O- terphenyl), on the other hand, have non- Arrhenius relaxation properties and typically consist of molecules interacting through nondirectional and noncovalent interactions (dispersion forces). In hydrate melts which also behave like fragile liquids ion- dipole interactions may be responsible for their fragility.

1.4 Glasses

As a supercooled liquid is cooled to lower temperatures its viscosity increases and its constituent molecules move more and more slowly. At some temperature the movement of the molecules will become so slow that they do not have a chance to rearrange sufficiently before the temperature is lowered further. Since these rearrangements are necessary for the liquid to find the equilibrium specific volume V_{sp} value for that temperature, the experimentally observed V_{sp} will begin to deviate from the equilibrium value at this point. At temperatures not much lower than this, the time scale for molecular rearrangements become extremely long compared to the time scale of the experimental observations . The structure of this material is then frozen for the practical purpose and we call it a glass. V_{SP} continues to decrease as the temperature is lowered, but the thermal expansion coefficient in the glassy state is significantly smaller than in the liquid or supercooled liquid states. Thermal expansion coefficient and specific heat values in the glassy and crystalline states are similar. Glass transition is a second-order phase transition

unlike crystallization (or melting) which is a first-order phase transition. Glass transition does not occur suddenly, but rather over a range of temperatures. Moreover the glass transition temperature T_g is different for different cooling rates. As the cooling rate lowered lower value for T_g is observed. However, the dependence of T_g upon cooling rate is relatively weak. Recently a report has been made on the appearance of first-order phase transition in supercooled triphenyl phosphite and it has been visualized by considering that polyamorphous states probably exist in a material instead of a single amorphous or glassy state.[112] A first-order liquid-glass transition was predicted by the free- volume approach of Cohen and Grest [113] as well as by other workers.[114, 115]

On the basis of entropy considerations Kauzmann[116] explained the occurrence of glass transition as a thermodynamic requirement to avert a situation where supercooled liquid may otherwise have lower entropy than crystalline state or violation of third law of thermodynamics will take place. This is known as Kauzmann paradox. The temperature at which the supercooled liquid eventually would have the same entropy as the crystal is known as Kauzmann temperature, T_k .[111] The specific entropy, s, of a supercooled liquid below T_m is calculated from the measured specific heat C_p (T) values using the thermodynamic relation

$$s(T_2) - s(T_1) = \int_{T_1}^{T_2} (C_p(T) / T)\, dT \qquad (1.1)$$

The value of T_g is correlated to T_k as $T_g >= \approx T_k$.

Thermodynamically glassy state is considered as unstable. A glass is continually relaxing, possibly too slowly to measure, toward a more stable state, a state of local free energy minimum. If experimental observations are made on time scales fast compared to the molecular motion which allow the glass to relax, then the glass is mechanically stable for practical purposes, even though it is thermodynamically unstable.

T_g is an important property of a material. The dynamics of supercooled liquids and glasses and the theory of glass transition have not been fully understood. Consequently, in recent years there has been a tremendous increase of activity in this field.[61-63, 111, 117- 127] Some of the most commonly used theories of glass transition which, in turn, also describe the non-Arrhenius temperature dependence of transport properties or of relaxation times in general are presented below.

1.5 Free - Volume Theories

Cohen and Turnbull[128] presented an interpretation of diffusion and the glass transition in molecularly simple liquids based on the idea that molecular transport occurs by the movement of molecules into voids formed by distribution of free volume or density fluctuation. For the diffusion or transport of a molecule to take place, it was considered that the void must have a volume greater than some critical value. Cohen and Turnbull[128, 129] regarded the distribution of free volume as random or free and as taking place without any energy requirement. The average free volume per molecule v_f is defined as

$$v_f = v - v_o \qquad (1.2)$$

where v is the average volume per molecule in the liquid and v_o is the van der Waals volume of the molecule which is also known as intrinsic volume. Cohen and Turnbull[128] using statistical-mechanical approach derived an expression for the probability, p(v*), of finding a void of volume exceeding the critical value, v*. It is of the form

$$p(v^*) = \exp(-\gamma v^*/ v_f) \qquad (1.3)$$

where γ is a numerical factor introduced to correct for overlap of free volume during random distribution. Presuming that the molecules move with gas kinetic velocity u, the expression obtained by Cohen and Turnbull[128] for diffusion coefficient, D is of the form,

$$D = A \exp[-\gamma v^*/ v_f] \qquad (1.4)$$

where A is a constant having a temperature dependence of the form $T^{1/2}$. Eq (1.4) gave a theoretical basis to the empirical equation of Doolittle.[130] Expressing v_f in terms of temperature as

$$v_f = \alpha v (T - T_o) \qquad (1.5)$$

Cohen and Turnbull[128] obtained another expression for D which is of the form

$$D = A \exp[-B/(T - T_o)] \qquad (1.6)$$

In eq (1.5) α is the average value of the coefficient of thermal expansion and T_0 is the temperature at which free volume disappears. In eq (1.6) B is a free parameter related to γv^*. T_0 is identified approximately with the glass transition temperature T_g. T_0 is actually same as the Kauzmann temperature T_k and hence mostly lies below (up to ~ 50 K) T_g.[131, 132] Using Nernst-Einstein and Stokes-Einstein relations one obtains from eq (1.6) equations for electrical conductivity or fluidity[30-32, 131-134] as

$$y = A_y \exp [- B_y / (T - T_{0y})] \qquad (1.7)$$

where y is either electrical conductivity or fluidity. For viscosity η the corresponding expression is

$$\eta = A\eta \exp [B\eta / (T - T_{0\eta})] \qquad (1.8)$$

For relaxation times of liquids also an equation similar to eq (1.8) can be written. In eqs (1.7) and (1.8) A's and B's are adjustable parameters. Eqs (1.7) or (1.8) is similar to the Vogel-Tammann-Fulcher (VTF) equation[135] and the Williams-Landel-Ferry (WLF) equation[136] thus providing theoretical basis to the VTF and WLF equations. The temperature dependence of pre-exponential factors of eqs (1.4) - (1.8) is generally ignored although a mild temperature dependence is expected from the free volume theory of Cohen and Turnbull as pointed out above.

The free volume theory of Cohen and Turnbull described above was subsequently improved and modified by several workers.[113, 137-145] Naghizadeh[137] accounted for the energy requirement for distribution of free volume and thus removed from the model of Cohen and Turnbull the assumption that the exchange

of free volume takes place freely among the liquid molecules. Macedo and Litovitz[138] as well as Chung[139] considered that in addition to free volume requirement there is also an energy requirement to be fulfilled before the diffusion or transport of a molecule in liquid can take place. Interestingly, the expressions derived separately by Naghizadeh, Macedo and Litovitz, and Chung are similar and of the form

$$y = A_{1y} \exp \{ - [B_{1y} / (T - T_0)] - [E^*_y / T] \} \qquad (1.9)$$

Eq (1.9) is known as a hybrid equation in which E^*_y is the minimum activation energy required for the transport to take place. Hybrid equations of different types[140, 141] are also employed to describe the non-Arrhenius temperature dependence of transport properties.

Cohen and Grest[113] extended further the free volume theory by considering liquidlike and solidlike cells to exist in a liquid. A cell is treated as liquidlike or solidlike depending upon the free volume of a molecule. In this model, the free exchange of free volume among the liquidlike cells is responsible for the fluid properties whereas glass transition occurs when the solidlike cells span the entire sample. Combining percolation theory and free volume concept Cohen and Grest[113] obtained an expression for viscosity of the type

$$\eta = A_2 \exp (2B_2 / \{ (T - T_0) + [(T - T_0)^2 + 4CT]^{1/2} \}) \qquad (1.10)$$

where A_2, B_2 and C are free parameters. This extended free volume model of Cohen and Grest accounted for the thermodynamic behaviour of the supercooled liquids near the glass transition as well.[142]

It may be commented that the expression used extensively to describe the non-Arrhenius temperature dependence of transport properties of supercooling liquids is, however, of the type given by eq (1.7) and is commonly referred as the VTF equation. Recently Mansfield[125] reassessed the validity of VTF equation and other models of glass transition on the basis of statistical-thermodynamical arguments.

1.6 Configurational Entropy Theory

Gibbs and DiMarzio[146,147] developed a statistical-mechanical quasilattice theory and predicted a second-order phase transition to occur as the number of occupied sites on a lattice became sufficiently large and the configurational entropy vanished. The configurational entropy is that part of the entropy which is due to configurational rather than vibrational degrees of freedom . It can be calculated by subtracting the entropy of the crystal from that of the supercooled liquid. Adam and Gibbs[148] defined a cooperatively rearranging region as a subsystem of the sample which, upon a sufficient fluctuation in energy, can rearrange into another configuration independently of its environment. At the glass transition the cooperatively rearranging region comprises of the whole sample since at this temperature only one configuration will be available to the entire system.

Considering the probability of a cooperative rearrangement in a fixed subsystem as a function of its size, Adam and Gibbs[148] derived an expression for the temperature dependence of relaxation process in glass-forming liquids. It is of the form

$$y = A_{2y} \exp[- B_{2y} / T S_c] \qquad (1.11)$$

where A_{2y} is a frequency factor and $B_{2y} = s^*_c \Delta G$. ΔG is the free energy barrier per mole of particles hindering the cooperative rearrangement. s^*_c is the critical configurational entropy which a region of a liquid must possess in order to undergo cooperative rearrangement and may be approximated to k ln2 where k is the Boltzman constant . S_c is the configurational entropy per mole of the macroscopic system and may be evaluated from the expression[148, 149]

$$S_c \simeq \Delta C_p \ln (T / T_o) \qquad (1.12)$$

ΔC_p is the change in the molar heat capacity at the glass transition. Substituting for S_c in eq (1.11) we obtain an expression for the temperature dependence of relaxation processes as

$$y = A_{2y} \exp [-B_{3y} / T \ln(T / T_o)] \qquad (1.13)$$

where $B_{3y} = B_{2y} / \Delta C_p$. Eq (1.13) is also reduced to the VTF equation by approximating at temperatures not too far above T_o that $T \ln (T / T_o) \approx (T - T_o)$. Angell and coworkers[5,17,30-33,35-37,64,74,131-134] initiated the extensive use of the free-volume and configurational entropy models, essentially the VTF equation, to

describe both temperature and concentration dependences of transport properties of glass-forming molten salt systems consisting of anhydrous and hydrate melts and of concentrated electrolytic systems. Later, other workers also contributed to this field.[34,38-41,55,65,66,68,70-73,85-87,89-91,99-106,150-159]

1.7 Mode Coupling Theory

A second-order phase transition must be associated with a diverging correlation length. However, there has so far been no success in detecting directly a diverging correlation length, or even the diverging susceptibility. The mode coupling theory,[160-162] which has generated in recent years considerable interest in the dynamics of supercooled liquids and the mechanism of liquid-glass transition,[62,63,111,118,120-122,127], provides a way of understanding diverging correlation times in the absence of diverging correlation lengths or susceptibilities. The basic quantity of this theory is the dynamical structure factor describing the dynamical properties of density fluctuations. The relaxation time of density fluctuations is coupled via a nonlinear feedback mechanism to the slowly decaying density fluctuation itself. This causes a divergence of the structural relaxation time at a certain critical coupling constant or at a critical temperature T_c. In fact, the T_c predicted on the basis of the first stages of viscous slowdown is greater than T_g. A crossover of relaxation mechanisms at T_c has been demonstrated.[111,163] One of the great successes of mode coupling theory has been its prediction of a relaxation scenario consisting of several different and distinct regimes. The mode coupling

theory predicts a power-law equation for relaxation time and relaxation processes. This power-law equation for electrical conductivity k is of the form

$$k = k_o[(T / T_o) - 1]^{\beta} \qquad (1.14)$$

where k_o and β are constants. The value of the exponent β predicted by mode coupling theory is ~ 2. This power-law equation is being used in recent years increasingly more for describing the non-Arrhenius temperature dependence of relaxation time and processes of supercooled liquids.[111,118,120-122,127,140,159,163-166]

1.8 Scope and Scheme of the Present Work

The importance and necessity of room temperature molten salt systems are highlighted above and three categories of such systems which are in use have also been described. Hardly any study has been done on another potential and useful type of room temperature molten salt system containing a mixture of hydrate melt and organic compound. This fourth type of room temperature molten salt systems may be expected to have a high degree of supercooling tendency and it is worthwhile to explore their physicochemical properties . A direct consequence of the low liquidus temperature of this type of room temperature molten salt systems would be their fragile nature exhibited in the form of non-Arrhenius temperature dependence of transport properties. This provides an excellent new type of systems for testing the applicability of statistical-mechanical models for transport mechanism in liquids (some are explained above) in the light of the fact that inadequacy of free

volume theory[35,167-169], VTF equation[159,163,166] and mode coupling theory[111] has been reported.

Therefore, in the present work our main objective is to make some physicochemical studies on systems containing hydrate melts and organic compounds.

In **Chapter 2** a general description of the experimental techniques used in our study has been given.

In **Chapter 3** electronic spectral study has been made of systems containing calcium nitrate tetrahydrate melt and organic indicator dyes.

In **Chapter 4** an attempt has been made to study the kinetics of the reaction between calcium nitrate tetrahydrate melt and methyl red spectrophotometrically.

In **Chapter 5** we have made a study on the density and electrical conductivity of a room temperature molten salt system containing calcium nitrate tetrahydrate melt and acetamide as a function of temperature and concentration.

In **Chapter 6** the room temperature molten salt system chosen for study in Chapter 5 has been used as a molten salt medium to study one of the important phenomena in Physical Chemistry , that is, micellization.

In **Chapter 7** electrical conductivity measurements of three mixtures of calcium nitrate tetrahydrate with methanol, ethanol and propanol have been made as functions of temperature and compositiion.

References

1. A. R. Ubbelohde, ' The Molten State of Matter', John Wiley, New York, **1978**, Ch. 8.
2. J. O'M. Bockris and A. K. N. Reddy ' Modern Electrochemistry ', Plenum Press, New York, **1970**, Vol. 1, Ch. 6.
3. C. T. Moynihan, in ' Ionic Interactions ', Ed. S. Petrucci, Academic Press, New York, **1971**, Vol. 1, Ch. 5.
4. C. L. Hussey, in ' Advances in Molten Salt Chemistry ', Ed. G. Mamantov, Elsevier, Amsterdam, **1983**, Vol. 5 .
5. C. A. Angell and C. T. Moynihan, in ' Molten Salts', Ed. G. Mamantov, Mercel Dekker, New York, **1969.**
6. J. Braunstein, in ' Ionic Interactions ', Ed. S. Petrucci, Academic Press, New York, **1971**, Vol. 1, Ch. 4.
7. P. Tissot, in ' Molten salt Techniques', Eds. D. G. Lovering and R. J. Gale, Plenum Press, New York, **1983**, Vol. 1, Ch. 6.
8. R. J. Gale and R. A. Osteryoung, in ' Molten Salt Techniques', Eds. D. G. Lovering and R. J. Gale, Plenum Press, New York, **1983**, Vol. 1, Ch. 3.
9. H. L. Chum and R. A. Osteryoung, in ' Ionic Liquids', Ed. D. Inman and D. G. Lovering, Plenum Press, New York, **1981**, Ch. 19.
10. I. M. Hodge and C. A. Angell, in ' Ionic Liquids' Eds. D. Inman and D. G . Lovering, Plenum Press, New York, **1981**, Ch. 3.
11. C. L. Hussey, P. A. Barnard, I-W . Sun, D. Appleby, P. B. Hitchcock, K.

R. Seddon, T. Welton, and J. A. Zora , J. Electrochem. Soc., **1991**, 138, 2590.

12. C. J. Dymek Jr., G . F. Reynolds, and J. S. Wilkes, J. Eletrochem. Soc., **1987**, 134, 1658 .

13. J . A. Boon, J . S. Wilkes, and J. A. Lanning, J. Electrochem. Soc., **1991**, 138, 145.

14. (a) J. L. E. Campbell and K. E. Johnson, J. Am. Chem. Soc., **1995**, 117, 7791.

(b) R. A. Mantz, P. C. Trulove, R. T. Carlin, and R. A. Osteryoung, Inorg. Chem., **1995**, 34, 3846.

15. P. Singh, K. Rajeshwar, J. DuBow, and R. Job., J. Am. Chem. Soc., **1980**, 102, 4676.

16. R. Thapar and K. Rajeshwar, J. Electrochem. Soc., **1982**, 129, 560.

17. A. J. Easteal and C. A. Angell, J. Phys. Chem., **1970**, 74, 3987.

18. R. Narayan and K. L. N. Phani, in 'Molten salt Techniques' Ed. R. J. Gale and D. G. Lovering, Plenum Press, New York, **1991**, Ch. 1.

19. S. Sampath and R. Narayan, J. Electrochem. Soc., **1991**, 138, 2267.

20. D. S. Reid and C. A. Vincent, J. Electroanal. Chem., **1968,** 18, 427.

21. G. E. Mcmanis, A. N. Fletcher, D. E. Bliss, and M. H. Miles, Electrochim. Acta, **1986**, 31, 1271.

22. G. E. Mcmanis, A. N. Fletcher, D. E. Bliss, and M. H. Miles, J. Appl. Electrochem., **1986**, 16, 101.

23. G. E. Mcmanis, A. N. Fletcher, D . E. Bliss, and M. H. Miles, J. Electroanal. Chem. , **1985**, 190, 171.

24. G. Berchiesi, G. Vitali , and A. Amico, J. Chem. Eng. Data, **1985**, 30, 208.

25. A. Amico, G. Berchiesi, C. Cametti, A. DiBiasio, J.Chem. Soc. Faraday Trans.2, **1987**, 83, 619.

26. G. Berchiesi, F . Farhat, and M. De Angelis, J. Mol. Liq. , **1992**, 54,103.

27. G. Berchiesi, G. Vitali, R. Plowiec, and S. Baroeci, J. Chem. Soc. Faraday Trans. 2, **1989**, 85, 635.

28. R. Plowiec, A. Amico, and G. Berchiesi, J. Chem. Soc. Faraday Trans. 2, **1985**, 81, 217.

29. R. Nikolic and G. Ristic, J. Sol. Chem. , **1994**, 22, 787.

30. C. A. Angell, J. Electrochem. Soc. , **1965**, 112, 1224.

31. C. A. Angell, J. Phys. Chem., **1965,** 69, 2135.

32. C. A. Angell, J. Phys. Chem., **1966**, 70, 3988.

33. C. A. Angell , E. J. Sare, and R. D. Bressel, J. Phys. Chem., **1967**, 71, 2759.

34. C. T. Monihan , J. Phys. Chem., **1966,** 70, 3399.

35. E. Williams and C. A. Angell , J. Phys. Chem., **1977**, 81, 232.

36. C. A. Angell and R. D. Bressel, J. Phys. Chem., **1972**, 76, 3244.

37. C. A. Angell, L. J. Pollard, and W. Strauss, J. Sol. Chem., **1972**, 6, 517.

38. S. I. Smedley and D. R. MacFarlane, J. Electroanal. Chem., **1981**, 118, 445.

39. D. R. MacFarlane, J. Scheirer, and S. I Smedley, J. Phys. Chem., **1986**, 90, 2168.

40. L. Pickston, S. I. Smedley, and G. Woodall, J. Phys. Chem., **1977**, 81, 581.

41. S. I. Smedley and I. Torrie, J. Phys. Chem., **1978**, 82, 238.

42. R. E. Hester and R. A. Plane, J. Chem. Phys., **1964**, 40, 411.

43. B. Balshaw and S. I. Smedley, J. Phys. Chem., **1975,** 79, 1323.

44. R. E. Hester and R. A. Plane, J. Chem. Phys., **1966**, 45, 4588.

45. R. E. Hester and C. W. J. Scaife, J. Chem. Phys., **1967**, 47, 5253.

46. M. Peleg, J. Phys. Chem., **1972,** 76, 1019.

47. T. G. Chang and D. E. Irish, J. Phy. Chem., **1973**, 77, 52.

48. C. T. Moynihan and A. Fratiello, J. Am. Chem. Soc., **1967**, 89, 5546.

49. V. S. Ellis and R. E. Hester, J. Chem. Soc. A, **1969**, 607.

50. E. J. Sare, C. T. Moynihan, and C. A. Angell, J. Phys. Chem., **1973**, 77, 1869.

51. C. A. Angell and J. C. Tucker, J. Phys. Chem., **1974**, 78, 278.

52. J. A . Duffy and M. D. Ingram, Inorg. Chem. , **1978**, 17, 2798.

53. D. H. McDaniel, Inorg. Chem., **1979**, 18, 1412.

54. R. D. Dyer III, R. M. Fronko, M. D. Schiavelli, and M. D. Ingram, J. Phys. Chem., **1980**, 84, 2338.

55. J. H. Ambrus, C. T. Moynihan, and P. B. Macedo, J. Electrochem. Soc., **1972**, 119, 192.

56. K. E. Johnson and F. W. Yerhoff, J. Electrochem. Soc., **1985**, 132, 2399.

57. H. Kimura, Ind. Eng. Chem. Fundam., **1980**, 19, 251.

58. H. Kimura and I. Karino, Ind. Eng. Chem. Fundam., **1985**, 24, 192.

59. G. C. Lisensky and H. A. Levy, Acta. Cryst., **1978**, B34, 1975.

60. E. Bossmann, J. Richter, and A. Stark, Ber. Bunsenges. Phys. Chem., **1993**, 97, 240.

61. E. Mayer, A. Hallbrucker , G. Sartor, and G. P. Johari, J. Phys. Chem., **1995**, 99, 5161.

62. B. Privel, J. F. Jal, J. Dupuy- Philon, and A. K. Soper, J. Chem. Phys., **1995**, 103, 1886.

63. B. Privel, J. F. Jal, J. Dupuy- Philon, and A. K. Soper, J. Chem. Phys., **1995**, 103, 1897.

64. C. T. Moynihan, C. R. Smalley, C. A. Angell, and E. J. Sare, J. Phys. Chem., **1969**, 73, 2287.

65. S. K. Jain, J. Phys. Chem., **1978**, 82, 1272.

66. N. Islam, K. P. Singh, and S. Kumar, J. Chem. Soc. Faraday Trans. 1, **1979**, 75, 1312.

67. N. Islam, S. Kumar,and K. P. Singh, J. Chem. Soc. Faraday Trans. 1, **1979**, 75, 1830.

68. N. Islam and A. Ali, Can. J. Chem., **1979**, 57, 2028.

69. H. H. Emons, W. Voigt, and G. Wolf, J. Sol. Chem., **1983**, 12, 855.

70. R. C. Sharma and H. C. Gaur, Electrochim. Acta, **1976**, 21, 997.

71. R. C. Sharma and H.C. Gaur, J. Chem. Eng. Data, **1977**, 22, 41.

72. R. C. Sharma and H.C. Gaur, Indian. J. Chem., **1977**, 15A, 84.

73. R. C. Sharma , R. K. Jain, and H. C. Gaur, Electrochim. Acta., **1979**, 24, 139.

74. A. J. Easteal, E. J. Sare, C. T. Moynihan, and C. A. Angell, J. Sol. Chem., **1974**, 3, 807.

75. J. Braunstein, A. R. Alvarez-Funes, and H. Braunstein, J. Phys. Chem., **1966**, 70, 2734.

76. J. Braunstein, L. Orr, A. R. Alvarez-Funes, and H. Braunstein, J. Electroanal. Chem., **1967**, 15, 337.

77. J. Braunstein, J. Chem. Educ., **1967**, 44, 223.

78. J. Braunstein and H. Braunstein, J. Chem. Soc. D, **1971**, 565.

79. H. Braunstein, J. Braunstein, and P. T. Hardesty, J. Phys. Chem., **1973**, 77, 1907.

80. D. G. Lovering and D. J. Alner, J. Chem. Soc. D, **1970**, 570.

81. D. G. Lovering, Collec. Czecho. Chem. Commun., **1972**, 37, 3697.

82. D. G. Lovering, Collec. Czecho. Chem. Commun., **1973**, 38, 1719.

83. C. T. Moynihan and C. A. Angell, J. Phys. Chem., **1970**, 74, 736.

84. C. A. Angell and D. M. Gruen, J. Am. Chem. Soc., **1966**, 88, 5192.

85. N. Islam and K. Ismail, J. Phys. Chem., **1975**, 79, 2180.

86. N. Islam and K. Ismail, J. Phys. Chem., **1976**, 80, 1929.

87. N. Islam and K. Ismail, Indian. J. Chem., **1977**, 15A, 857.

88. N. Islam and K. Ismail, J. Polymer Sci., **1979**, 17, 4021.

89. N. Islam. S. Kumar, and K. P. Singh, Can. J. Chem., **1978**, 56, 1231.

90. N. Islam, K. P. Singh, and S. Kumar, Bull. Chem. Soc. Jpn., **1979**, 52, 579.

91. N. Islam , K. Ismail, and A. Ali, Indian. J. Chem., **1980**, 19A, 254.

92. A. J. Easteal and M. C. Emson, J. Phys. Chem., **1980**, 84, 3330.

93. A. J. Easteal, Aus. J. Chem., **1981**, 34, 1853.

94. C. Nanjundiah and R. Narayan, J. Electroanal. Chem., **1979**, 103, 295.

95. C. Nanjundiah and R. Narayan, Electrochim. Acta,**1981**, 26, 203.

96. C. Nanjundiah and R. Narayan, Electrochim. Acta., **1981**, 26, 367.

97. R. Narayan and C. Nanjundiah, J. Electroanal. Chem., **1982**, 136, 159.

98. R. Narayan and K. T. Valsaraj, Electrochim. Acta, **1982**, 27, 153.

99. S. Mahiuddin and K. Ismail, Bull. Chem. Soc. Jpn., **1981**, 54, 2525.

100. P. Sangma, S. Mahiuddin, and K. Ismail, J. Phys. Chem., **1984.**, 88, 2378.

101. S. Mahiuddin and K. Ismail, Bull. Chem. Soc. Jpn., **1984**, 58, 313.

102. C. Bhattacharjee, S. Ismail, and K. Ismail, J. Chem. Eng. Data, **1986**, 31, 117.

103. S. S. Islam and K. Ismail, Can. J. Chem., **1988**, 66, 242.

104. S. S. Islam and K. Ismail, J. Chem. Eng. Data., **1988**, 33, 472.

105. S. S. Islam and K. Ismail, J. Chem. Eng. Data., **1990**, 35, 348.

106. S. S. Islam and K. Ismail, J. Electrochem. Soc., **1990**, 137, 3148.

107. D. H. Kerridge and S. A. Tariq, Sci. Int. (Lahore), **1990**, 2, 23 (Chem. Abst. **1991**, 113, 223600y).

108. R. F. Bartholomew and H. M. Garfinkel, J. Inorg. Nucl. Chem., **1969**, 31, 3655.

109. D. Turnbull and M. H. Cohen, J. Chem, Phys., **1958**, 29, 1049.

110. C. A. Angell, J. Non- Cryst. Solids, **1991**, 131-133, 13.

111. M. D. Ediger, C. A. Angell, and S. R. Nagel, J. Phys. Chem., **1996**, 100, 13200.

112. A. Ha, I. Cohen, X. Zhao, M. Lee, and D. Kivelson, J. Phys. Chem., **1996**,100,1

113. M. H. Cohen and G. S. Grest, Phys. Rev. B, **1979**, 20, 1077.

114. T. R. Kirkpatrick, D. Thirumalai, and P. G. Wolynes, Phys. Rev. A, **1989**, A40. 1045.

115. T. R. Kirkpatrick and D. Thirumalai, Transp. Theory Stat. Phys., **1995**, 24, 927.

116. W. Kauzmann, Chem. Rev., **1948**, 43, 219.

117. S. S. N. Murthy and D. Kumar, J. Chem. Soc. Faraday Trans., **1993**, 89, 2423.

118. W. Kob and H. C. Anderson, Phys. Rev. Lett., **1994**, 73, 1376.

119. T. Fehr and H. Lowen, Phys. Rev. E, **1995**, 52, 4016.

120. S. K. Lai and S. Y. Chang, Phys. Rev. B, **1995**, 51, 12869.

121. A. P. Sokolov, W. Steffen, and E. Rossler, Phys. Rev. E, **1995**, 52 , 5105.

122. A. P. Sokolov, J. Hurst, and D. Quitmann, Phys. Rev. B, **1995**, 51, 12865.

123. J. Wuttke, W. Petry, G. Coddens, and F. Fujara, Phys. Rev. E, **1995**, 52, 4026.

124. Y. Yang and K. A. Nelson, J. Chem. Phys., **1995**, 103, 7722.

125. M. L. Mansfield, J. Chem. Phys., **1995**,103, 8124.

126. G. Sartor, K. Hofer, and G. P. Johari, J. Phys. Chem., **1996**., 100, 6801.

127. S. S. N. Murthy, J. Phys. Chem. B, **1997**, 101, 6043.

128. M. H. Cohen and D. Turnbull , J. Chem. Phys., **1959**, 31, 1164.

129. D. Turnbull and M. H. Cohen, J. Chem. Phys., **1961**, 34, 120.

130. A. K. Doolittle, J. Appl. Phys. **1951**, 22, 1471.

131. C. A. Angell, J. Am. Ceram. Soc., **1968**, 51, 117.

132. C. A. Angell, J. Am. Ceram. Soc., **1968**, 51, 125.

133. C. A. Angell, J. Phys. Chem., **1964**, 68, 218.

134. C. A. Angell, J. Phys. Chem., **1964**, 68, 1917.

135. (a) H. Vogel, Physik. Z., **1921**, 22, 645 ;

(b) V. G. Tammann and W. Hesse, Z. Anorg. Allg. Chem., **1926**, 156, 245 ;

(c) G. S. Fulcher, J. Am. Ceram. Soc., **1925**, 8, 339.

136. M. L. Williams, R. F. Landel, and J. D. Ferry, J. Am. Chem. Soc., **1955**, 77, 3701.

137. J. Naghizadeh, J. Appl. Phys., **1964**, 35, 1162.

138. P. B. Macedo and T. A. Litovitz, J. Chem. Phys., **1965**, 42, 245.

139. H. S. Chung, J. Chem. Phys., **1966**, 44, 1362.

140. R. J. Speedy, J. A. Ballance, and B. D. Cornish, J. Phys. Chem., **1983**, 87, 325.

141. A. A. Ruth, B. Nickel, and H. Lesche, Z. Phys. Chem., **1992**, 175, 91.

142. G. S. Grest and M. H. Cohen, Phys. Rev. B, **1980**, 21, 4113.

143. H. Vogel and A. Weiss, Ber. Bunsenges. Phys. Chem., **1981**, 85, 539.

144. H. Vogel and A. Weiss, Ber. Bunsenges. Phys. Chem., **1981**, 85, 1022.

145. J. Fisher and A. weiss, Ber. Bunsenges. Phys. Chem., **1986**, 90, 896.

146. J. H. Gibbs and E. A. DiMarizio, J. Chem. Phys., **1958**, 28, 373.

147. J. H. Gibbs and E. A. DiMarizio, J. Chem. Phys., **1958**, 28, 807.

148. G. Adams and J. H. Gibbs, J. Chem. Phys., **1965**, 43, 139.

149. V. P. Privalko, J. Phys. Chem., **1980**, 84, 3307.

150. J. Barthel, H.-J. Gores, and G. Schmeer, Ber. Bunsenges. Phys. Chem., **1979**, 83, 911,

151. J. Barthel, H.-J. Gores, P. Carlier, F. Feuerlein, and M. Utz, Ber. Bunsenges. Phys. Chem., **1983**, 87, 436.

152. J. Barthel, Pure Appl. Chem., **1985**, 57, 355.

153. N. Islam, M. R. Islam, S. Ahmed, and B. Waris, J. Am. Chem.

Soc., **1975**, 97, 3026.

154. N. Islam, M. R. Islam, B. Waris, and K. Ismail, J. Phys. Chem., **1976**, 80, 291.

155. N. Islam, A. Maroof,and K. Ismail, Can. J. Chem., **1979**, 57, 147.

156. S. Mahiuddin and K. Ismail, Can. J. Chem., **1982**, 60, 2883.

157. S. Mahiuddin and K. Ismail, J. Phys. Chem., **1983**, 87, 5241.

158. S. Mahiuddin and K. Ismail, J. Phys. Chem., **1984**, 88, 1027.

159. A. Das, S. Dev, H. Shangpliang, K. L. Nonglait, and K. Ismail, J. Phys. Chem. B, **1997**, 101, 4166.

160. E. Leutheusser, Phys. Rev. A, **1984**, 29, 2765.

161. U. Bengtzelius, W. GÖtze, and A. SjÖlander, J. Phys. C, **1984**, 17, 5915.

162. W. GÖtze, in ' Liquids, Freezing, and the Glass Transition', Eds. J. P. Hansen, D. Levesque, and J. Zinn- Justin, Elsevier, Amsterdam, **1991**.

163. S. S. N. Murthy, J. Chem. Soc. Faraday Trans. 2, **1989**, 85, 581.

164. S. S. N. Murthy, J. Chem. Soc. Faraday Trans. 2, **1988**, 84, 671.

165. R. J. Speedy, J. Phys. Chem., **1983**, 87, 320.

166. H. Weingärtner, R. Haselmeirr, and M. Holz, J. Phys. Chem., **1996**, 100, 1303.

167. M. Goldstein, J. Chem. Phys., **1963**, 39, 3369.

168. M. Goldstein, J. Phys. Chem., **1973**, 77, 667.

169. C. A. Angell, L. J. pollard, and W. Strauss, J. Chem. Phys., **1969**, 50, 2694.

CHAPTER 2

EXPERIMENTAL TECHNIQUES AND DATA ANALYSIS

2.1 Sample Preparation

Details of the chemicals used and of sample preparation are given in the respective chapters. Samples were prepared generally by weighing directly the components of a mixture. Sometimes while using liquid component it was added by measuring its volume and the corresponding weight was determined from the density data. Weighing was done using a Shimadzu Libror AEL-200 electronic analytical balance having 0.1 mg readability. Wherever required doubly distilled water having conductivity about 2 $\mu S\ cm^{-1}$ has been used.

Since hydrate melts are used during this study, it may be worthwhile to mention about the concentration scale used for representing the composition of a hydrated salt. This new concentration unit was introduced by Angell and Gruen[1] and is denoted by R which is equal to the water-to-salt molar ratio. This unit is particularly more useful than the conventional units like molality or molarity when one discusses the composition region where there are insufficient water molecules to fill more than one or two hydration shells per cation or anion. For example, for the hydrated salt $Ca(NO_3)_2.4.1H_2O$, R=4.1 which is equivalent to 13.55 mol kg^{-1} on molality scale. R of a hydrated salt can be determined by the conventional titration method or by comparing the density or specific conductance of the hydrated melt with the density versus concentration or specific conductance versus concentration calibration curves for the aqueous solution of the salt, respectively.

2.2 Temperature Control

The temperatures of the test solutions above 25°C were controlled using INSREF IRI 015A thermostat equipped with a digital proportional temperature controller. The digital temperature display of the thermostat was first calibrated against a reference mercury thermometer. Either water or oil was used as bath liquid depending upon the highest temperature required to be controlled. The oil used was the commercially available refined oil. Using this thermostat, temperature can be controlled with a thermal stability better than ± 0.05°C.

We also used sometimes a thermostatic bath of ~10 litre capacity which was set up by assembling an immersion heater (1 kW), stirrer (Remi make), mercury contact thermometer, mercury vertical relay (Jumo-type GKT 15-0, 22V, 15A), calibrated mercury check thermometer, and a voltage divider. Using such a thermostat a thermal stability better than ± 0.02°C could be obtained by appropriately adjusting the output voltage from the voltage divider.

2.3 Density Measurement

Density measurements were made using a glass pycnometer of apporximately 7 cm^3 capacity having a stem of about 10 cm length graduated to about 0.01 cm^3 divisions. Each mark on the stem of the pycnometer was calibrated using n-octane

(Fluka) as a reference liquid. The reported density, d, of n-octane as a function of temperature (t°C) which is required for calibration is given by[2]

$$d = 0.71848 - 0.8239\times10^{-3}t + 0.4459\times10^{-6}t^2 - 5.293\times10^{-9}t^3 \qquad (2.1)$$

Samples were introduced into the pycnometer with the help of a hypodermic syringe with ca. 10 cm long needle. On the other hand, viscous samples were filled in the pycnometer by applying vacuum. Densities were determined by recording the volume changes as a function of temperature. Using this method it is possible to measure density with an accuracy of 0.01%.

2.4 Conductance Measurement

All conductance measurements were made at 1kHz using Wayne Kerr B905 Automatic Precision Bridge. This LCR meter has 0.01nS resolution and measures conductance with an accuracy of 0.05%. It also has an averaging facility and averages 2 ('average 1') to 128 ('average 9') measurements in a time span of about 670ms to 36s. We have used throughout 'average 9' option and therefore each conductance reading corresponds to an average of 128 measurements. The Bridge works basically on the principle of Ohm's law. Matching currents are passed through the standard resistor and the solution under test. The corresponding two voltages produced, whose values depend upon the impedences at the standard resistors and the test solution, are measured, resolved and computed to give the

desired information on the display. All functions of the instrument are under direct control of a micro-processor.

A dip-type conductivity cell having platinized platinum electrodes was used for conductance measurement. The cell constant was determined using standard KCl solution.[3-6]

2.5 Spectral Measurements

Visible absorption spectra of indicators in molten media were recorded using Beckmann DU- 650 spectrophotometer. Quartz cells of 1 cm path length were used for holding the samples. This spectrophotometer has a resolution of ± 1 nm and the measured absorbance has an accuracy of 0.01%. For maintaining the temperature of the samples thermostated water was circulated around the cell holder.

2.6 Data Analysis

The experimental data were analyzed by fitting the data to different equations as explained in the succeeding chapters. For this purpose, we have used two types of computer programs. In the simple least-squares method, values of the constant parameters of the equations used were computed by directly minimizing the square of the deviation in a single cycle. For example, fitting of data to linear equations was done by this method in order to get least-squares fitted values of slope and intercept. In the other method an iterative least-squares method has been used.

The computer program for this method was developed essentially on the basis of the Newton-Raphson method.[7-9] In this program, approximate values of the unknown parameters of the equations used are initially fed into the computer. The computer then improves the values of the parameters in every cycle by minimizing the square of the deviation. Refined values of the parameters become their initial values for the next cycle. The cycle is continued till the best-fit is obtained.

The deviation of the calculated values from the observed values has been expressed in terms of standard deviation, σ, which is defined as

$$\sigma = [(\text{cal. value} - \text{obs. value})^2 / \text{no. of data points}]^{1/2} \qquad (2.2)$$

For linear fits, the linearity of the fits is also checked sometimes by calculating the correlation coefficients which is defined as

$$\text{Correlation Coefficient} = S_{xy} / (S_{xx} S_{yy})^{1/2} \qquad (2.3)$$

S_{xx}, S_{yy} and S_{xy} are given by

$$S_{xx} = \Sigma x_i^2 - (\Sigma x_i)^2 / n \qquad (2.4)$$

$$S_{yy} = \Sigma y_i^2 - (\Sigma y_i)^2 / n \qquad (2.5)$$

$$S_{xy} = \Sigma x_i y_i - \Sigma x_i \Sigma y_i / n \qquad (2.6)$$

where x_i is the independent variable, y_i is the dependent variable and n is the number of data points. For a perfect linear fit correlation coefficient is equal to ± 1. All the computations were done using HCL HP Infiniti (Pentium, 100 MHz) Personal Computer.

References

1. C. A. Angell and D. M. Gruen, J. Am. Chem. Soc., **1966**, 88, 5192.
2. S.W. Washburn, ' International Critical Tables of Numerical data ', vol. 3, McGraw Hill, New York, **1928**.
3. J. Barthel, F. Feuerlein, R. Neueder, and R. Wachter, J. Sol. Chem., **1980**, 9, 209.
4. Y.C. Wu, W.F. Koch, W.J. Hamer, and R.L. Kay, J. Sol. Chem., **1987**, 16, 985.
5. Y.C. Wu, K.W. Pratt, and W.F. Koch, J. Sol. Chem., **1989**, 18, 515.
6. Y.C. Wu, W.F. Koch, W.J. Hamer, and R.L. Kay, J. Sol. Chem., **1990**, 19, 1053.
7. J.B. Scarborough, ' Numerical Mathematical Analysis ', Oxford & IBH Pub., New Delhi, **1966**, p. 201.
8. D.P. Shoemaker and C.W. Garland, ' Experiments in Physical Chemistry ', McGraw Hill Kogakusha, Tokyo, **1962**, p. 26.
9. R.L. Kay, J. Am. Chem. Soc., **1960**, 82, 2099.

CHAPTER 3

ELECTRONIC SPECTRA OF MELTS CONTAINING CALCIUM NITRATE TETRAHYDRATE AND ORGANIC INDICATORS

3.1 Introduction

As highlighted in Chapter 1 a considerable amount of research in the field of molten salt chemistry deals with the development of room temperature molten electrolytes which are important for use as electrolytes for high-voltage batteries and as solvent media for carrying out chemical reactions and other physicochemical studies. Different types of room temperature molten salt systems are described in chapter 1. As stated in the scope of the present work (chapter 1, section 1.8) our main objective is to study the behaviour of molten systems containing hydrated inorganic salt and organic compound which form an almost unexplored category of room temperature molten salt systems.

Hydrate melts are one kind of room temperature molten electrolyte (cf. chapter 1, sec 1. 2) which possess remarkable chemical properties.[1-7] Due to the presence of aquometal complexes, hydrate melts and highly concentrated solutions of certain metal salts have high acidic behaviour.[1,4-8] The acidity of hydrate melts can also be controlled by the addition of a second salt.[4] Sare et al.[8] showed that mixtures of $Al(NO_3)_3.10H_2O$ and $AlCl_3.10H_2O$ dissolve noble metals more rapidly than boiling aqua regia.

The acidic behaviour of hydrate melts may be understood from the following equilibria :

$$[M(H_2O)_4]^{n+} \rightleftharpoons H^+ + [M(OH)(H_2O)_3]^{(n-1)+} \qquad (3.1)$$

where M represents a metal ion of oxidation number, n. Several dissociation equilibria of the above type may be written until the final equilibrium :

$$[MO_3(OH)]^{(7-n)-} \rightleftharpoons H^+ + [MO_4]^{(8-n)-} \qquad (3.2)$$

is reached. The actual species predominating under a given set of conditions depends upon the oxidation number n of the metal ion and also the chemical nature of M. For example, under mildly acidic conditions, if n = 2, then the predominant species is $[M(H_2O)_4]^{2+}$, whereas if n = 6 it is $[MO_4]^{2-}$.

Different attempts have been made to find a suitable scale for expressing the acidity of hydrate melts or of concentrated aqueous solutions.

Duffy and Ingram[1,9] used a new scale known as optical basicity scale for expressing the acidity of concentrated aqueous solutions and of Lewis acids in general. The application of optical basicity scale is restricted to oxide-containing systems (oxidic systems) and thus excluding hydrogen halide acids from consideration. The basicity of oxyanions are therefore compared by the electron donor power of the oxygens present in the oxyanions. The electron donor power of the oxygens is probed by introducing small concentrations of metal ions which, by their acidic nature, accept negative charge . Metal ions such as Tl^+, Pb^{2+}, and Bi^{3+} are used as probes and these ions accept varying amounts of negative charge depending upon the basicity of the environment . The amount of negative charge donated to the metal ion affects the frequency, γ, of its $^1S_0 \rightarrow {}^3P_1$ absorption band, which occurs in the uv region. In the case of Pb^{2+}, the $^1S_0 \rightarrow {}^3P_1$ transition

involves excitation of an electron from the 6s orbital to the 6p and occurs at γ = 60,700 cm^{-1} for the condition where there is zero donation, while for the condition approaching maximum donation in CaO melt γ = 29,700 cm^{-1} causing a maximum spectroscopic shift of 31,000 cm^{-1}. The quantity λ defined as $\lambda = (60{,}700 - \gamma_{oxyanion}) / 31{,}000$ is termed as optical basicity. A link between λ and pK for the dissociation of the parent acid of the oxidic species (conjugate base) was established by Duffy and Ingram.[1] However, the correlation between optical basicity and acid strength is entirely empirical and the existence of such a relationship has not been fully justified in terms of thermodynamic arguments. Attempt has also been made by Sare et al.[8] to use proton nmr data in the estimation of acidity of concentrated aqueous electrolytes.

A commonly used scale for expressing the acidity of a system is the pH scale. However, the determination of acidity of a metal aquo complex demands reference to the conditions pertaining in concentrated solutions rather than in dilute solutions. Thus the pH scale or the method involving the measurement of hydrogen ion concentration cannot be employed to hydrate melts. In fact, the break down of pH as a useful measure of acidity occurs for solutions whose ion strength is > ca. 0.1 mol. dm^{-3}. Instead, acidity must be viewed in terms of the tendency of the aquo complex to donate protons to some suitable acceptor. For concentrated solutions of oxy acids, the tendency to donate protons is measured using weak organic bases which are normally organic indicators. This equilibrium for the protonation of organic base, B may be represented as

$$HX + B \rightleftharpoons BH^+ + X^- \qquad (3.3)$$

where HX denotes the acid. The acid dissociation constant, K_a of BH^+ is written as

$$K_a = a_B\, a_{H^+} / a_{BH^+} \qquad (3.4)$$

where a's represent the activities of the different species in the concentrated solution or hydrate melt. Eq (3.4) takes the form

$$H_0 = pK_a + \log [\, C_B / C_{BH^+}] \qquad (3.5)$$

where C's indicate concentrations of the different species. H_o is the Hammett acidity function[10] and is given by

$$H_0 = - \log [\, a_{H^+} f_B / f_{BH^+}] \qquad (3.6)$$

where f ' s indicate the activity coefficients. It may be noted that in dilute aqueous solutions H_0 becomes identical with pH. The concentration ratio C_B / C_{BH^+} can be correlated to the optical densities by the expression[10]

$$C_B / C_{BH^+} = (A - A_a) / (A_B - A) \qquad (3.7)$$

where A is the absorbance of the organic indicator in the experimental system which may be a concentrated solution. A_a and A_B are the absorbances of the indicator in the most acidic and basic solutions, respectively. Thus the quantity C_B / C_{BH^+} in eq (3.5) is measurable spectrophotometrically.

The above method of measuring acidity in terms of H_0 can be applied to estimate the acidity of concentrated aqueous solutions of metal salts or of hydrate melts.[1,4-6] However, some difficulties are faced while applying the above method to hydrate melts. These are : (1) A hydrate melt may not be chemically inert and might cause some side reactions of the organic indicator. (2) A hydrate melt may not have good UV transparency for the necessary spectrophotometric analysis.

The spectrophotometric technique for the determination of H_0 has been found to be however not applicable to hydrate melts containing nitrate ions due to the above mentioned two difficulties. In this chapter we have recorded visible spectra of molten systems containing calcium nitrate tetrahydrate melt and various organic indicators with a view to employ the spectrophotometric technique for determining the H_0 value of calcium nitrate tetrahydrate (CNTH) melt by overcoming the difficulties mentioned above.

3.2 Experimental Section

The indicators used for spectral study are p- nitrophenol (CDH,analytical reagent), p-nitroaniline (SISCO,extrapure), methyl red (SD, analytical reagent), methyl orange (E. Merck), and bromophenol blue(SM, 0.05 % w/v solution, density = 0.9882 g cm^{-3}). All indicators except p-nitrophenol which was recrystallized from doubly distilled water were used without further purification.

CNTH (SD, Analytical reagent) melt was prepared by heating the hydrated salt in a water bath (INSREF) around 45°C and then allowing it to cool very slowly. Melt was made acidic by adding an weighed amount of nitric acid (GLAXO, analytical reagent) to a known amount of the melt. To make the melt basic, excess of NaOH pellets (SD, analytical reagent) were added to the melt and heated at about 45°C in the thermostat for an hour. The undissolved NaOH was removed from the melt by vacuum filtration using a sintered crucible. Stock solutions of the indicators of known concentrations were prepared in doubly distilled water. In some cases when the preparation of stock solution of indicator in water was found to be difficult due to low solubility, the indicator solution was made in an alkaline solution and was neutralized later by the addition of appropriate amount of acid (for example in the case of methyl red). Spectra were taken immediately after the addition of the weighed amounts of indicator solution to the melt using the Beckmann DU - 650 Spectrophotometer. The temperature of the sample was maintained at 25°C by circulating thermostated water around the cell holder.

3.3 Results and Discussion

The absorption spectra of methyl red (MR), p-nitrophenol (PNP), bromophenol blue (BPB), methyl orange (MO), and p-nitroaniline (PNA) taken in neat, acidic and basic CNTH melts at 25°C are shown in Figs. 3.1-3.17. The values of λ_{max} for the acidic and basic forms of indicators and of absorbance A_B in basic melt for the different indicators are given in Table 3.1. The λ_{max} values were found to be

reproducible within ± 2nm. The structures of the indicators are shown in Fig. 3.18. The literature[6,11-13] values of λ_{max} in aqueous medium are also given in Table 3.1 for the sake of comparison. Compared to the values of λ_{max} in aqueous medium the corresponding values in the melt are either in close agreement or red shifted. Red shifting of λ_{max} in hydrate melt compared to its position in water was also reported by Dyer et al.[4] In the case of PNA the λ_{max} for the acidic form could not be located accurately due to non-transparency of the pure melt below ~ 330nm. Dyer et al.[4] also pointed out about such a difficulty in locating λ_{max} for the protonated PNA in nitrate melts. In Table 3.1 the literature[6,14] values of pK_a of the indicators used are also listed. It may be noted that for the calculation of H_0 of hydrate melts pK_a values of indicators in water are generally used since pK_a values in hydrate melts are not known.

It has been observed that in acidic CNTH melt the absorbance values are not stable and vary with time. This is attributed to the reaction of these organic indicators with the acidic melt. Nitration of organic substances in CNTH, which is favoured by the presence of acid, has been reported.[2] Owing to this problem, experimental determination of meaningful values of H_0 of CNTH melt using eqs (3.5) and (3.7) has been considered to be difficult.[4,6] To overcome this problem we made an attempt to determine the value of the ratio C_B / C_{BH}^+ using the spectral data of an indicator in neat and basic CNTH only. For this purpose, it is considered that an indicator exists completely in the deprotonated form in basic CNTH melt. Knowing the absorbance of the indicator and its total cocentration (indicated in the

figure captions) in the basic melt, the value of the extinction coefficients for the basic form of the indicator was evaluated. To get the value of C_B, the absorbance corresponding to the basic form of the indicator in the neat melt was divided by the value of extinction coefficient evaluated above. The value of C_{BH}^+ was then determined by deducting C_B from the total concentration of the indicator in the neat melt. An almost similar approach was used by Duffy and Ingram[6] to estimate C_B / C_{BH}^+ in concentrated aqueous solutions of $ZnCl_2$ by considering that the organic indicator exists almost completely in the basic form in dilute $ZnCl_2$ solution. We however observed that the above method adopted by us for estimating C_B/C_{BH}^+ cannot be satisfactorily applied in the case of every indicator. For instance, MR, MO, and PNP indicators exist predominantly in the protonated forms in neat melt thereby making the amount of their basic forms so small that direct estimation of C_B was not possible. Consequently, using MR, MO, and PNP indicators the above method cannot be employed for the determination of H_0 of CNTH melt . From the above observation it is implied that in nitrate ion containing hydrate melts in order to employ the present method of estimating C_B / C_{BH}^+ the indicator to be used must have a low pK_a value. This is in accordance with the suggestion made by Duffy and Ingram[6] that the H_0 value is more meaningful when C_B and C_{BH}^+ are within a factor of 10 of each other since pK_a value of an indicator determines the relative values of C_B and C_{BH}^+ in a melt. Therefore, an attempt has been made to evaluate H_0 of CNTH melt from the spectral data of BPB and PNA.

Although the pK_a (= 4.1) value of BPB is more than that of MO, the value of C_B corresponding to BPB could be estimated accurately in spite of the fact that the

amount of the basic form of the indicator in neat melt is low. This was possible because in BPB the difference between the λ_{max} values of its acidic and basic forms is 143nm whereas in MO this difference is only 40nm. In MR and PNP the differences between the two λ_{max} values are 58 and 75 nm, respectively. The lower differences in the λ_{max} values of acidic and basic forms of MO, MR, and PNP compared to that observed in BPB cause the overlapping of the spectra due to the two forms of the indicators rendering determination of the precise value of the absorbance of basic form in neat melt difficult. On the other hand, in the case of BPB the spectra due to acidic and basic forms are well separated as evident from Fig 3.7 and also from the overlay spectra of BPB given in Fig 3.10. The value of H_0 for CNTH melt calculated using BPB was found to be 2.6. Thus an indicator having $pK_a \approx 4$ can still be used for determining C_B directly in a neat hydrate melt if the spectra due to acidic and basic forms of the indicator are well separated.

The pK_a value of PNA is 0.99 which is the lowest among the pK_a values of the indicators used in this study. Duffy and Ingram[6] used this indicator for determining H_0 of concentrated $ZnCl_2$ solutions having water to salt molar ratio ≥ 11. Dyer et al.[4] also used PNA indicator for evaluating H_0 of binary mixtures of CNTH melt with HNO_3 , $Al(NO_3)_2.9H_2O$ and $Cd(NO_3)_2.4H_2O$. However, H_0 for pure CNTH melt was not reported by Dyer et al.[4] A low value of pK_a ensures that, as mentioned above, the amount of basic form of the indicator in the neat hydrate melt can be so high that its precise direct estimation may be possible. As expected, in the neat melt a clear band at 394 nm due to the basic form of PNA was observed (Figs. 3.13 and

3.17). Thus, the value of C_B was directly evaluated and the value of H_0 for CNTH melt obtained using PNA indicator is found to be 1.8 (Table 3.1). This value of H_0 is about 0.8 units less than that obtained using BPB indicator. Based on the uncertainties involved in concentration values of the indicators the error limits of H_0 values were estimated to be nearly $\pm$ 0.2. Dependence of H_0 value on the pK_a of the indicator used can also be noticed in the values of H_0 reported by Duffy and Ingram[6] for concentrated $ZnCl_2$ solutions. For example, the H_0 values reported[6] for $ZnCl_2.4.43$ and $ZnCl_2.5.66H_2O$ melts using 4-chloro-2-nitroaniline (pK_a = -1.03), 4-nitrodiphenylamine (pK_a = - 2.38), and 2,5-dichloro-4-nitroaniline (pK_a = -1.82) indicators are -2.35, -2.10, and -1.86 and -1.45, -0.83, and -0.78, respectively. A direct correlation exists between the H_0 value of a hydrate melt and the pK_a of the corresponding aquometal ion. For instance, based on the optical basicity value Duffy and Ingram[6] predicted a value of - 4.1 for the pK_a of $Zn(H_2O)_4^{2+}$ whereas the H_0 value measured for zinc chloride tetrahydrate melt is in the range -2.35 to -1.86 as given above. Similarly, from the value 2.6 predicted[6] for the pK_a of $Ca(H_2O)_4^{2+}$ based on its optical basicity value, H_0 value in the range 1.5 to 1.2 may be anticipated for CNTH melt. Furthermore, on extrapolating separately the H_0 values reported[4] for the binary molten mixtures CNTH+ $Al(NO_3)_3.9H_2O$ and CNTH + $Cd(NO_3)_2.4H_2O$, we obtained the H_0 value of CNTH melt as 1.5 $\pm$ 0.1 and 2.6 $\pm$ 0.1, respectively. It is worthwhile to note that the H_0 values of CNTH melt estimated thus are comparable with the present measured values using BPB and PNA.

It may therefore be concluded that : (1) Spectrophotometric technique using organic indicators can be employed for the determination of H_0 function of hydrate

melts even if the indicator undergoes reaction in the acidic melt and the melt has no UV transparency. (2) From the spectra of an indicator in neat and basic hydrate melt it is possible to estimate C_B / C_{BH}^+. (3) For obtaining meaningful value of H_0, indicators to be used must have low pK_a value preferably $\leq \sim 1$. (4) Indicators having high pK_a value in the range ~ 4 are also found to be useful for the determination of H_0 provided such indicators have well separated absorption bands for their acidic and basic forms in neat hydrate melt.

Table 3.1 : Spectral Data and Parameters of Eq (3.5) for Different Indicators in Calcium Nitrate Tetrahydrate Melt at 25°C (λ_{max} in Aqueous Medium are Given in the Parentheses)

Indicator	λ_{max} (nm) in Melt		A_B	C_B	$\log[C_B/C_{BH^+}]$	H_0 ± 0.2
	Acidic	Basic		(mol kg^{-1})		
MR (pK_a=5.0)	520 (522)	462 (423)	0.4544	—	—	—
PNP (pK_a=7.1)	333 (317)	408 (407)	2.4940	—	—	—
BPB (pK_a=4.1)	447 (440)	590 (595)	0.9124	3.19×10^{-5}	-1.5	2.6
MO (pK_a=3.7)	510 (507)	470 (462)	0.2273	—	—	—
PNA (pK_a=.99)	—	394 (380)	2.0061	8.07×10^{-5}	0.8	1.8

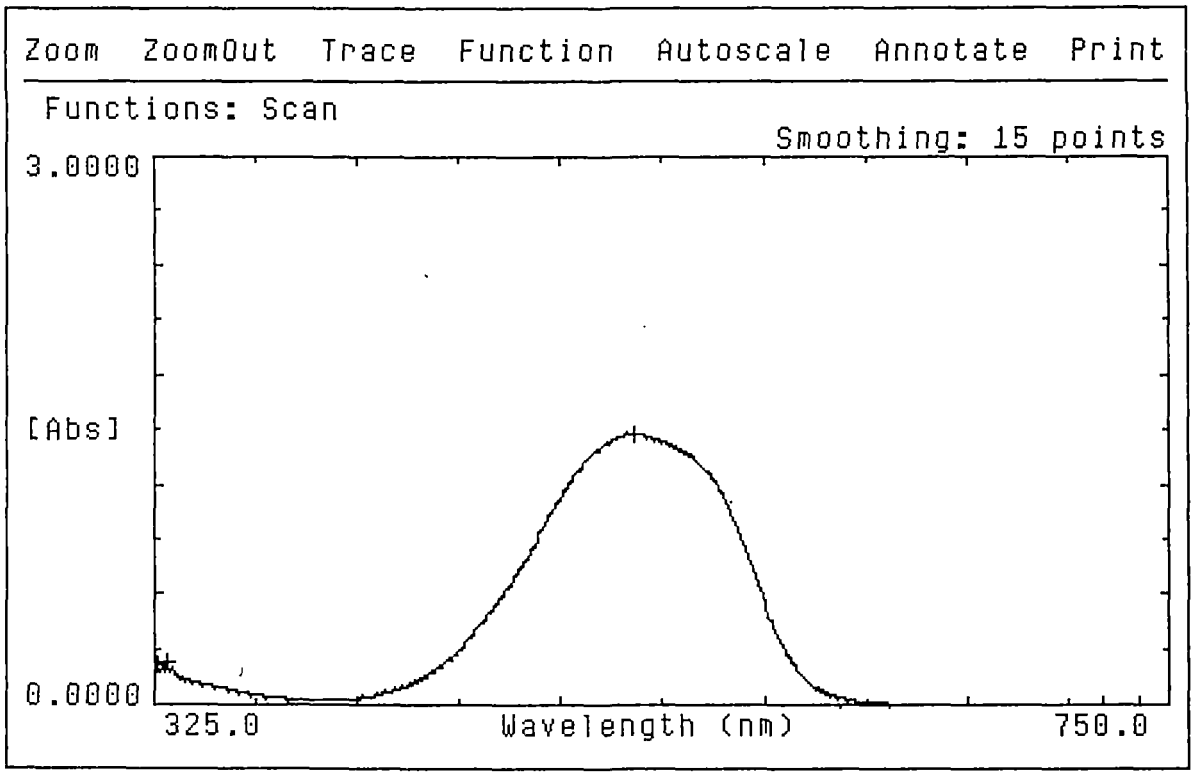

Fig. 3.1 Spectra of methyl red (2.47×10^{-5} mol kg^{-1}) in neat Calcium nitrate tetrahydrate melt at 25°C.

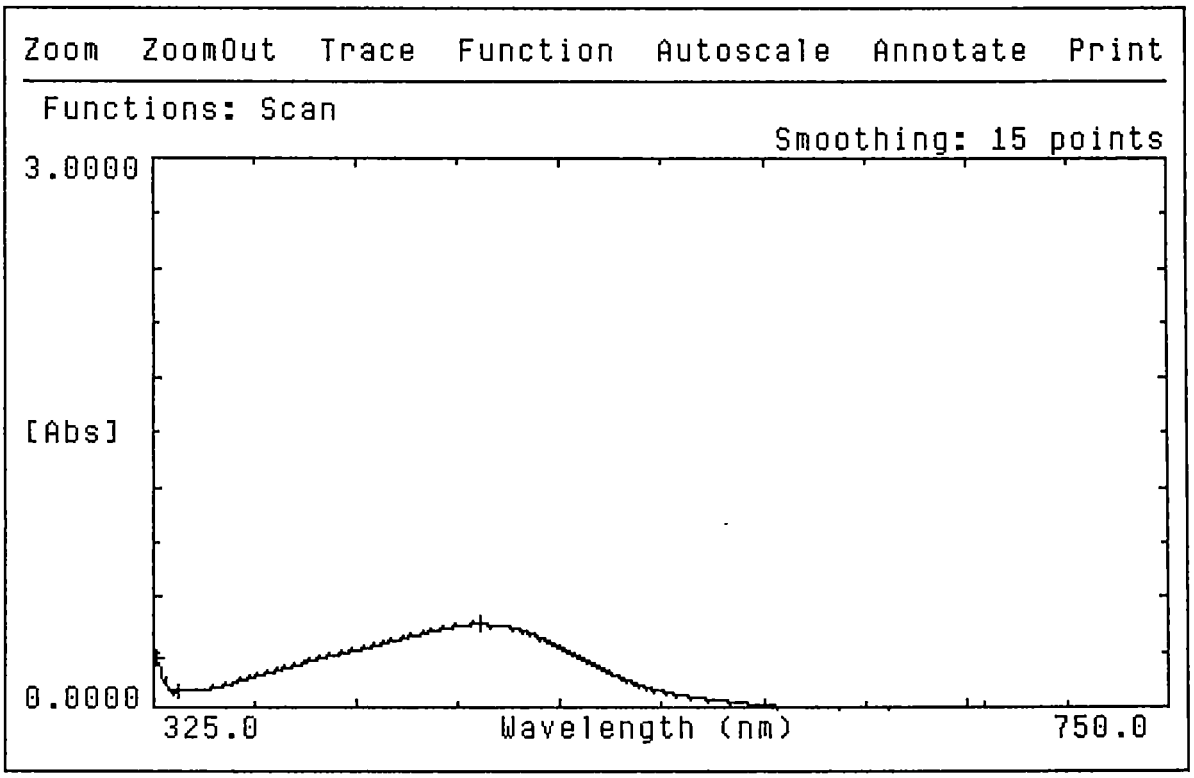

Fig. 3.2 Spectra of methyl red (1.87×10^{-5} mol kg^{-1}) in basic Calcium nitrate tetrahydrate melt at 25°C.

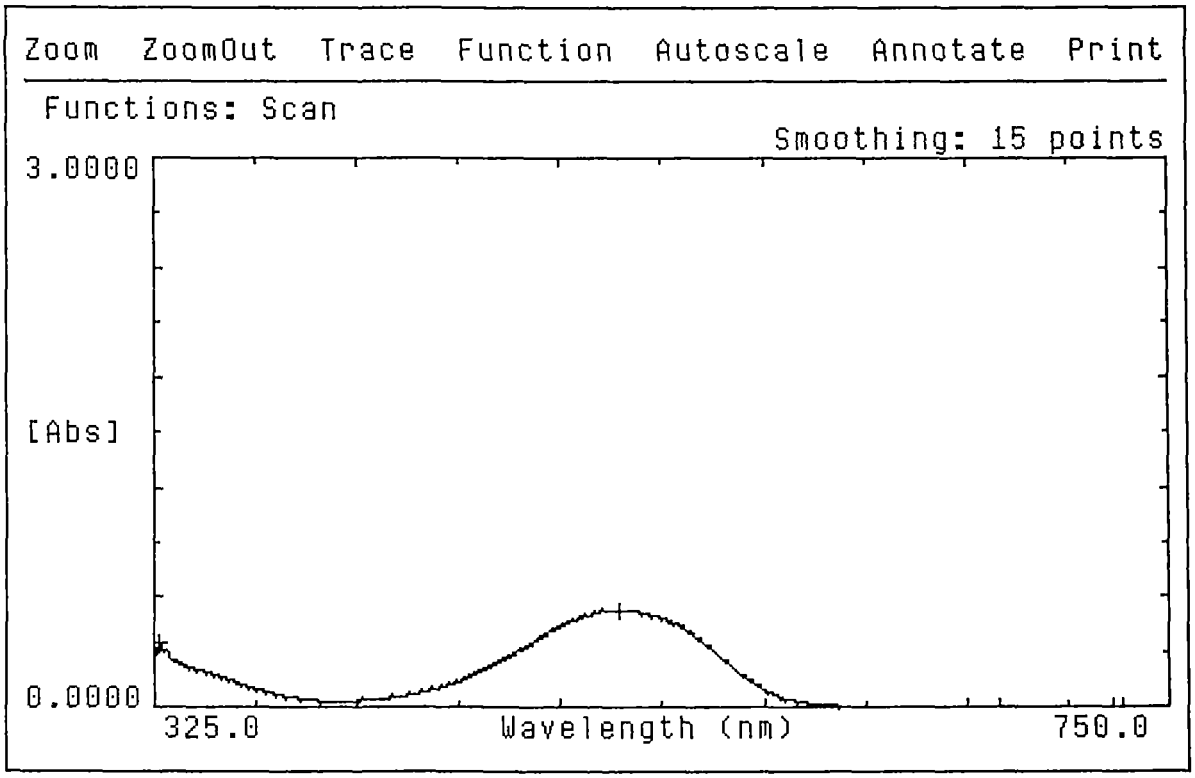

Fig. 3.3 Spectra of methyl red (2.26×10^{-5} mol kg^{-1}) in acidic Calcium nitrate tetrahydrate melt at 25°C.

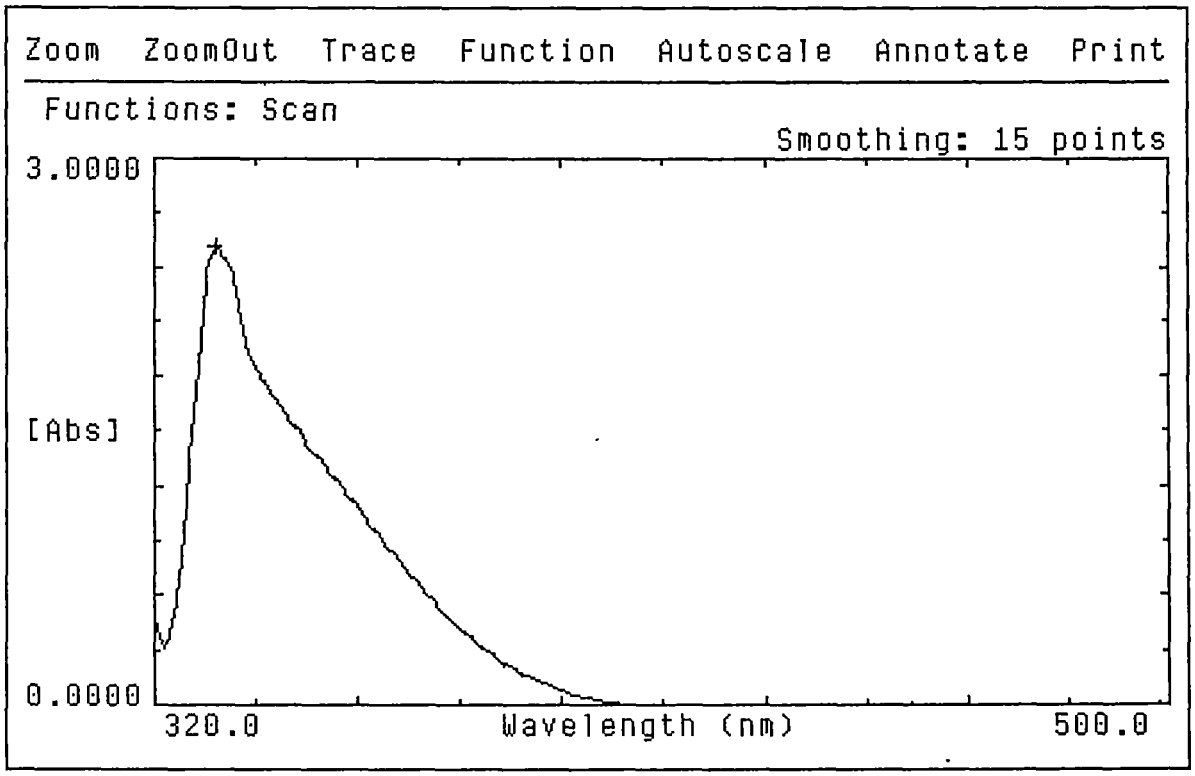

Fig. 3.4 Spectra of p-nitrophenol (1.49×10^{-4} mol kg^{-1}) in neat Calcium nitrate tetrahydrate melt at 25°C.

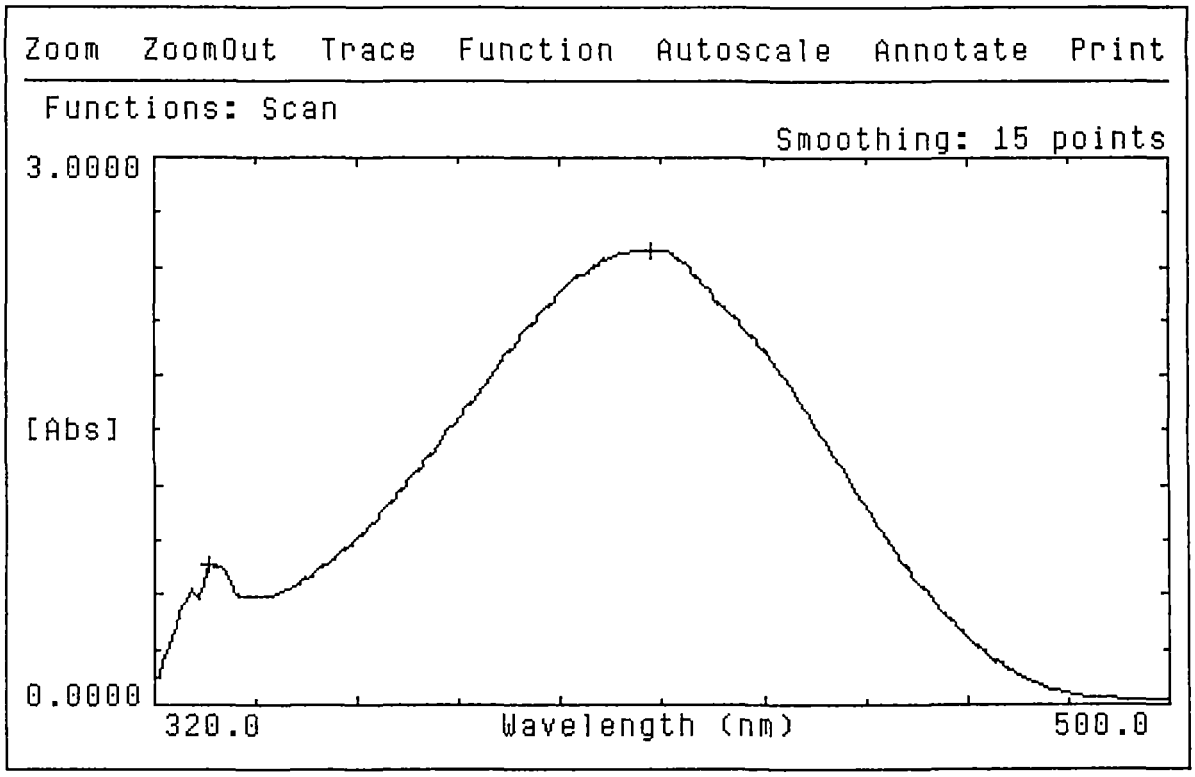

Fig. 3.5 Spectra of p-nitrophenol (1.00×10^{-4} mol kg^{-1}) in basic Calcium nitrate tetrahydrate melt at 25°C.

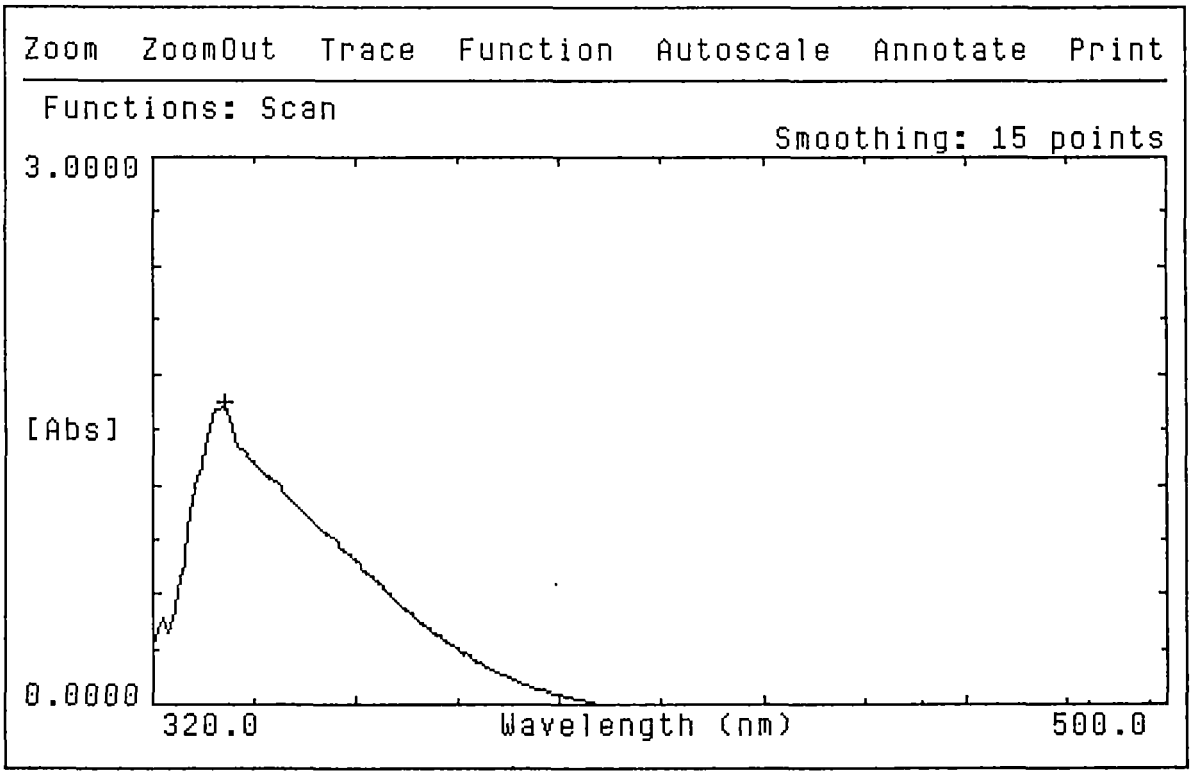

Fig. 3.6 Spectra of p-nitrophenol (1.13×10^{-4} mol kg^{-1}) in acidic Calcium nitrate tetrahydrate melt at 25°C.

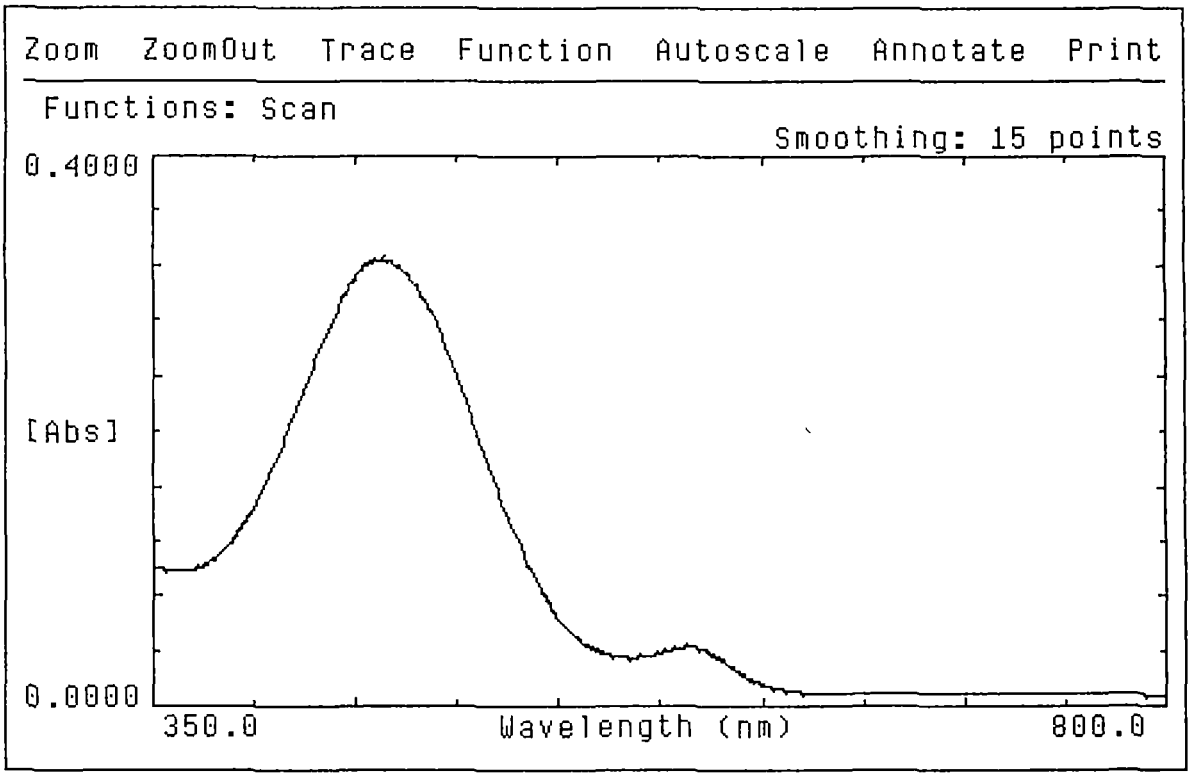

Fig. 3.7 Spectra of bromophenol blue (1.14×10^{-3} mol kg^{-1}) in neat Calcium nitrate tetrahydrate melt at 25°C.

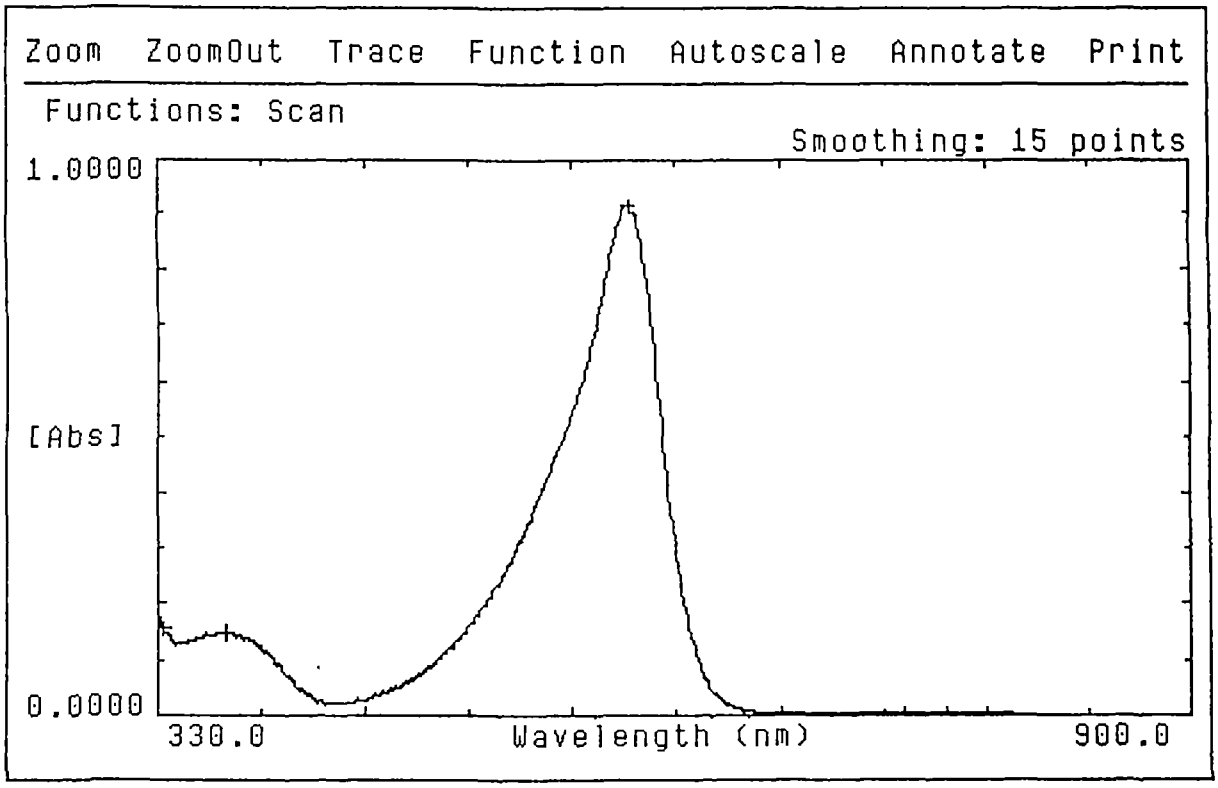

Fig. 3.8 Spectra of bromophenol blue(1.24×10^{-3} mol kg^{-1}) in basic Calcium nitrate tetrahydrate melt at 25°C.

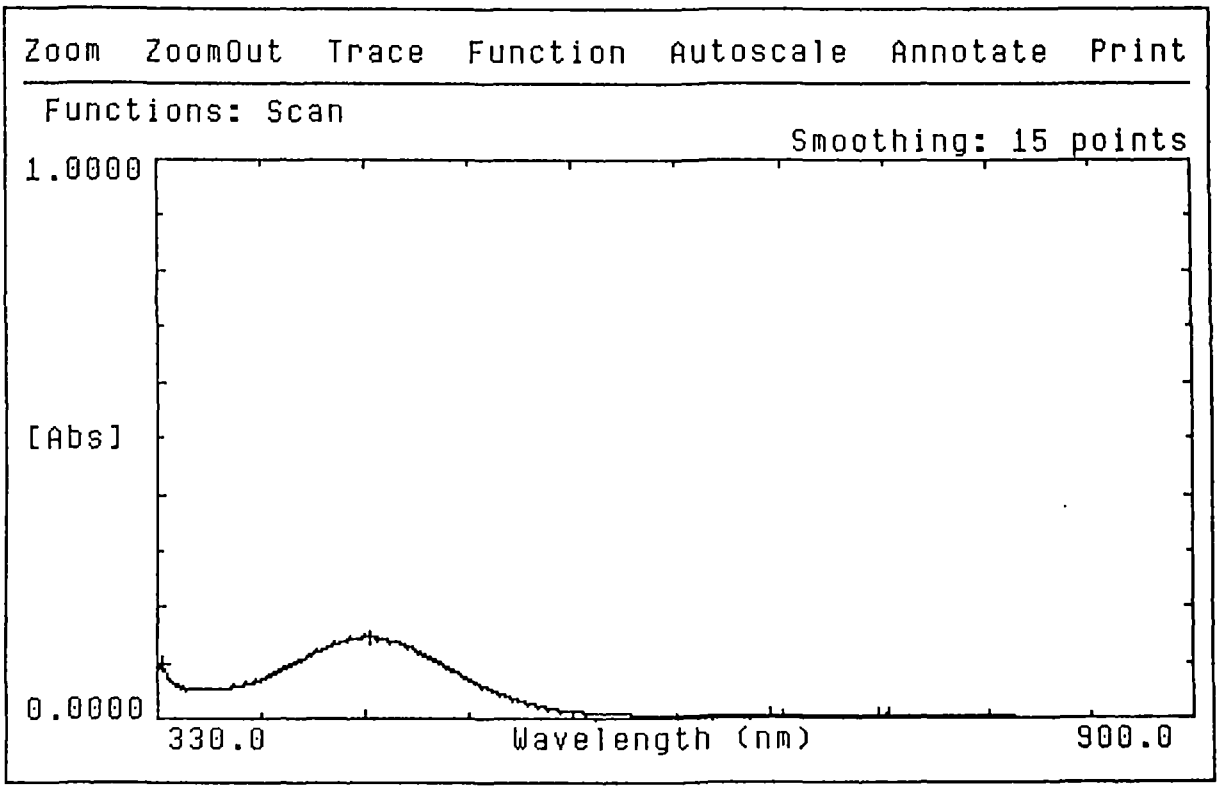

Fig. 3.9 Spectra of bromophenol blue(1.12×10^{-3} mol kg^{-1}) in acidic Calcium nitrate tetrahydrate melt at 25°C.

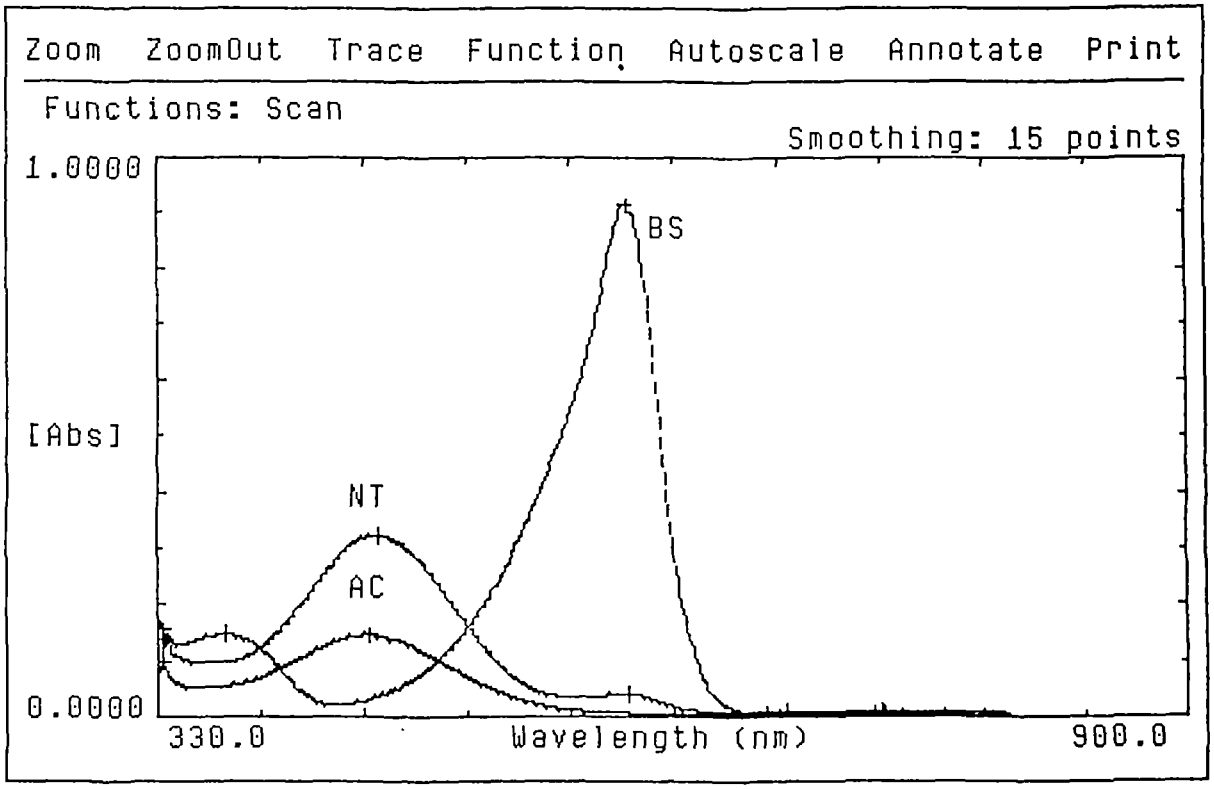

Fig. 3.10 Overlay spectra of bromophenol blue in neat(NT), basic(BS), and acidic(AC) calcium nitrate tetrahydrate melt at 25°C.

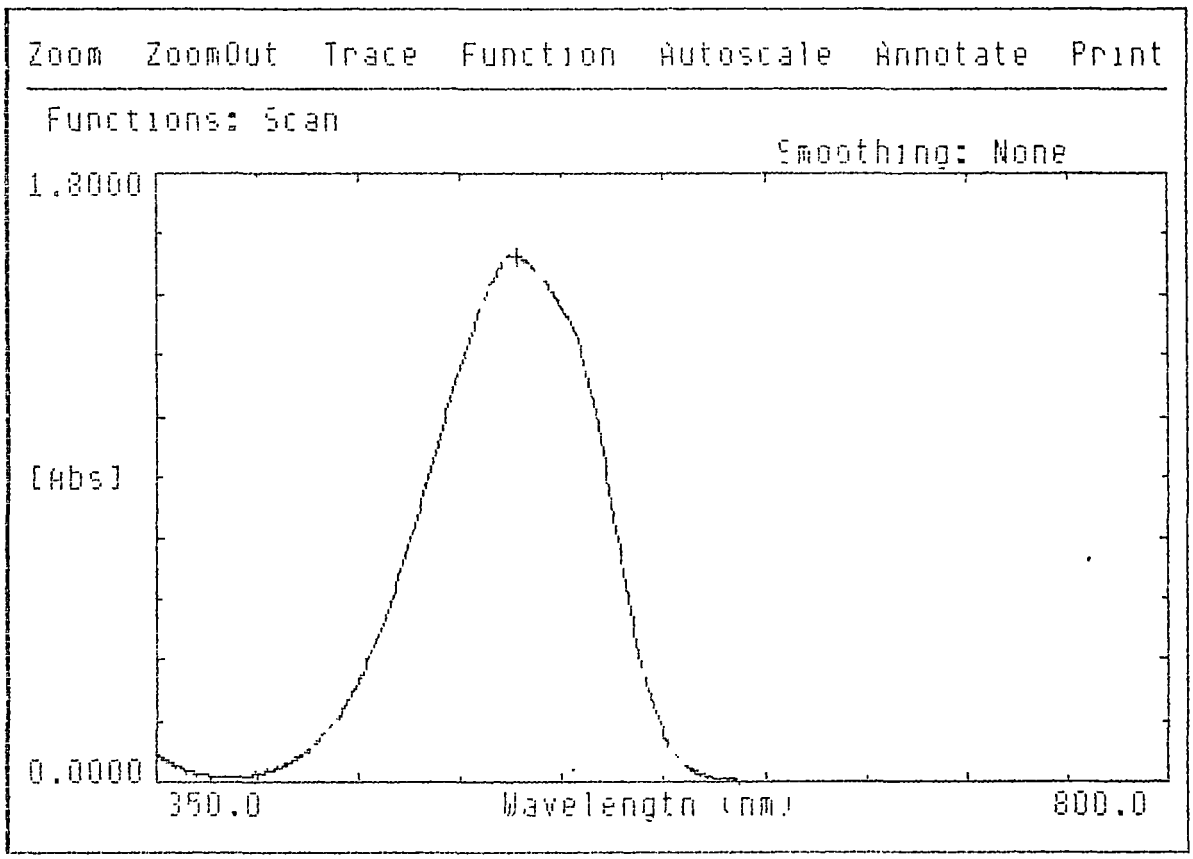

Fig. 3.11 Spectra of methyl orange(2.35×10^{-5} mol kg^{-1}) in neat Calcium nitrate tetrahydrate melt at 25°C.

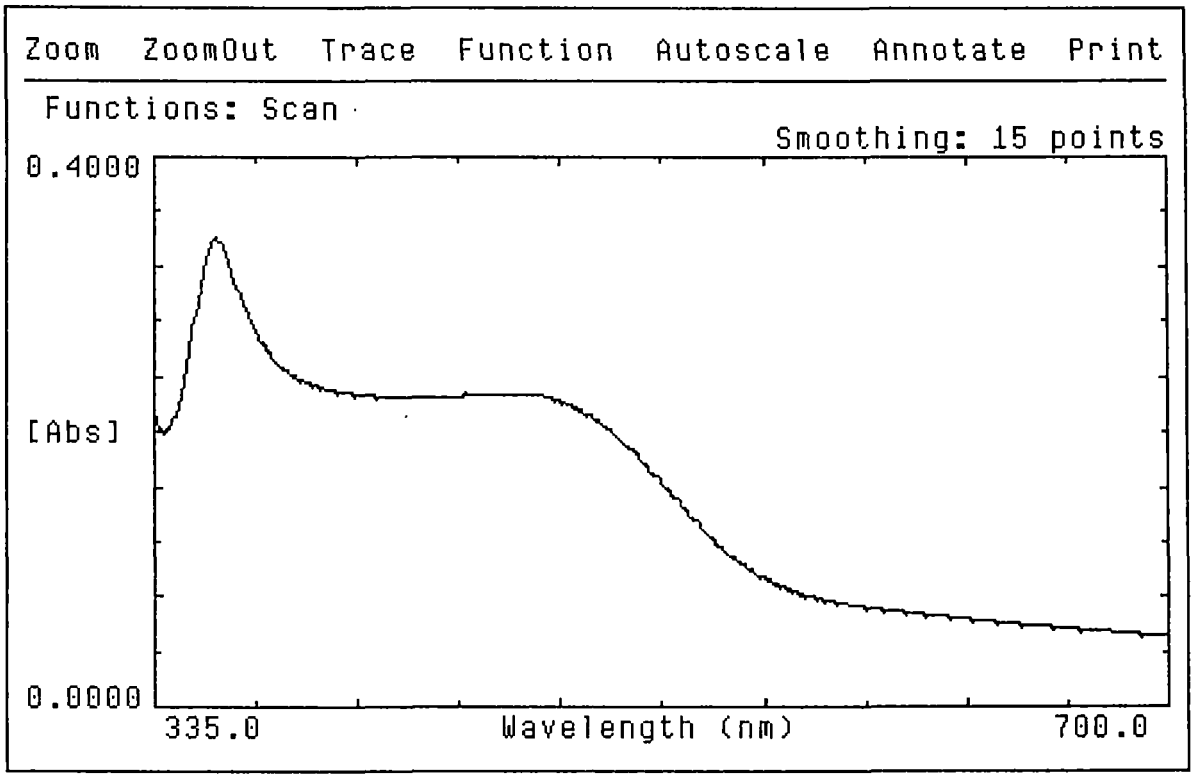

Fig. 3.12 Spectra of methyl orange(5.10×10^{-5} mol kg^{-1}) in basic Calcium nitrate tetrahydrate melt at 25°C.

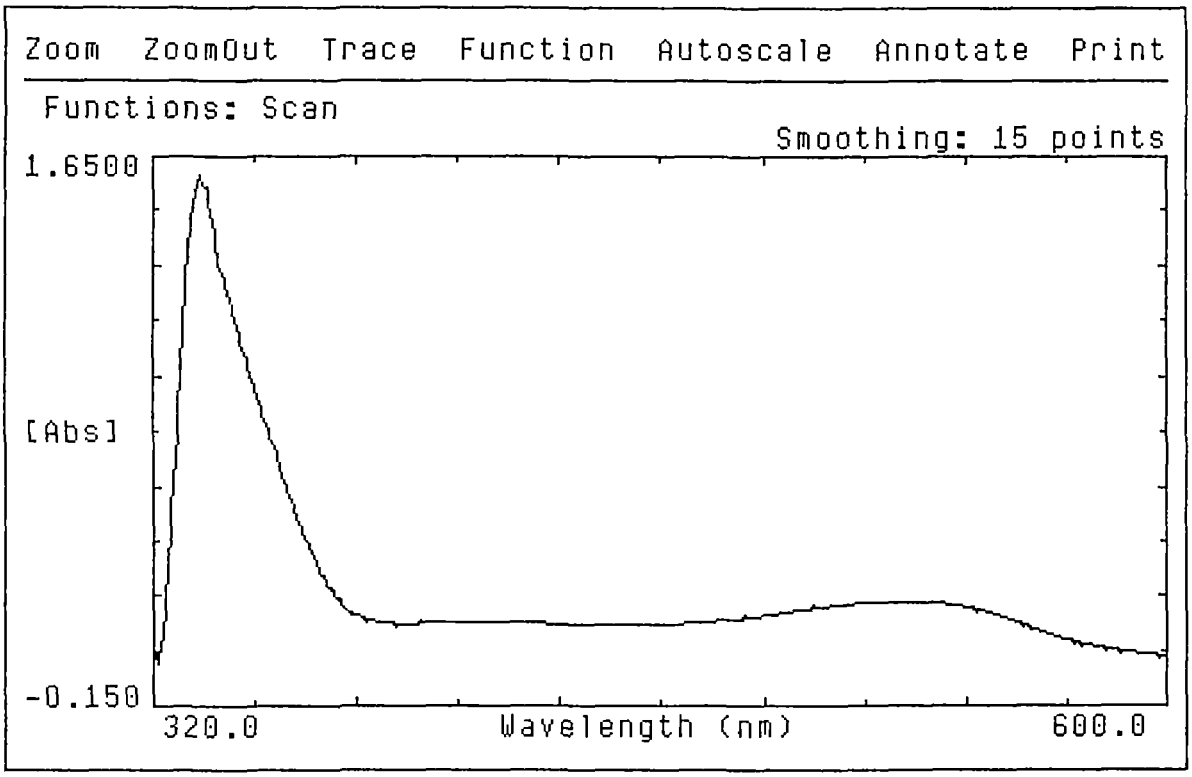

Fig. 3.13 Spectra of methyl orange(9.46×10^{-5} mol kg^{-1}) in acidic Calcium nitrate tetrahydrate melt at 25°C.

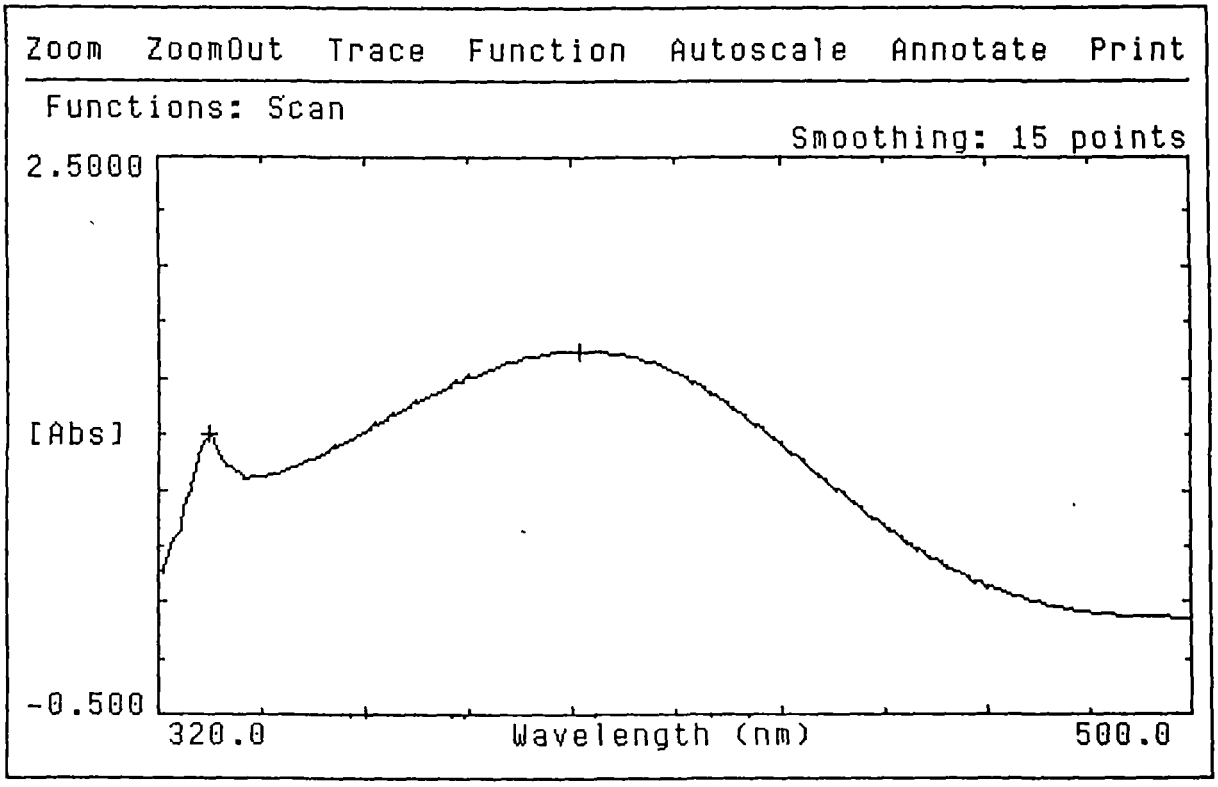

Fig. 3.14 Spectra of p-nitroaniline (9.37×10^{-5} mol kg^{-1}) in neat Calcium nitrate tetrahydrate melt at 25°C.

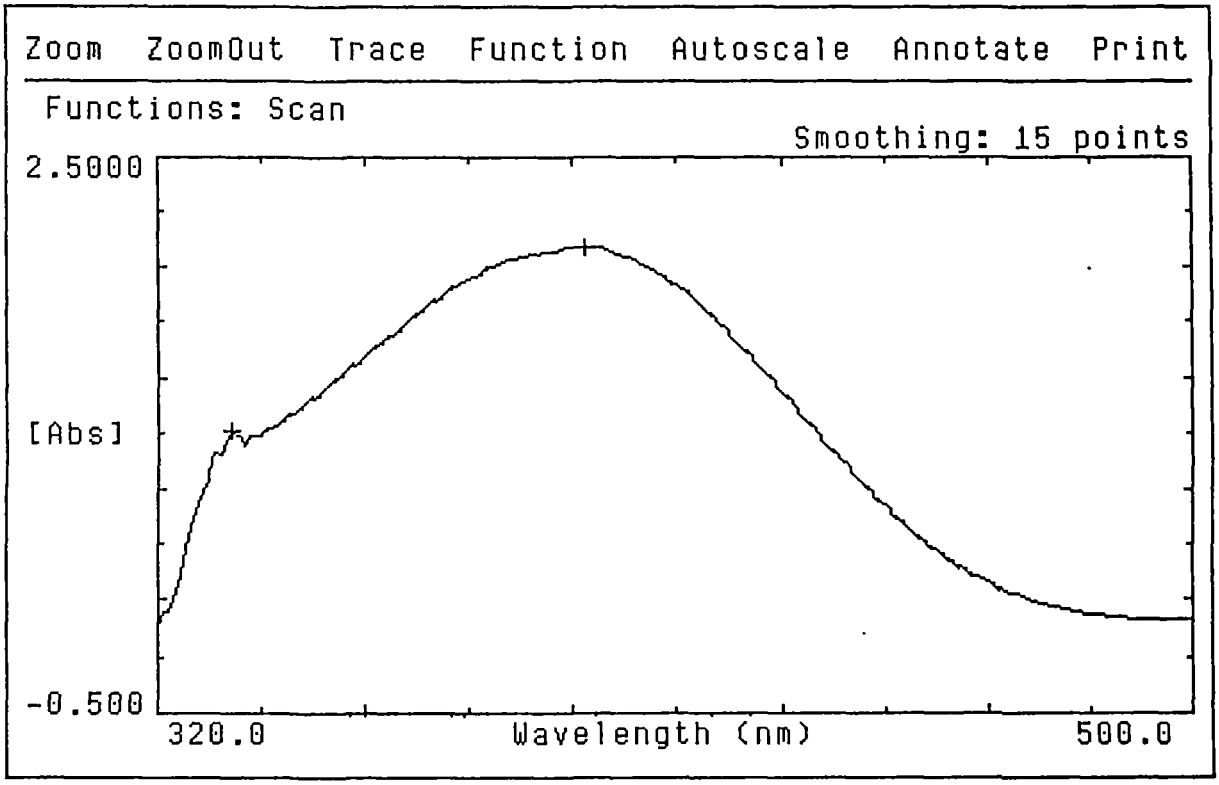

Fig. 3.15 Spectra of p-nitroaniline(1.12×10^{-4} mol kg^{-1}) in basic Calcium nitrate tetrahydrate melt at 25°C.

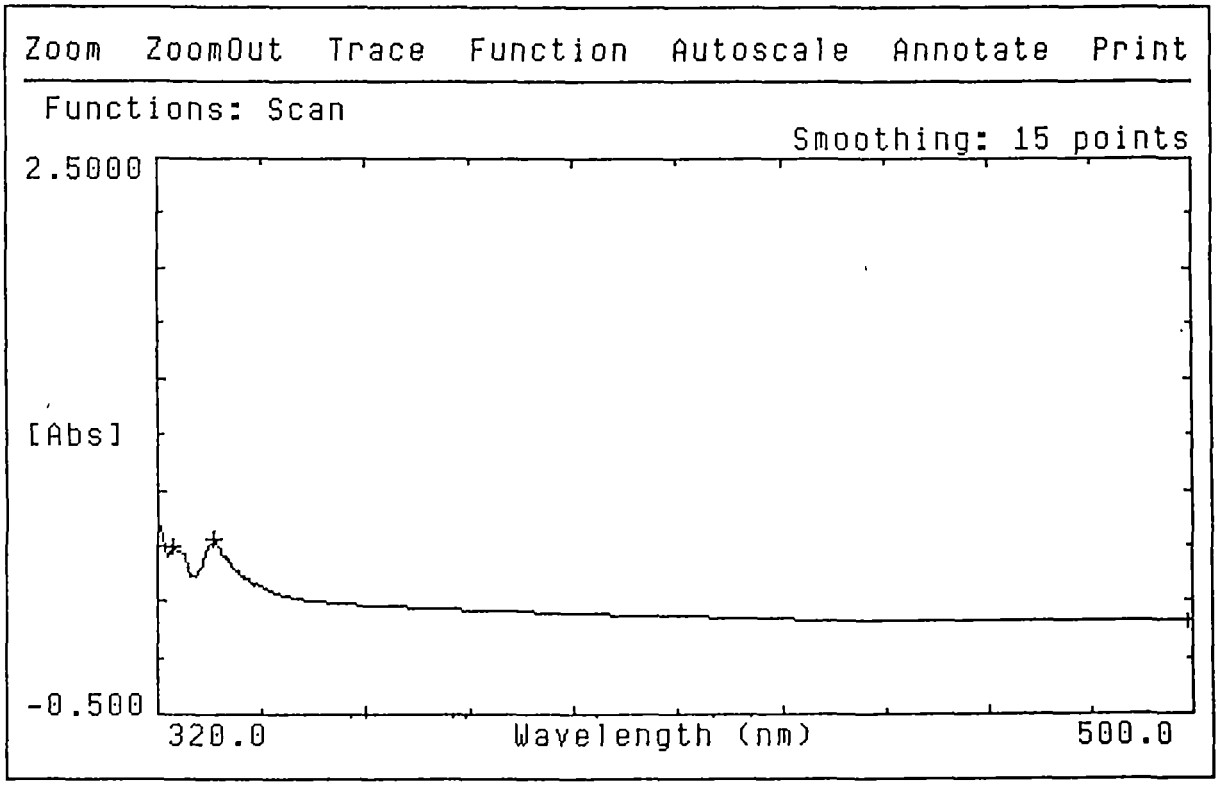

Fig. 3.16 Spectra of p-nitroaniline(1.08×10^{-4} mol kg^{-1}) in acidic Calcium nitrate tetrahydrate melt at 25°C.

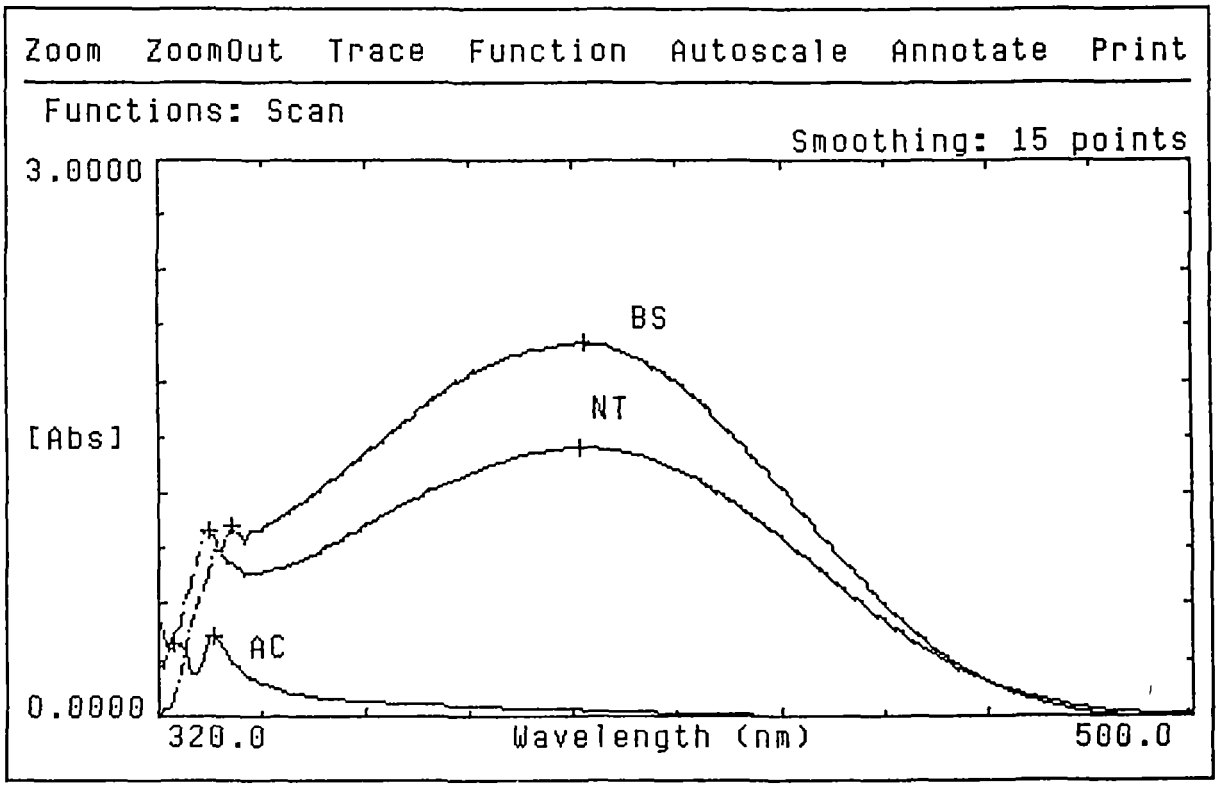

Fig. 3.17 Overlay spectra of p-nitroaniline in neat(NT), basic(BS), and acidic(AC) calcium nitrate tetrahydrate melt at 25°C.

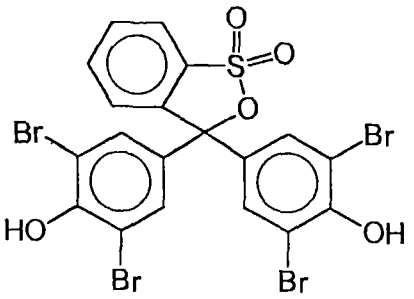

Bromophenol Blue

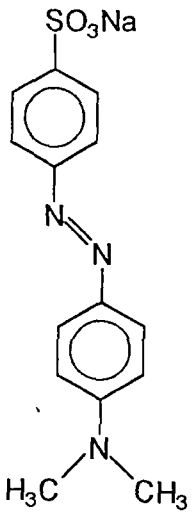

Methyl Orange

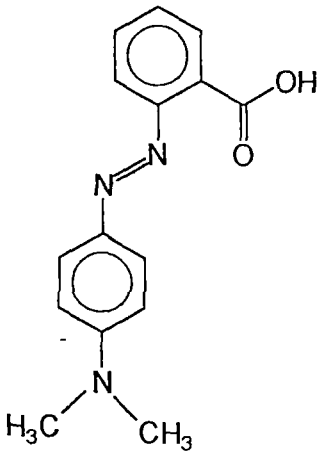

Methyl Red

p-Nitrophenol

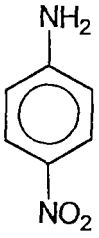

p-Nitroaniline

Fig 3.18 Structures of the indicators used.

References

1. J. A. Duffy and M. D. Ingram, in 'Ionic Liquids', Eds. D. Inman and D. G. Lovering, Plenum Press, New York, **1981**.
2. R. F. Bartholomew and H. M. Garfinkel, J. Inorg. Nucl. Chem., **1969**, 31, 3655.
3. J. Braunstein, in 'Ionic Interactions', Ed. S. Petrucci, Academic Press, New York, **1971**, vol.1.
4. R. D. Dyer III, R. M. Fronko, M. D. Schiavelli, and M. D. Ingram, J. Phys. Chem., **1980,** 84, 2338.
5. J. A. Duffy and M. D. Ingram, Inorg. Chem., **1977,**16, 2988.
6. J. A. Duffy and M. D. Ingram, Inorg. Chem., **1978,**17, 2798.
7. D. H. McDaniel, Inorg. Chem., **1979**, 18, 1412.
8. E. J. Sare, C. T. Moynihan, and C. A. Angell, J. Phys. Chem., **1973,** 77, 1869.
9. J. A. Duffy and M. D. Ingram, J. Am. Chem. Soc., **1971,** 93, 6448.
10. C. H. Rochester, 'Acidity Function', Academic Press, London, **1970**.
11. C. J. Drummond, F. Grieser, and T. W. Healy, J. Chem. Soc. Faraday Trans. 1 , **1989**, 85, 561.
12. A. I. Biggs, Trans . Faraday Soc., **1954**, 50, 800.
13. R. C. Weast, 'Handbook of Chemistry and Physics', CRC Press, Ohio, **1977**, p. C-215.

14. J. Bassett, R. C. Denney, G. H. Jeffery, and J. Mendham, 'Vogel's Textbook of quantitative Inorganic Analysis', ELBS and Longman, London, **1978**, p. 241.

CHAPTER 4

A SPECTRAL STUDY OF THE BEHAVIOUR OF METHYL RED IN ACIDIC CALCIUM NITRATE TETRAHYDRATE MELT

4.1 Introduction

In chapter 3 we recorded the electronic spectra of five different organic indicators in neat, basic and acidic calcium nitrate tetrahydrate (CNTH) melts at 25°C with a view to determine the acidity function of the hydrate melt. While recording such spectra we observed that the absorbance values of protonated indicators in the acidic CNTH melt vary with time thereby envisaging that the indicators take part in some chemical reaction. In the case of methyl red (MR), for instance, it was visually noticed that the red colour of the acidic melt starts disappearing with time. An attempt has therefore been made in this chapter to study the kinetics of the reaction of MR in acidic CNTH melt by recording the time dependent absorption spectra.

4.2 Experimental Section

CNTH (SD, AR grade) and MR (Merck) were used without further purification. Attempts to recrystallize CNTH failed as usual due to its high supercooling tendency. CNTH melt was prepared as described in chapter 3. The solubility of MR in CNTH melt is extremely low. Therefore two different stock solutions of MR were prepared, one in 1:1 mixture of ethanol (Bengal Chemicals) and water (double distilled) and another in acetic acid (BDH, AR grade). The concentrations of these stock solutions of MR in alcohol + water mixture and acetic acid were found to be 1.300×10^{-4} and 8.975×10^{-4} mol kg^{-1}, respectively. The CNTH

melt was made acidic by adding known amount of acetic acid. All solutions were made by weight.

For recording the spectra known amount of the stock solution of MR in either alcohol + water mixture or acetic acid was added to the CNTH melt. In every case, λ_{max} for MR in acidic CNTH melt was determined first. After that using a fresh sample of MR in acidic CNTH melt and fixing the wavelength at λ_{max}, variation of absorbance with time was recorded. The time gap between the addition of the indicator to the melt and the first recording of the absorbance by the spectrophotometer (zero time of absorbance measurement) was noted everytime from which absorbance at the zero time of addition of MR was estimated.

All spectra were recorded at 25°C using Beckmann DU-650 spectrophotometer as described in chapter 3.

4.3 Results and Discussion

Visible spectra obtained by the addition of MR in alcohol + water mixture to acidic CNTH melt is shown in Fig 4.1a. The λ_{max} occurs at 522nm which is comparable to the λ_{max} value reported in water[1] and the same observation was made in the preceding work also (cf. chapter 3). However, the variation of absorbance at 522nm with time, which is shown in Fig 4.1b, is found to be of unusual type. The nature of the kinetics of the reaction of MR in acidic CNTH melt changed further by the addition of more ethanol to the acidic melt as apparent from

the absorbance versus time plot given in Fig 4.2. Furthermore, it was observed that if nitric acid is used instead of acetic acid to make the melt acidic, then the reaction of MR in the presence of ethanol becomes very vigorous and exothermic. It was therefore inferred that the presence of ethanol in acidic CNTH melt affects the kinetics of the reaction which MR undergoes in the melt. Accordingly, an attempt was made to measure the absorbance of MR in acidic CNTH melt as a function of time in the absence of ethanol. For this purpose, the stock solution of MR prepared in acetic acid was used. Visible spectra of MR in acidic CNTH melt recorded after the addition of different amounts of the solution of MR in acetic acid into the melt are shown in Fig 4.3 - 4.7.

In order to understand the kinetics of the reaction of MR in acidic CNTH melt, the values of $\ln(A_0 / A_t)$ are plotted against time in Fig 4.8. Here A_0 is the absorbance of protonated MR at zero time and A_t that at time t. From these plots it is apparent that the reaction of MR in the hydrate melt follows a pseudo - first - order kinetics upto a particular time duration. This time limit of applicability of pseudo - first - order rate expression changes with the change in the amount of acetic acid added to the hydrate melt. The least - squares fitted values of the first - order rate constant, k_1 as a function of acid concentration and the corresponding time duration of applicability of pseudo - first - order rate expression are given in Table 4.1. From Fig 4.8 it is also apparent that above the time limit of applicability of pseudo - first - order rate expression, the value of k_1 tends to decrease for 0.2488 and 0.5352 mol kg^{-1} acetic acid concentrations whereas for the remaining acid concentrations equal to 0.6987, 0.8683, and 1.1077 mol kg^{-1} the value of k_1 seems

to increase. Furthermore, by the addition of acetic acid the rate of reaction of MR increases initially, reaches an optimum value, and then decreases. Such a variation of k_1 with acetic acid concentration is illustrated in Fig 4.9. The decrease in rate of nitration of MR with increase in acetic acid concentration above ~ 0.54 mol kg^{-1} also became obvious by the fact that in CNTH melt containing 1.1077 mol kg^{-1} acetic acid nitration occurred only after a lapse of ~ 150s.

Both in anhydrous nitrate melts and in CNTH melt nitration of organic compounds has been reported[2-5] to take place. The reactive species in these melts is considered to be NO_2^+. NO_2^+ is actually considered to be the species responsible for the nitration of organic materials in nitric acid or in a mixture of nitric and sulfuric acids. The generation of NO_2^+ in CNTH melt may take place according to the following reactions,[4,6]

$$Ca(NO_3)_2.4H_2O \longrightarrow [Ca(H_2O)_4]^{2+} + 2NO_3^- \qquad (4.1)$$

$$[Ca(H_2O)_4]^{2+} \rightleftharpoons [Ca(OH)(H_2O)_3]^+ + H^+ \qquad (4.2)$$

$$CH_3COOH \rightleftharpoons CH_3COO^- + H^+ \qquad (4.3)$$

$$NO_3^- + 2H^+ \rightleftharpoons NO_2^+ + H_2O \qquad (4.4)$$

Topol et al.[2] however could not confirm the existence of NO_2^+ species in anhydrous nitrate melt at 275 - 350°C.Temple and Thickett,[5] on the other hand, reported that in

anhydrous nitrate melts (temperature ≈ 310°C) nitration of aromatic compounds takes place in the vapour phase above the melt and the yield of the product increases by the addition of water into the melt. Consequently it was commented by Temple and Thickett[5] that nitration itself does not offer support to the existence of NO_2^+ in molten salts and suggested that in the vapour phase HNO_3 (g) is probably responsible for nitration. However, in CNTH melt since the temperature of the experiment is 25°C and the vapour pressure is low the above argument of Temple and Thickett[5] may not be applicable and NO_2^+ may still be considered as the species responsible for nitration of MR. Moreover, it was observed that (I) in CNTH melt nitration of MR is extremely slow, (ii) addition of acetic acid increases the rate of nitration, and (iii) addition of nitric acid makes the reaction much faster. These observations can be explained in the light of the equilibrium (4.4) and therefore emphasizes that NO_2^+ is responsible for nitration in CNTH melt. The rate of the nitration can be written as

$$\text{rate} = k' [NO_2^+][MR] \qquad (4.5)$$

In eq (4.5) the rate constant term k' may contain activity coefficients of NO_2^+, MR and transition state complex.[7] Considering the concentration of NO_2^+ to be relatively large in comparison to the low amount of MR taken in the melt, $[NO_2^+]$ may be presumed to remain almost constant initially. With this approximation, eq (4.5) takes the form of a pseudo - first - order rate equation which may be written as

$$\text{rate} = k_1 [MR] \qquad (4.6)$$

where $k_1 = k' [NO_2^+]$. The integrated form of eq (4.6) can easily be written as

$$k_1 = (1/t) \ln (A_0 / A_t) \qquad (4.7)$$

Thus the observed pseudo-first order kinetics of the reaction of MR in acidic CNTH melt at the initial stages of the reaction can be accounted for. A similar pseudo-first-order kinetics is reported[7] to be followed by the nitration reactions of deactivated aromatics in concentrated nitric acid. On continuation of nitration for some time, a considerable decrease in NO_2^+ concentration may occur which may in turn be responsible for the observed decrease in k_1 above the time limits of applicability of eq (4.7) in the case of acidic CNTH melt containing 0.2488 and 0.5352 mol kg^{-1} acetic acid. On the other hand, the initial increase in k_1 caused by the addition of acetic acid into the CNTH melt as shown in Fig 4.9 can be explained in the light of the equilibrium (4.4) as due to the increase in NO_2^+ concentration because of increase in H^+ amount. It may be noted that the dissociation of acetic acid in the hydrate melt given in equilibrium (4.3) can suppress the dissociation equilibrium (4.2). The increase in k_1 by the addition of acetic acid is similar to the reported[7] trend observed on adding small amounts of sulfuric acid during the nitration of deactivated aromatics in concentrated nitric acid. Furthermore, it is interesting to note that in CNTH melt the nature of the dependences of k_1 on acetic acid concentration (Fig 4.9) is similar to such a dependence of rate constant on the per

cent of sulfuric acid reported for the nitration of trimethylanilinium ion, nitrobenzene, and anthraquinone in a mixture of sulfuric and nitric acids.[7] For these three compounds the decrease in rate of nitration above 90% sulfuric acid was attributed to their protonation as well as to media effects like change in dielectric constant. In the present study the decrease in k_1 with increasing acetic acid concentration above ~0.54 mol kg^{-1} acetic acid seems to be attributable only to protonation of MR since it is unlikely that addition of ~1.1 mol kg^{-1} acetic acid to CNTH produces significant change in the media effect on k_1. The reported[1] protonation equilibria of MR are shown in Fig. 4.10. According to this dissociation equilibrium of protonated MR, if nitration of deprotonated species of MR is considered to take place then in the course of reaction more of protons may be expected to be produced in the hydrate melt. This may again cause an increase in the amount of NO_2^+ and may therefore account for the increase in k_1 observed above ~ 800s (Fig. 4.8) particularly in CNTH melt containing higher concentrations of acetic acid. Moreover, in view of the fact that the red colour of the acidic melt containing MR slowly disappears, nitration of the phenyl rings of the MR does not seem to take place. In the light of the above discussion it may be proposed that nitration of azo nitrogen of MR takes place and the probable reaction is given in Fig. 4.11

Table 4.1 Pseudo-First-Order Rate Constants for the Reaction of Methyl Red in Acidic Calcium Nitrate Tetrahydrate Melt

Initial Conc. of MR / mol kg^{-1}	**Acetic acid conc. /mol kg^{-1}**	**kx10^4/s**	**Time duration/s**
1.32 x 10^{-5}	0.2488	4.2233	0 - 400
2.79 x 10^{-5}	0.5352	8.5982	0 - 300
3.61 x 10^{-5}	0.6987	4.5871	0 - 700
4.44 x 10^{-5}	0.8683	4.2974	0 - 750
5.59 x 10^{-5}	1.1077	2.3147	150 - 800

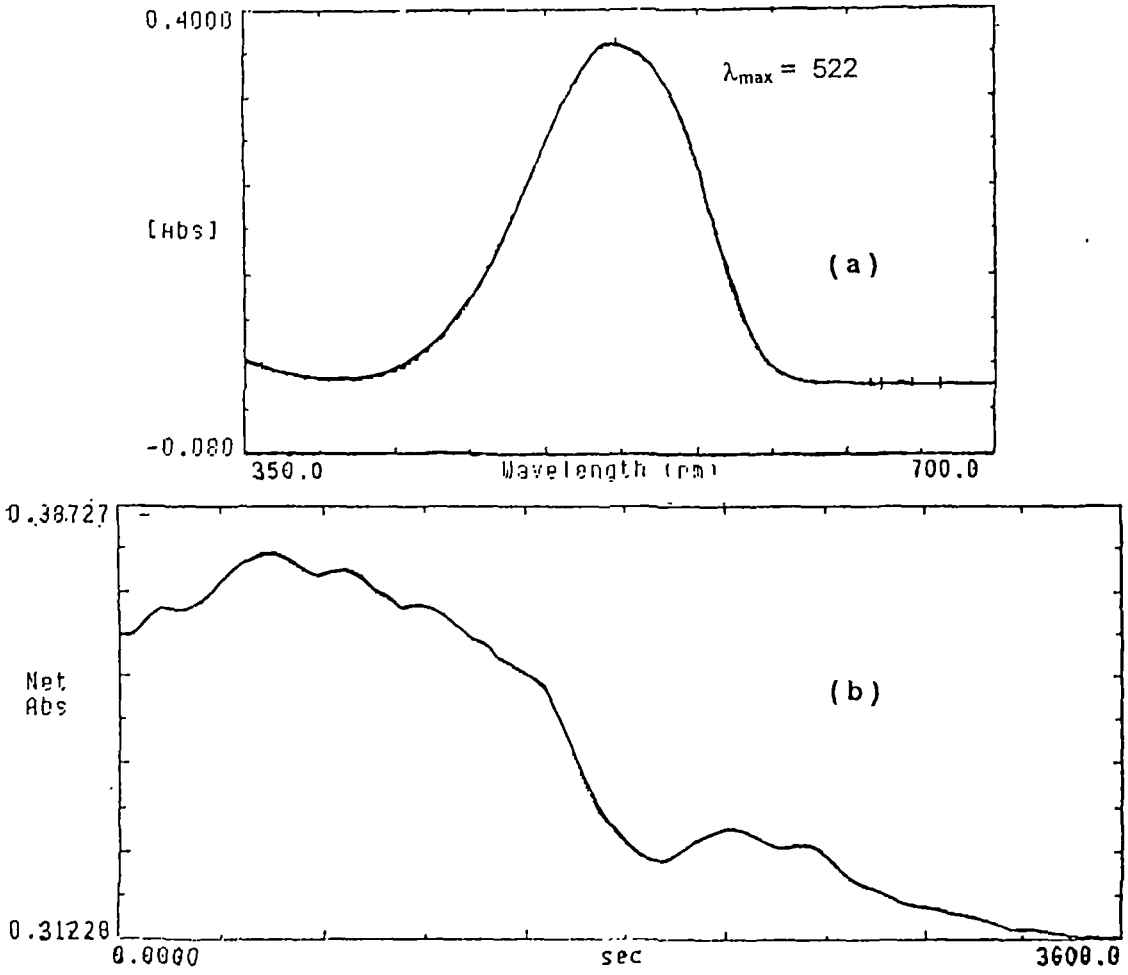

Fig. 4.1: (a) Visible absorption spectrum and (b) plot of absorbance versus time at 522nm for MR (MR dissolved in water + alcohol mixture) in CNTH melt + acetic acid at 25°C (Conc. of MR = 3.79x 10^{-6} mol kg^{-1}, Conc. of acetic acid = 0. 3465 mol kg^{-1}).

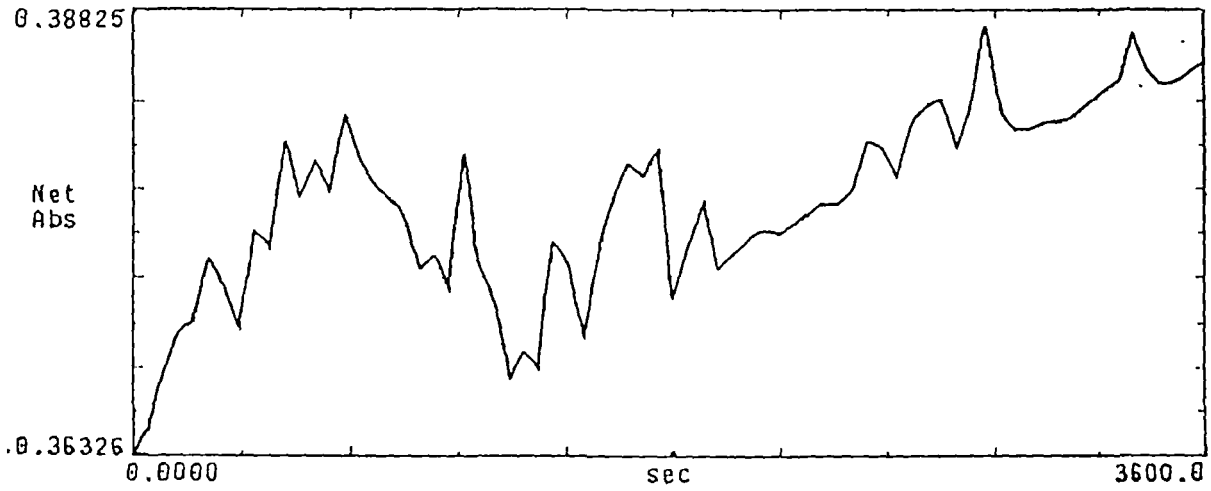

Fig. 4.2: Plot of absorbance versus time at 522nm for MR (MR dissolved in water + alcohol mixture) in CNTH melt + acetic acid + ethanol (0.2 cm^3) at 25°C (Conc. of MR = 4.19x 10^{-6} mol kg^{-1},Conc. of acetic acid = 0.3465 mol kg^{-1}).

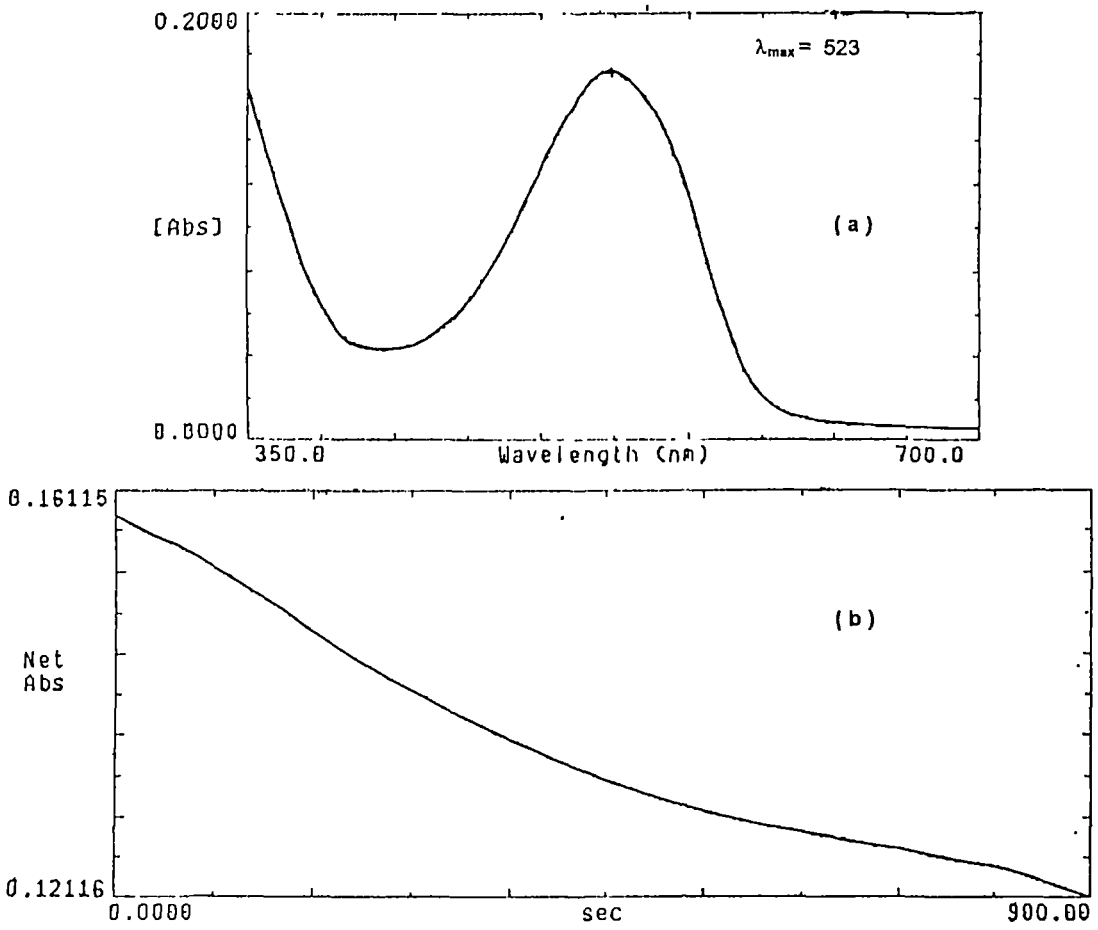

Fig. 4.3: (a) Visible absorption spectrum and (b) plot of absorbance versus time at 523nm for MR (MR dissolved in acetic acid) in CNTH melt + acetic acid at 25°C (Conc. of MR = 1.32×10^{-5} mol kg^{-1}, Conc. of acetic acid = 0. 2488 mol kg^{-1}).

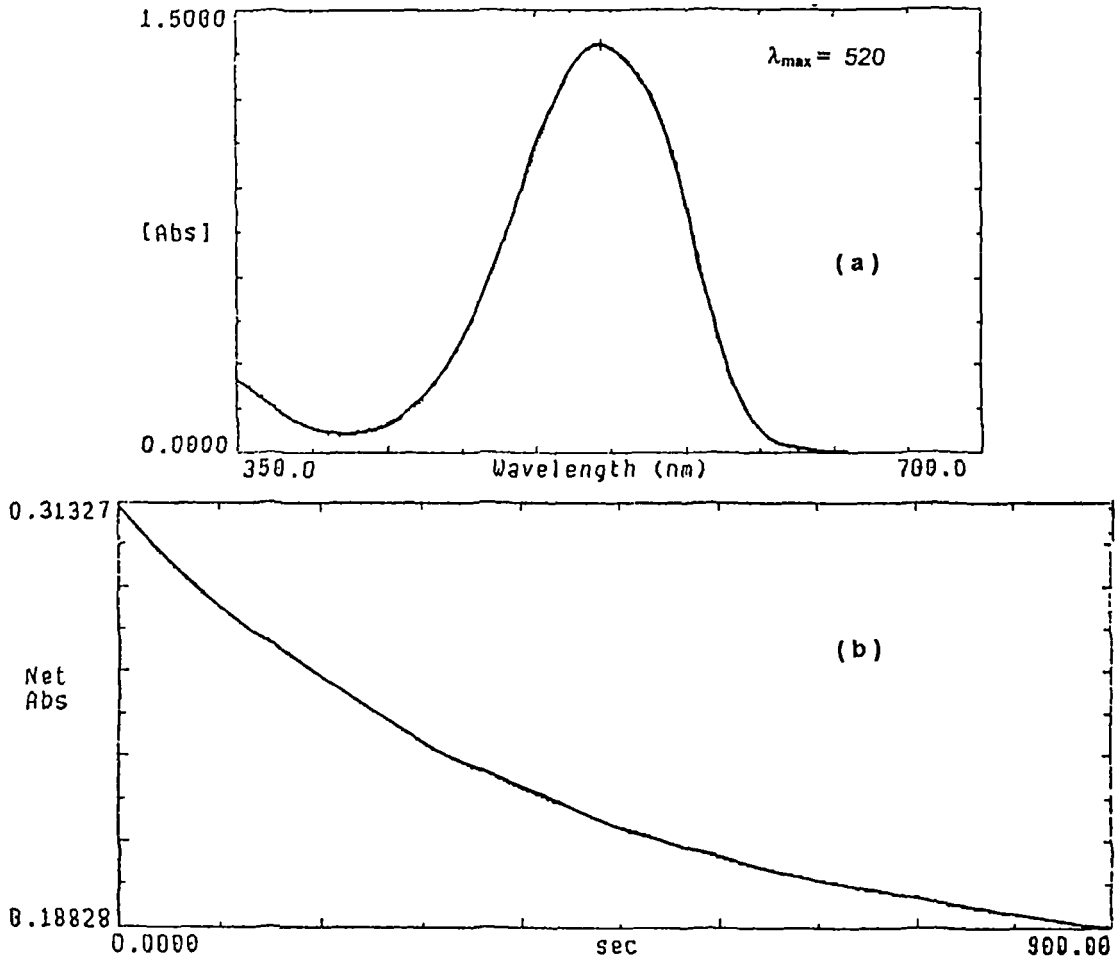

Fig. 4.4: (a) Visible absorption spectrum and (b) plot of absorbance versus time at 520nm for MR (MR dissolved in acetic acid) in CNTH melt + acetic acid at 25°C (Conc. of MR = 2.79x 10^{-6} mol kg^{-1}, Conc. of acetic acid = 0. 5352 mol kg^{-1}).

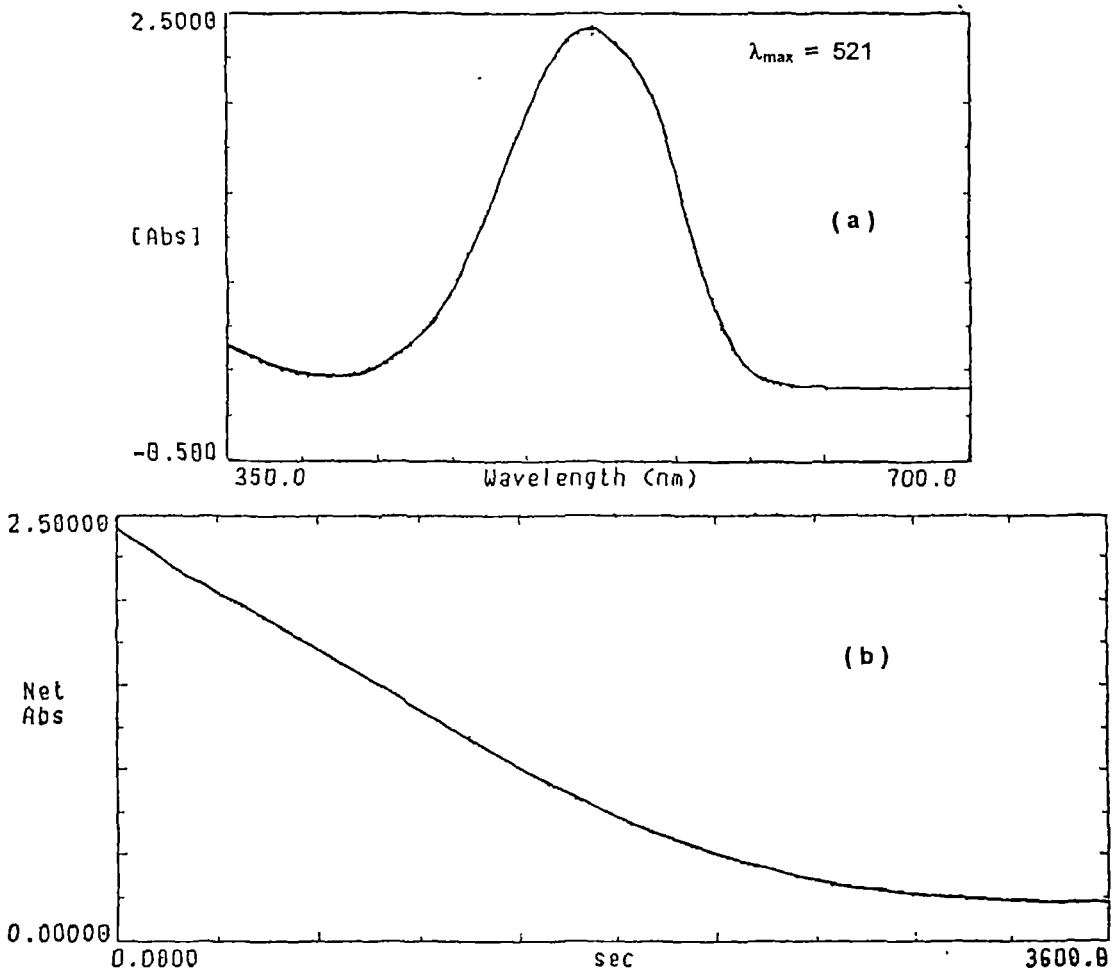

Fig. 4.5: (a) Visible absorption spectrum and (b) plot of absorbance versus time at 521nm for MR (MR dissolved in acetic acid) in CNTH melt + acetic acid at 25°C (Conc. of MR = 3.61×10^{-5} mol kg^{-1}, Conc. of acetic acid = 0. 6987 mol kg^{-1}).

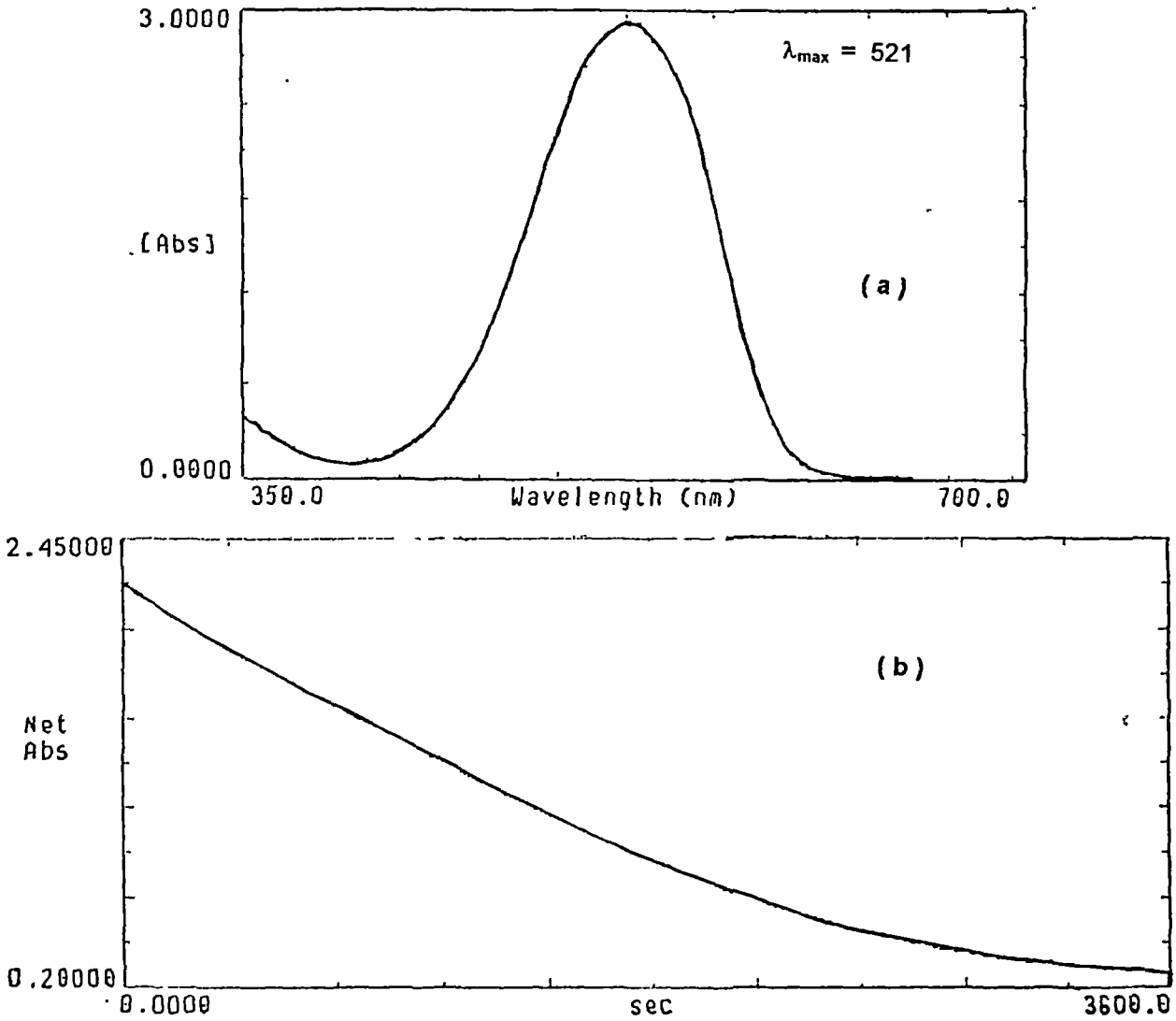

Fig. 4.6: (a) Visible absorption spectrum and (b) plot of absorbance versus time at 521nm for MR (MR dissolved in acetic acid) in CNTH melt + acetic acid at 25°C (Conc. of MR = 4.44x 10^{-5} mol kg^{-1}, Conc. of acetic acid = 0. 8683 mol kg^{-1}).

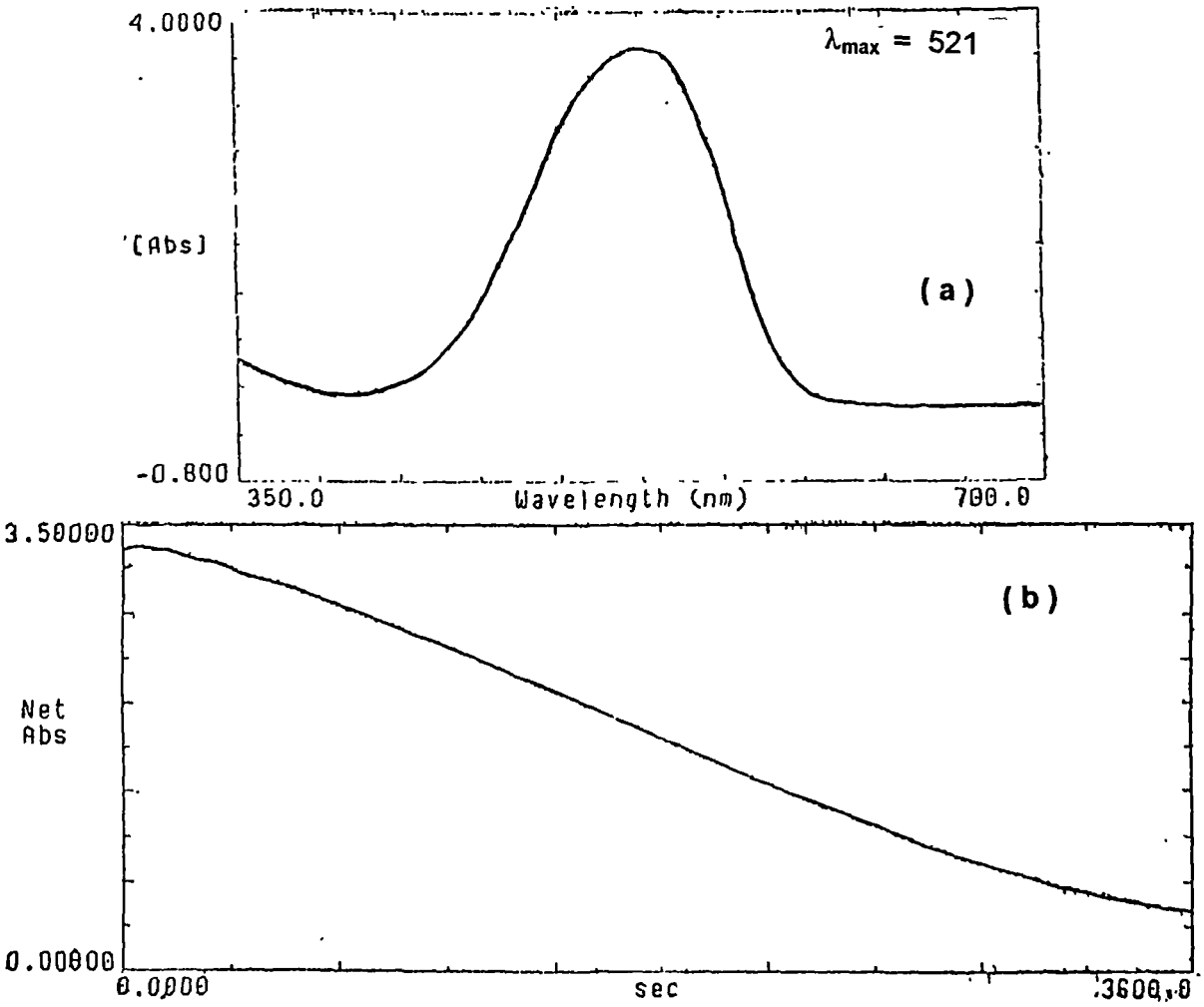

Fig. 4.7: (a) Visible absorption spectrum and (b) plot of absorbance versus time at 521nm for MR (MR dissolved in acetic acid) in CNTH melt + acetic acid at 25°C (Conc. of MR = 5.59x 10^{-6} mol kg^{-1}, Conc. of acetic acid = 1.1077 mol kg^{-1}).

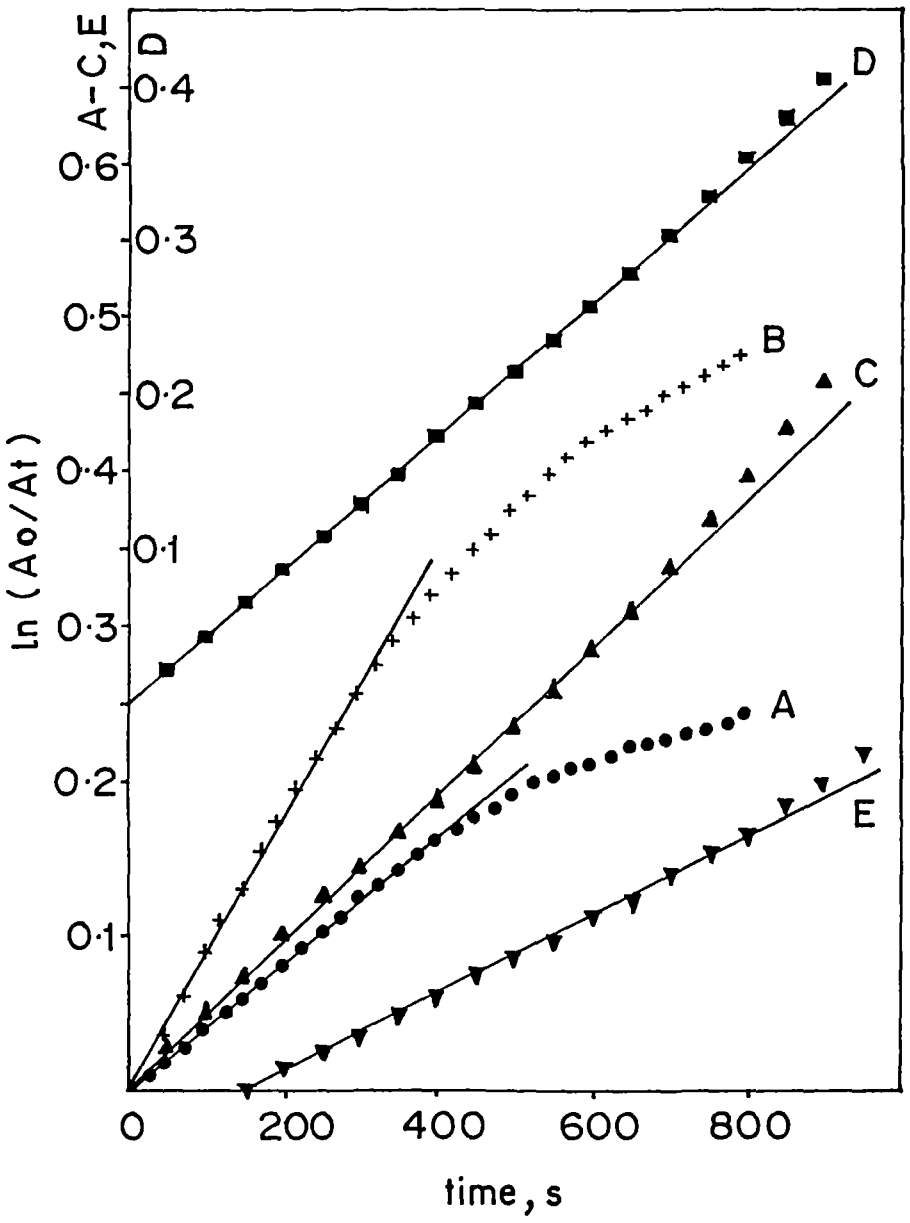

Fig. 4.8: Plot of $\ln(A_0 / A_t)$ versus time for the reaction of MR in acidic CNTH melt at 25^0C.

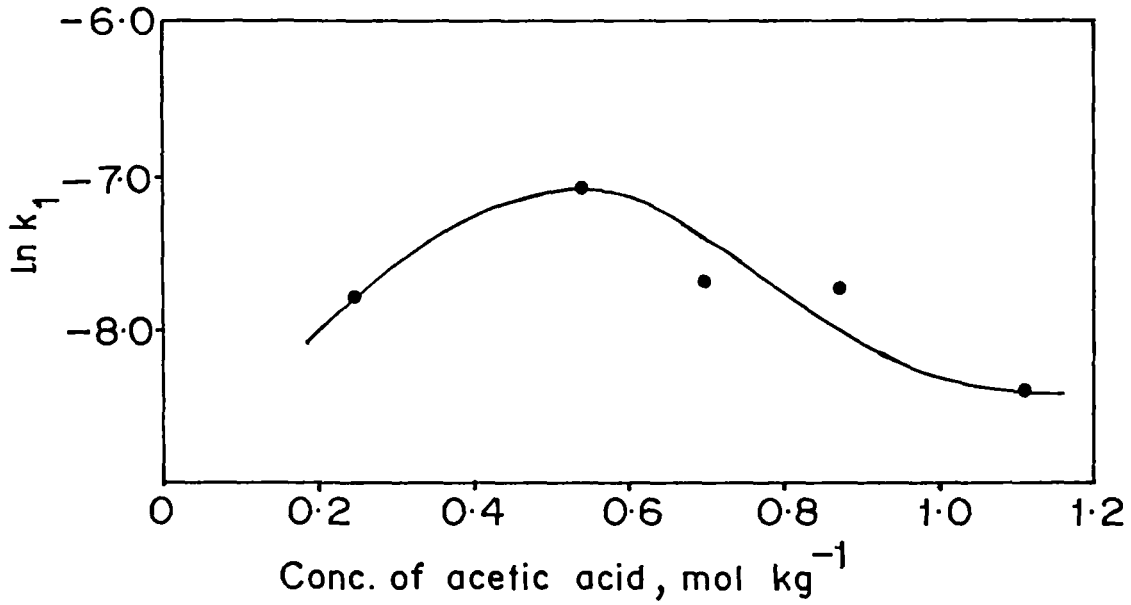

Fig. 4.9: Variation of pseudo-first-order rate constant for the reaction of MR in acidic CNTH melt with acetic acid concentration.

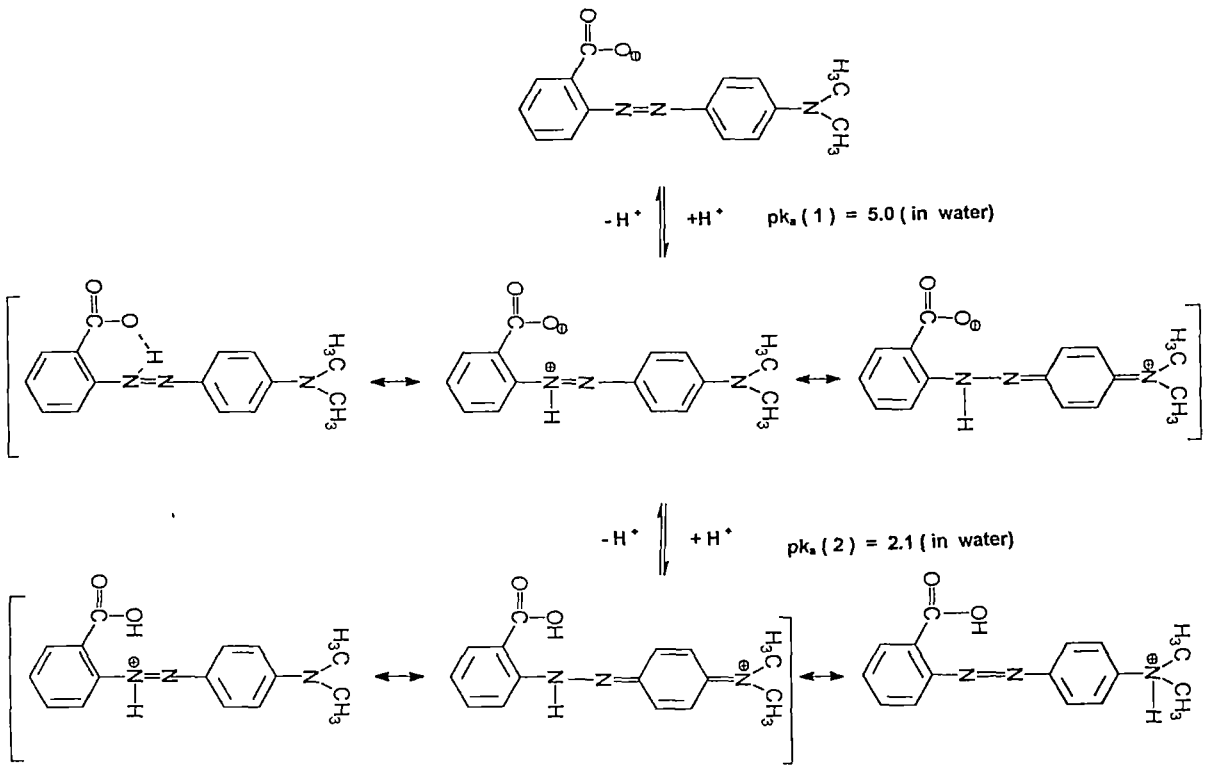

Fig. 4.10. Species considered to be involved in the acid-base equilibria of MR in water . 1a- deprotonated MR, 1b-singly protonated MR, 1c- doubly protonated MR(taken from ref. 1).

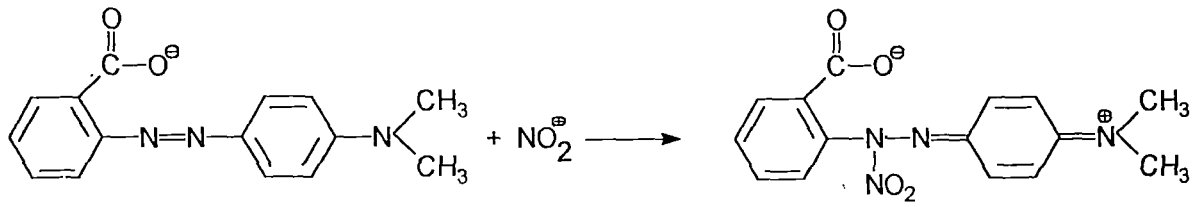

Fig. 4.11. Probable nitrated species of MR.

References

1. C. J. Drummond, F.Grieser, and T. W. Healy, J. Chem. Soc. Faraday Trans. 1, **1989**,85, 561.
2. L. E. Topol, R. A. Osteryoung, and J. H. Christie, J. Phys. Chem., **1966**, 70, 2857.
3. R. B. Temple, C. Fay, and J. Williamson, Chem. Commun., **1967**, 966.
4. R. F. Bartholomew and H. M. Garfinkel, J. Inorg. Nucl. Chem., **1969**, 31, 3655.
5. R. B. Temple and G. W. Thickett, Aust. J. Chem., **1973**, 26, 667.
6. J. A. Duffy and M. D. Ingram, in 'Ionic Liquids', D. Inman and D. G. Lovering, Eds., Plenum Press, New York, **1981**.
7. R. D. Gilliom, 'Introduction to Physical Organic Chemistry', Addison - Wesley Pub. Co., Reading, **1970**, pp. 237 - 241.

CHAPTER 5

VOLUMETRIC AND ELECTRICAL CONDUCTANCE BEHAVIOUR OF CALCIUM NITRATE TETRAHYDRATE+ ACETAMIDE MELT : A ROOM TEMPERATURE MOLTEN SALT SYSTEM

This work has been published in J. Chem. Eng. Data, 1995, 40, 12

5.1 Introduction

In continuation of our study on room temperature molten salt systems containing hydrate melt and organic compounds, we have made in this chapter a study on the volumetric and transport behaviour of a melt containing calcium nitrate tetrahydrate (CNTH) and acetamide by measuring its density and electrical conductivity as a function of temperature and composition . CNTH has been found to have a good solvent property as it can dissolve a variety of inorganic salts.[1-7] Except for a report on the density and viscosity measurement of a melt containing CNTH and urea,[8] to our knowledge no other study has been made on the transport behaviour of room temperature molten salts containing hydrate melt and organic compound. Acetamide melt has attracted the attention of many molten salt chemists because of its ability to act as an excellent polar solvent and to form room temperature molten salts on mixing with inorganic salts (cf. chapter 1).[9-25] Acetamide is found to be readily soluble in CNTH melt. In view of the above considerations , CNTH + acetamide melt was chosen for our present study.

5.2 Experimental Section

CNTH (Merck) was used without further purifications. Acetamide (Thomas Baker) was recrystallized from its solution in ethanol and stored in vacuum desiccator before use.

Accurately weighed amounts of CNTH and acetamide, as required, were taken in several air - tightly capped corning glass sample tubes and heated in the water thermostat at ~ 50°C. The mixtures were heated for several hours with occasional shaking of the sample tube till homogeneous solutions were obtained. These samples were cooled slowly and stored in vacuum desiccators

Density was measured using a pycnometer described in chapter 2. Due to high viscosity of the samples, it was found to be difficult to introduce the sample in the pycnometer with the help of a hypodermic syringe. Therefore, the sample was filled in the pycnometer by applying vacuum. Reproducibility of density data was checked by making duplicate measurements and was found to be within ± 0.1%. After the density measurements were over, the samples were drained out from the pycnometer by applying vacuum again.

Electrical conductivity measurements were made as explained in chapter 2 using Wayne Kerr B905 Automatic Precision Bridge and dip - type cell of cell constant 120.6 m^{-1}.

A thermostated oil bath controlled by a Jumo relay and contact thermometer (description given in chapter 2) was used to regulate the temperature.

5.3 Results and Discussion

With the help of the reported density versus concentration isotherm of the $Ca(NO_3)_2 + H_2O$ system,[26] the actual H_2O/Ca^{2+} mole ratio in the CNTH sample used was estimated to be 4.26 ± 0.01.

The experimental values of density, d, of molten (1-x) $Ca(NO_3)_2.4.26\ H_2O + xCH_3CONH_2$ system, which are given in Table 5.1, vary linearly with temperature, t, and were therefore least-squares fitted to the expression

$$d = a - bt \qquad (5.1)$$

The least-squares fitted values of the constants a and b for the melts of different x are given in Table 5.2. x denotes the mole fraction of acetamide. It has been found that the measured values of density of pure acetamide at 86, 94, and 105°C are higher than the reported values[12] by 0.4, 0.16 and 0.13%, respectively.

Although addition of acetamide to molten CNTH causes the density to decrease nonlinearly, the molar volume V decreases linearly with increasing x at all experimental temperatures. Such a non - linear and linear dependences of d and V, respectively on x are illustrated in Fig 5.1 for two different temperatures. Similar behaviour of d and V was reported in the molten mixture of CNTH and urea also.[8] It may be noted that this type of variation of d and V with the mole fraction of solute is

also a general observation made in molten mixtures consisting of a hydrate melt and an anhydrous inorganic salt.[1,3,27,28] Furthermore, from the linear variation of V with x we obtained, on least - squares fitting, the value 56.90×10^{-6} m^3 mol^{-1} for V of pure acetamide at 25°C. This estimated value of V agrees within 0.63% with its value 56.54×10^{-6} m^3 mol^{-1} obtained from the high - temperature density data of molten CH_3CONH_2 (Table 5.1) indicating thereby additivity of molar volume. In binary mixtures containing hydrate melt and anhydrous inorganic salt, molar volume is reported[28] to be additive if the solute added is not capable of displacing water from the coordinating sphere of the cation of the hydrate melt. In the present system under study the high solubility of acetamide in CNTH may be due to the hydrogen bonding of acetamide with $Ca(H_2O)_4^{2+}$ ions. This type of interaction between hydrate melt and CH_3CONH_2, however, does not appear to cause non - ideality in molar volume. Thus room temperature molten salt systems containing hydrate melt and inorganic or organic solutes appear to behave as an ideal mixture of hydrate melt and hypothetical supercooled liquid solute.

The observation made in the present and previous studies[1,3,8,27,28] regarding the molar volume of binary mixtures consisting of a hydrate melt as one of the components indicates the possibility of employing an alternative method to estimate the densities of high- or low-melting anhydrous inorganic and organic compounds.The proper choice of a hydrate melt as the solvent medium is what is most important in this method. This alternative method will be quite useful to measure indirectly the density of molten salts both above and below (supercooled)

the melting points especially when the salts either decompose on melting or have high melting points.

The experimental values of the specific conductance, k, of (1-x) $Ca(NO_3)_2.4.26$ H_2O + x CH_3CONH_2 melts are given in Table 5.3 as functions of temperature t and x. The variation of the molar conductance, Λ (=kV), with temperature is non-Arrhenius and is illustrated in Fig 5.2. Non - Arrhenius type of temperature dependence of electrical conductivity was also reported[16] for molten mixtures of $LiNO_3$, $NaNO_3$ and NH_4NO_3 with an amide mix consisting of 0.6 mole fraction of acetamide and 0.4 mole fraction of urea. Therefore, molten mixtures containing acetamide behave like fragile liquids. Accordingly the molar conductance data of the present system under study were least - squares fitted to the VTF equation of the form (cf. chapter 1)

$$\Lambda(S\ m^2\ mol^{-1}) = A \exp [-B / (T - T_0)] \qquad (5.2)$$

The significances of A, B and T_0 are explained in chapter 1 and their best - fit values are listed in Table 5.4. The variation of best fit values of the ideal glass transition temperature, T_0 with x does not appear to follow a regular trend. This kind of observation regarding the concentration dependence of T_0 was normally made in molten mixtures containing hydrate melts.[2,3] Under such a condition an alternative least - squares fitting of the conductance (or fluidity) data by keeping the value of B parameter almost constant was suggested.[2] The constancy of B parameter was also explained in the light of the free volume theory.[3] The molar conductance data

were therefore fitted to the VTF eq (5.2) by keeping the value of B ≈ 508 so that the standard deviations of this alternative fit are not very much higher than the corresponding standard deviations for the best - fit. The values of A, B and T_0 obtained thus are listed in Table 5.5. The variation of T_0 with x is shown in Fig 5.3. Up to $x \approx 0.5$ T_0 appears to remain almost constant and in the region $x > 0.5$ T_0 tends to decrease. The value of T_0 computed for $Ca(NO_3)_2.4.26H_2O$ is comparable with the reported values.[2,3,29] By extrapolating T_0 vs. x plot to x = 1, the T_0 of pure acetamide melt can be estimated to be equal to ~ 191 K. The T_0 values of $Ca(NO_3)_2.4.26H_2O$ + acetamide systems are comparable with the reported[8] T_0 values of $Ca(NO_3)_2.4.12H_2O$ + urea system. Experimental glass transition temperatures, T_g, of $Ca(NO_3)_2.4.26H_2O$ + CH_3CONH_2 or of pure CH_3CONH_2 are not available for comparison. An attempt has therefore been made to compare the value T_0 = 201K of $Ca(NO_3)_2.4.26H_2O$ + CH_3CONH_2 system of x =0.775 (from Fig 5.3) with the reported value of T_g = 234K of the eutectic mixture of NaCNS and CH_3CONH_2 having x = 0.775. The value of the ratio $T_g / T_0 \approx 1.16$ obtained from this comparison is comparable to the accepted range of value for T_g / T_0 .[2,30] It may be noted that in the entire composition region (x = 0 to 1) of $Ca(NO_3)_2.4.26H_2O$ + CH_3CONH_2 system, T_0 has an average value equal to 200 ± 9 and therefore the effect of addition of acetamide on T_0 is not very significant. Since no correlation has yet been established between T_0 (orT_g) and the supercooling tendency of a material, it is difficult to comment on whether the supercooling tendency of CNTH has enhanced or diminished by the addition of acetamide.

The variation of specific conductance,k with concentration has been illustrated in Fig 5.3 by plotting k/k_0 versus x, where k_0 is the specific conductance of the hydrate melt . k decreases as the amount of acetamide in the molten mixture increases. What is interesting is that even on adding an anhydrous inorganic salt to the hydrate melt k decreases as illustrated in Fig 5.3 by plotting , on the basis of reported[31] data , k/k_0 for the $Ca(NO_3)_2.4H_2O + KNO_3$ melt versus x of KNO_3 . The dependence of k on concentration is obviously controlled by the concentration of charged species and by the mobility of these charged species which,in turn, is dependent inversely on the viscosity of the medium. A recent study by Mahiuddin[32] on the viscosity of $Ca(NO_3)_2.4.37\ H_2O + CH_3CONH_2$ melt has revealed an overall decrease in the viscosity of the melt on going from pure hydrate melt to pure acetamide . Similarly decrease of viscosity of $Ca(NO_3)_2.4.12H_2O$ melt was reported on the addition of urea.[8] Therefore , the decrease in k caused by the addition of acetamide to CNTH may be due to an effective decrease in the amount of charged species per unit volume . On the other hand, in the case of addition of anhydrous inorganic salt to hydrate melt viscosity generally increases causing the mobility of ions to decrease thereby becoming responsible for the decrease of k. Furthermore, in the present system under study eventhough the viscosity decreases with the addition of acetamide,[32] the mobility of $Ca(H_2O)_4^{2+}$ and NO_3^- ions may still be considered to decrease due to their interaction with acetamide in the light of the ion-acetamide interactions reported in $Ca(NO_3)_2 + CH_3CONH_2$ and NaCNS + CH_3CONH_2 eutectic mixtures.[14,15,23,25] In NaCNS +CH_3CONH_2 eutectic mixture a polymeric structure is reported to exist due to the sodium ion- acetamide interaction.[15] However, in the present system under investigation polymeric

structure formation through ion-acetamide interaction may be unlikely since such a structure formation must cause a sharp increase of viscosity on the addition of acetamide.

. Table5.1: Experimental Values of the Density, d, of (1 - x) $Ca(NO_3)_2.4.26H_2O$ + x CH_3CONH_2 Melts

t/°C	10^{-3}d/kg m^{-3}	t/°C	10^{-3}d/kg m^{-3}	t/°C	10^{-3}d/kg m^{-3}
x = 0.0		**x = 0.111**		**x = 0.300**	
26.1	1.7283	33.6	1.6952	34.6	1.6193
30.0	1.7248	37.4	1.6918	38.4	1.6161
34.0	1.7214	41.2	1.6889	42.2	1.6127
37.9	1.7177	45.0	1.6857	45.9	1.6096
41.8	1.7145	48.7	1.6825	49.6	1.6067
45.6	1.7114	52.4	1.6794	53.2	1.6035
49.4	1.7079	56.0	1 .6762	57.0	1.6004
53.2	1.7047	59.8	1.6728	60.7	1.5975
57.1	1.7016	63.7	1.6697	64.5	1.5942
61.0	1.6981	67.6	1.6665	68.3	1.5914
65.0	1.6951	71.5	1.6633	71.9	1.5883
68.8	1.6918	75.4	1.6601	75.6	1.5855
72.7	1.6888	79.3	1.6569	79.3	1.5825
76.5	1.6856	83.1	1.6538	82.9	1.5796
80.4	1.6825	86.9	1.6507	86.6	1.5766

Table 5.1 continued

t/°C	10^{-3}d/kg m^{-3}	t/°C	t/°C	10^{-3}d/kg m^{-3}
x = 0.0		**x = 0.111**		**x = 0.300**
84.3	1.6793	90.6	90.4	1.5736
88.2	1.6761	94.4	94.1	1.5704
92.1	1.6728	98.2	97.9	1.5675
96.0	1.6696			
99.9	1.6664			

Table 5.1 continued

t/°C	10^{-3}d/kg m^{-3}	t/°C	10^{-3}d/kg m^{-3}	t/°C	10^{-3}d/kg m^{-3}
x =0.401		**x = 0.597**		**x = 0.801**	
21.7	1.5883	23.3	1.4704	24.5	1.2987
25.3	1.5851	26.4	1.4680	27.6	1.2964
28.8	1.5826	30.1	1.4648	30.7	1.2938
32.4	1.5791	33.8	1.4617	33.9	1.2912
36.4	1.5757	37.3	1.4586	37.1	1.2885
40.3	1.5724	40.5	1.4560	40.2	1.2860
44.2	1.5697	43.9	1.4531	43.4	1.2837
47.4	1.5665	47.4	1.4502	46.5	1.2811
51.1	1.5634	50.9	1.4471	49.6	1.2727
54.7	1.5601	54.2	1.4444	52.6	1.2764
62.0	1.5543	57.6	1.4418	55.8	1.2737
65.5	1.5512	61.0	1.4389	59.0	1.2715
69.0	1.5482	64.5	1.4361	62.1	1.2690
72.7	1.5454	67.9	1.4335	65.2	1.2668
76.2	1.5422	71.3	1.4306	68.3	1.2644
79.9	1.5395	74.7	1.4281	71.4	1.2620

Table 5.1 continued

t/°C	10^{-3}d/kg m^{-3}	t/°C	10^{-3}d/kg m^{-3}	t/°C	10^{-3}d/kg m^{-3}
x =0.401		**x = 0.597**		**x = 0.801**	
83.6	1.5365	78.1	1.4252	74.4	1.2596
87.3	1.5338	81.5	1.4227	77.4	1.2573
91.0	1.5309	84.9	1.4201	80.3	1.2547
94.5	1.5280	88.2	1.4174	83.3	1.2524
98.2	1.5251	91.5	1.4147	86.3	1.2500
		94.9	1.4121	89.5	1.2476
		98.3	1.4092	92.5	1.2452
				95.6	1.2428
				98.6	1.2405

Table 5.1 continued

t/°C	10^{-3}d/kg m^{-3}	t/°C	10^{-3}d/kg m^{-3}	t/°C	10^{-3}d/kg m^{-3}
x =0.900		x =0.900		x = 1.0	
25.7	1.1779	74.7	1.1401	58.3	1.0163
28.7	1.1756	77.6	1.1379	60.8	1.0148
31.7	1.1732	80.4	1.1358	63.1	1.0125
34.6	1.1707	83.2	1.1336	65.5	1.0107
37.5	1.1685	86.0	1.1314	67.9	1.0088
40.4	1.1664	88.9	1.1293	70.2	1.0069
43.4	1.1641	91.7	1.1271	72.4	1.0050
46.3	1.1618	94.4	1.1250	74.9	1.0031
49.3	1.1598	97.2	1.1229	77.3	1.0012
52.2	1.1574	100.0	1.1206	79.5	0.9993
55.2	1.1553			81.9	0.9975
58.1	1.1530			84.1	0.9956
61.0	1.1510			86.3	0.9938
63.9	1.1489				
66.7	1.1467				
69.3	1.1446				
71.9	1.1424				

Table5.2: Parameters of Eq 1 for [(1 - x) $Ca(NO_3)_2.4.26H_2O$ + x CH_3CONH_2]Melts

x	10^{-3}a/kg m^3	b/kg m^{-3} $°C^{-1}$	Correlation coefficient	Standard deviation in d/kg m^{-3}
0.0	1.7495	0.8340	-0.9999	0.2766
0.111	1.7231	0.8349	-0.9999	0.1490
0.300	1.6471	0.8152	-0.9999	0.1862
0.401	1.6059	0.8291	-0.9998	0.3527
0.597	1.4890	0.8140	-0.9999	0.2963
0.801	1.3177	0.7838	-0.9999	0.1614
0.900	1.1978	0.7678	-0.9999	0.3005
1.0	1.0637	0.8094	-0.9998	0.1212

Table 5.3 : Specific Conductance k of [(1-x) $Ca(NO_3)_2.4.26H_2O$ + xCH_3CONH_2] Melts

t/°C	10 k/S m^{-1}						
	x = 0.0	x = 0.111	x = 0.300	x = 0.401	x = 0.597	x = 0.801	x = 0.900
25.0	5.9193	4.3714	4.3976	4.0483	3.6102	3.1513	2.9369
30.0	7.8255	5.8092	5.8073	5.3603	4.7237	4.0049	3.6767
35.0	10.098	7.5614	7.5120	6.9007	6.0157	5.0137	4.5687
40.0	12.757	9.5763	9.3146	8.7540	7.4927	6.1350	5.5477
45.0	15.799	12.022	11.636	10.882	9.1748	7.4288	6.6426
50.0	19.095	14.654	14.200	13.098	10.915	8.8371	7.8279
55.0	22.854	17.661	16.870	15.724	13.296	10.365	9.1410
60.0	26.813	20.823	19.906	18.495	15.441	11.964	10.477
65.0	31.101	24.263	22.955	21.533	18.018	13.707	11.950
70.0	35.692	28.080	26.388	24.794	20.695	15.576	13.520
75.0	40.424	32.183	29.930	28.313	23.446	17.469	15.120
80.0	45.419	36.370	33.906	31.948	26.352	19.470	16.776
85.0	50.725	40.929	37.869	35.827	29.380	21.504	18.490
90.0	56.088	45.406	41.628	39.646	32.441	23.602	20.250
95.0	61.495	53.539	45.973	43.729	35.397	25.795	22.102
100.0	67.295	58.614	49.748	47.949	38.904	28.038	23.932

Table 5.4 : Best-Fit Values of Eq.(5.2) for (1-x) $Ca(NO_3)_2.4.26H_2O$ + xCH_3CONH_2 Melts and Standard Deviation (σ), in $\ln\Lambda$

x	-lnA	B	T_0/K	σ
0.0	4.0597	470.5	210.4	0.0028
0.111	3.5940	639.4	195.0	0.0135
0.300	4.4613	491.2	208.2	0.0076
0.401	4.4384	524.1	205.1	0.0028
0.597	4.7963	535.9	201.6	0.0071
0.801	5.5399	501.8	200.6	0.0029
0.900	5.9671	469.3	202.5	0.0156

Table 5.5 : Least-Squares Fitted Values of Eq.(5.2) for (1-x) $Ca(NO_3)_2.4.26H_2O$ + xCH_3CONH_2 Melts Selected to Give Almost Constant B Values and Standard Deviation (σ), in $\ln\Lambda$

x	-lnA	B	T_0/K	σ
0.0	3.9065	508.0	206.0	0.0055
0.111	4.0993	509.4	209.0	0.0195
0.300	4.3632	508.0	206.2	0.0078
0.401	4.5001	508.7	207.0	0.0033
0.597	4.9060	507.9	205.0	0.0078
0.801	5.5175	507.6	200.0	0.0030
0.900	5.8199	507.9	197.5	0.0161

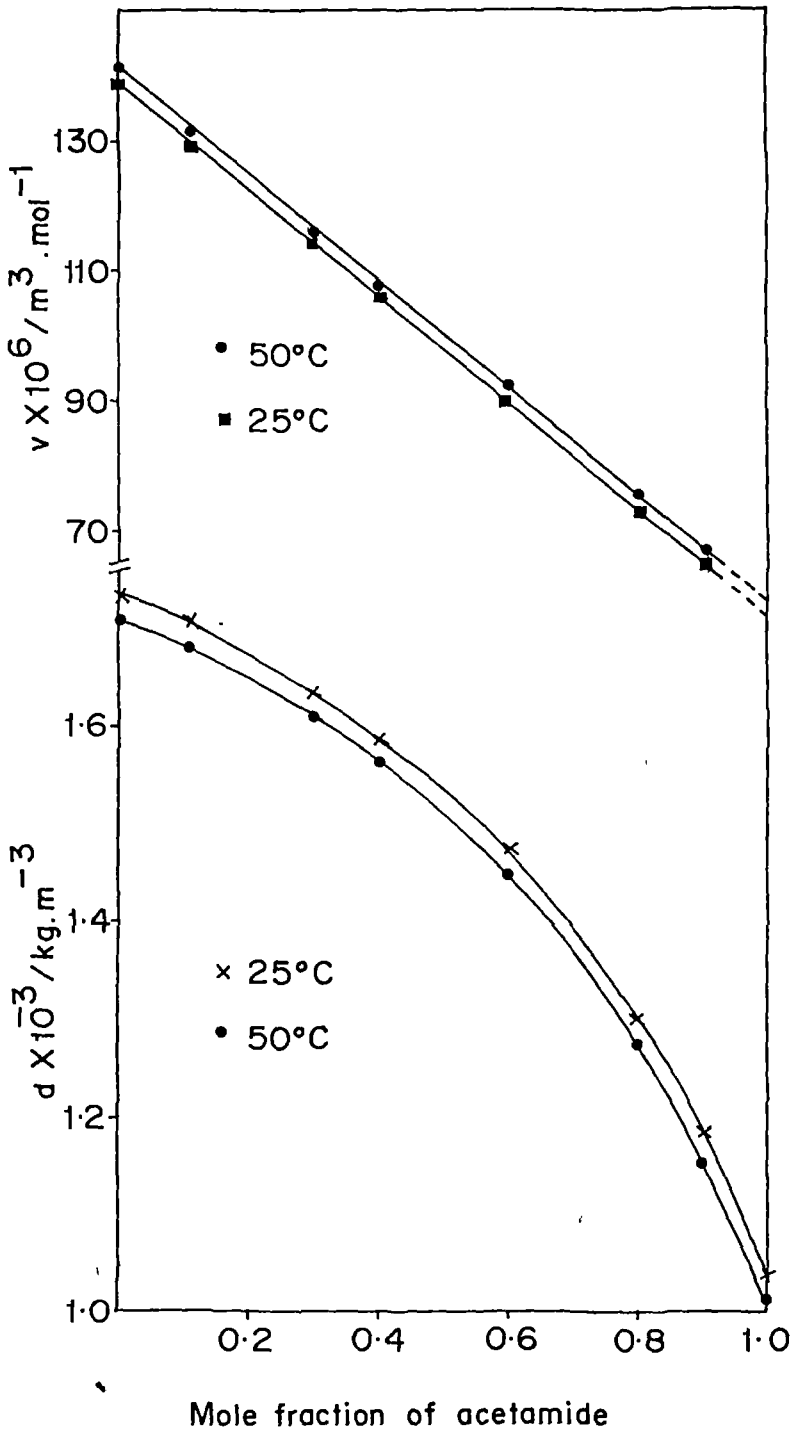

Fig. 5.1: Plot of density and molar volume of CNTH + acetamide melts versus mole fraction of acetamide

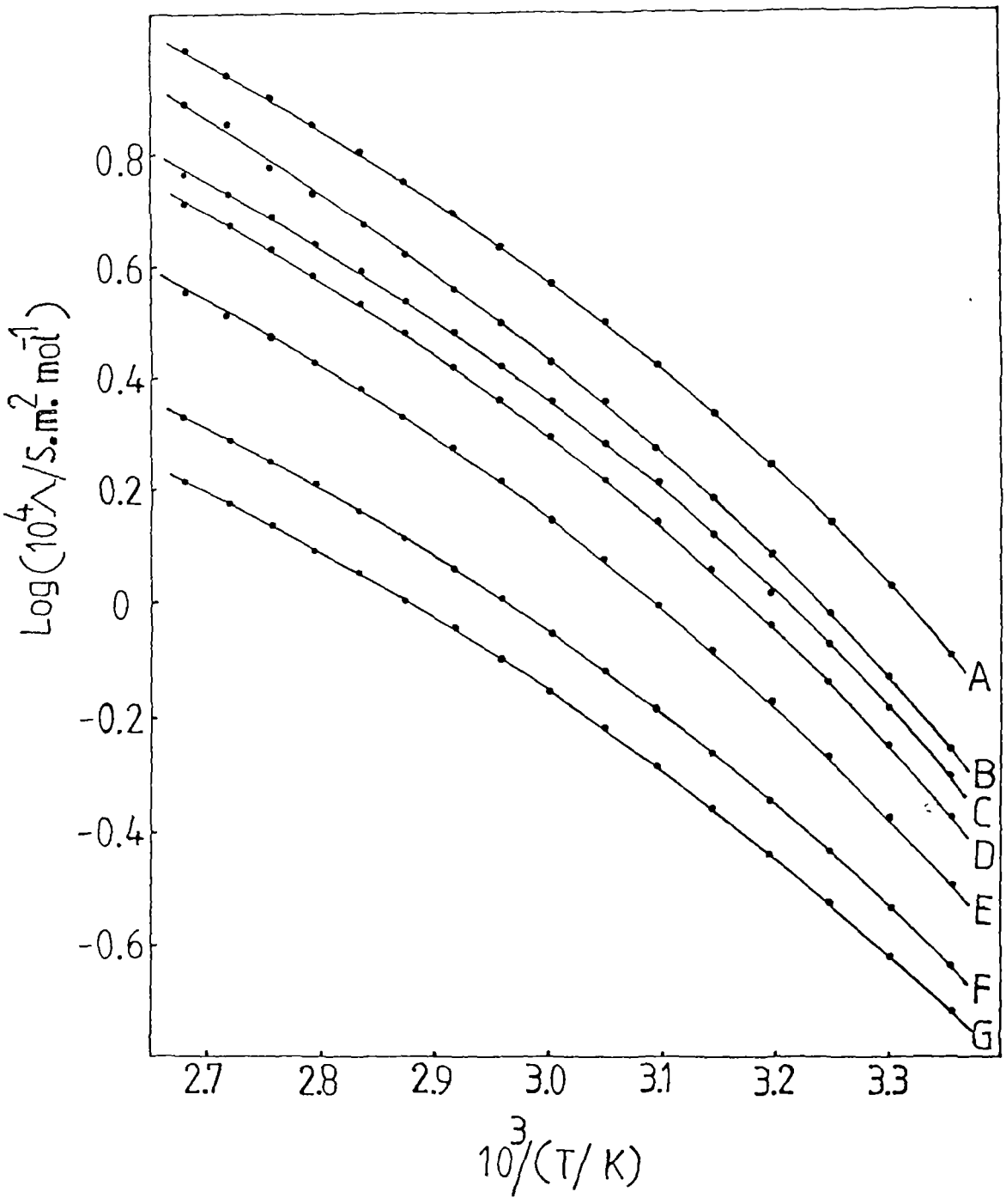

Fig. 5.2: Non - Arrhenius plots for the molar conductance of (1 - x) $Ca(NO_3)_2.4.26\ H_2O$ + xCH_3CONH_2 melts: A, x = 0.0; B, x = 0.111; C, x = 0.300; D, x = 0. 401; E, x = 0.597; F, x = 0.801; G, x = 0.900.

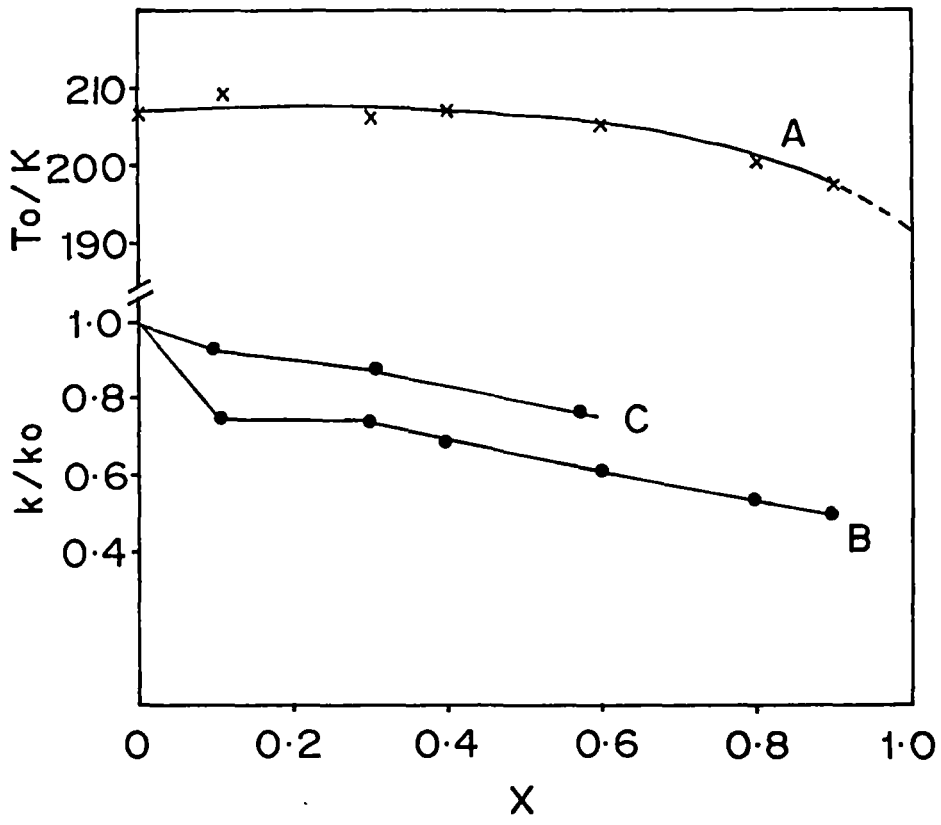

Fig. 5.3: Plot of (A) To and (B) k / ko versus x for (1-x) $Ca(NO_3)_2.4.26\ H_2O$ + xCH_3CONH_2 melts, and (c) plot of k / ko versus x for (1-x)$Ca(NO_3)_2.4\ H_2O$ + $xKNO_3$ melts (from ref . 31) . ko is the specific conductance of the hydrate melt.

References

1. J. Braunstein, L. Orr, and W. MacDonald, J. Chem. Eng. Data, **1967**, 12, 415.
2. C. T. Moynihan, C. R. Smalley, C. A. Angell, and E. J. Sare, J. Phys. Chem., **1969**, 73, 2287.
3. N. Islam and K. Ismail, J. Phys. Chem., **1975**, 79, 2160.
4. N. Islam and K. Ismail, J. Phys. Chem., **1976**, 80, 1929.
5. N. Islam and K. Ismail, Indian J. Chem., **1977**, 15A, 857.
6. S. K. Jain, J. Phys. Chem., **1978**, 82, 1272.
7. N. Islam, K. P. Singh, and S. Kumar, J. Chem. Soc. Faraday Trans. 1, **1979**, 75, 1312.
8. S. K. Jain, N. P. Kulshrestha, and V. V. Singh, J. Chem. Eng. Data,**1984**, 29, 14.
9. G. Charlot and B. Trimillon (Translated by P. J. J. Harvey), ' Chemical Reactions in Solvents and Melts, ' Pergamon Press, London, 1969, p. 321.
10. D. S. Reid and C. A. Vincent, J. Electroanal. Chem., **1968**, 18, 427.
11. R. Narayan and K. L. N. Phani, in ' Molten Salt Techniques,' Eds., R. J. Gale and D. G. Lovering, Plenum Press, New York, 1991, Vol. 4, p.1.
12. R. A. Wallace, J. Phys. Chem., **1971**, 75, 2687.

13. G. Berchiesi, G. Vitali, P. Passamonti, and R. Plowiec, J. Chem. Soc. Faraday Trans. 2, **1983**, 79, 1257.

14. G. Berchiesi, G. Vitali, and A. Amico, J. Chem. Eng. Data, **1985**, 30, 208.

15. R. Plowiec, A. Amico, and G. Berchiesi, J. Chem. Soc. Faraday Trans. 2, **1985**, 81, 217.

16. G. E. McManis, A. N. Fletcher, D. E. Bliss, and M. H. Miles, J. Electroanal. Chem., **1985**, 190, 171.

17. G. E. McManis, A. N. Fletcher, D. E. Bliss, and M. H. Miles, Electrochim. Acta, **1986**, 31, 1271.

18. G. E. McManis, A. N. Fletcher, D. E. Bliss, and M. H. Miles, J. Appl. Electrochem., **1986**, 16, 101.

19. A. Amico, G. Berchiesi, C. Cametti, and A. DiBiasio, J. Chem. Soc. Faraday Trans. 2, **1987**, 83, 619.

20. D. H. Kerridge, Chem. Soc. Rev., **1988**, 17, 181.

21. J. Tripkovic, R. Nikolic, and D. H. Kerridge, J. Serb. Chem. Soc., **1989**, 54, 527.

22. R. Nikolic, J. Tripkovic, and D. H. Kerridge, Thermochim. Acta, **1989**, 146, 353.

23. G. Berchiesi, G. Vitali, R. Plowiec, and S. Barocci, J. Chem. Soc. Faraday Trans. 2, **1989**, 85, 635.

24. G. Berchiesi, F. Farhat, and M. De Angelis, J. Mol. Liq., **1992**, 54, 103.

25. R. Nikolic and G. Ristic, J. Sol. Chem., **1994**, 22, 787.

26. W. W. Ewing and R. J. Mikovsky, J. Am. Chem. Soc., **1950**, 72, 1390.

27. S. Mahiuddin and K. Ismail, Bull. Chem. Soc. Jpn., **1981**, 54, 2525.

28. C. Bhattacharjee, S. Ismail, and K. Ismail, J. Chem. Eng. Data, **1986**, 31, 117.

29. C. T. Moynihan, J. Phys. Chem., **1966**, 70, 3399.

30. A. J. Easteal, E. J. Sare, C. T. Moynihan, and C. A. Angell, J. Sol. Chem., **1974**, 3, 807.

31. C. A. Angell, J. Electrochem. Soc., **1965**, 112, 1224.

32. S. Mahiuddin, J. Chem. Eng. Data, **1996**, 41, 231.

CHAPTER 6

A STUDY ON THE MICELLIZATION OF SURFACTANTS IN CALCIUM NITRATE TETRAHYDRATE + ACETAMIDE AND PURE ACETAMIDE MELTS USING CONDUCTANCE METHOD

6.1 Introduction

Surfactants, which are amphiphiles having both hydrophobic and hydrophilic characters in a molecule, form regular micelles in polar non-aqueous solvents including molten salt media. Reports on micellization in molten salt media are, however, very few. Reinsborough and coworkers[1-5] were the first to report about the formation of micelles by cationic surfactants in molten pyridinium chloride at 155°C. The second report of micelle formation in molten salt medium was made by Evans et al.[6,7] who reported micellization of alkyltrimethyl-ammonium bromide, alkylpyridinium bromides, and Triton X-100 in molten ethylammonium nitrate at 50°C. Recently Akhter[8] reported micellization of ionic surfactants in molten acetamide at 90°C. The study on the micellization of surfactants in ionic liquids is greatly hindered due to poor solubility of surfactants in ionic melts and secondly due to the high working temperature of ionic melts which cause thermal decomposition of surfactants. Thus in order to undertake the study of micellization of ionic surfactants in molten electrolyte media, it is necessary to select molten media such that the above mentioned difficulties can be overcome.

In the preceding chapter the volumetric and electrical conductance behaviours of a new room temperature molten salt system consisting of calcium nitrate tetrahydrate (CNTH) and acetamide were investigated.[9] This particular room temperature molten salt system was earlier used by Tripkovic et al.[10] as a medium for studying the spectral behaviour of transition metal ions. Since this room temperature molten salt system consists of a hydrated inorganic salt and an organic

compound it can be expected to dissolve ionic surfactants, even though ionic surfactants are insoluble in CNTH melt. Accordingly an attempt has been made in this chapter to study the micellization behaviour of sodium dodecyl sulfate (SDS) in CNTH + acetamide molten mixture. For this electrical conductance of SDS in CNTH + acetamide melt and of SDS, cetylpyridinium chloride (CPC), and $NaNO_3$ in pure acetamide melt were measured.

6.2 Experimental Section

CNTH (E. Merck), SDS (Sigma), and CPC (SISCO, extra pure grade) were used without further purification. Acetamide (E. Merck) was recrystallized from its solution in doubly distilled acetone whereas sodium nitrate (SD) was recrystallized from its solution in doubly distilled water.

Binary molten mixture of CNTH and acetamide of different compositions were prepared as described in chapter 5. For conductance measurement a weighed amount of CNTH+acetamide melt was taken in a sample tube and into it a dip-type conductivity cell was introduced. The sample tube was then closed air-tight using adhesive tapes and kept in the thermostat whose temperature was maintained at 38°C. After thermal equilibrium electrical conductance of the melt was measured. Then a weighed amount of SDS was quickly added into the melt and the sample tube was again closed air- tight. The system in the sample tube was then kept in the thermostat with occasional shaking till the added surfactant completely dissolves in the melt. After the system became homogeneous conductance of the

system was recorded. Similarly the conductance of the molten system was measured after each addition of SDS till the melt became almost saturated with SDS and the experiment was repeated using CNTH+acetamide melt of different compositions.

In a similar fashion conductances of solutions of SDS, CPC and $NaNO_3$ in pure acetamide melt were also measured.

Electrical conductance measurements were made at 1kHz using Wayne Kerr B905 Automatic Precision Bridge as described in chapter 2 and 5. Dip-type cells of cell constants 121.11 m^{-1} and 105.85 m^{-1} were used.

A thermostated oil bath was used to regulate temperature as described in chapters 2 and 5.

6.3 Results and Discussion

Specific conductances, k, of SDS in CNTH + acetamide melts of five different compositions containing 34.68, 68.38, 70.18, 73.47, and 78.30 weight % acetamide were measured at 38°C as a function of concentration of SDS. These data are presented in Table 6.1. Duplicate measurements have shown that the specific conductance data are reproducible within ± 2 % and this much deviation in the data is attributable mainly to slight variations in the water to salt molar ratio of CNTH.[11]

The solubility of SDS in the molten mixtures of CNTH and acetamide is found to be considerably less. For example, SDS is soluble in the melt containing 78.3 weight % (= 93.5 mole %) acetamide only about 0.12 mol kg^{-1} and this solubility decreased by about 3 times in the molten mixture of 34.68 weight % acetamide. Sometimes SDS was dissolved in the melt by heating the sample to higher temperature and then cooling the sample to the required temperature. The surfactant once dissolved in the melt at higher temperature remains in the dissolved state even at lower temperatures also. Such solutions are termed as supercooled surfactant solutions by Franses et al.[12] In fact, the temperature at which the solubility of a surfactant in a given solvent increases suddenly is called as Kraft temperature.[6,12,13] In melts containing less than 34.68 weight % acetamide solubility of SDS was found to be negligible.

The variation of k with concentration of SDS in the different CNTH + acetamide melts is shown in Fig 6.1. From Fig 6.1 it is apparent that the nature of the behaviour of k with respect to SDS concentration is dependent on the amount of acetamide present in the molten mixture. In molten mixtures containing 78.3 (melt A) and 73.47 (melt B) weight % acetamide the shape of the k versus concentration of SDS plots is similar to that in water and polar organic solvents. Thus SDS may be considered to micellize in melts A and B and the values of critical micelle concentrations (cmc) of SDS in these molten mixtures are found to be 0.017 ± 0.001 and 0.014 ± 0.001 mol kg^{-1}, respectively. In molten mixture containing 70.18 weight % acetamide (melt C), cmc of SDS is found to be 0.014 ±

0.001 mol kg^{-1} and the dependence of k on SDS concentration above cmc is seen to be similar to that found in melts A and B (Fig 6.1), the increase in k with SDS concentration is however not significant. On the other hand, in melt C below cmc k initially decreases with the addition of SDS upto ~ 0.004 mol kg^{-1} and above this concentration starts increasing. In molten mixture containing 68.38 weight % acetamide (melt D), k decreases with the addition of SDS upto ~ 0.012 mol kg^{-1}, remains almost constant in the SDS concentration range from ~ 0.012 to ~ 0.020 mol kg^{-1}, and then decreases continuously above 0.020 mol kg^{-1}. The cmc of SDS in melt D is found to be 0.020 $\pm$ 0.001 mol kg^{-1}. In the molten mixture containing 34.68 weight % acetamide (melt E), k decreases monotonically by the addition of SDS and the cmc value is found to be 0.021 $\pm$ 0.001 mol kg^{-1}. All the cmc values of SDS in CNTH + acetamide melts are listed in Table 6.2. In melt E the nature of the k versus concentration isotherm is similar to that of cetyldimethylbenzylammonium chloride in molten pyridinium choride at 155°C (Fig 6.2).[4] In CNTH melt also it has been observed that by the addition of inorganic or organic solutes k decreases (cf. chapter 5).[9] It may however be noted that in CNTH melt or other hydrate melts electrical conductance data of added inorganic salts in the low concentration region are not available for comparison.

In order to explain properly the conductance behaviour of SDS in melts A, B, C, D and E, one must also have the knowledge of the conductance behaviour of SDS in pure acetamide melt. Although Akhter[8] reported, on the basis of conductance measurements at 90°C, that SDS micellizes in acetamide melt, a

detailed study of the conductance behaviour of SDS in acetamide melt has not been done. In polar nonaqueous solvents electrical conductivity data of surfactants are known to provide misleading results about micellization.[13-16] Binana-Limbele and Zana[16] suggested that extreme caution must be exercised while using electrical conductivity data of surfactants in polar nonaqueous solvents for determining cmc values. In view of the above comments, a careful analysis of the electrical conductivity data of surfactants in acetamide melt is therefore required before drawing any conclusion about their micellization behaviour. Accordingly, we measured k of SDS and CPC in pure acetamide melt at 89 and 84°C as a function of SDS concentration and these data are given in Tables 6.3 and 6.4. In acetamide melt the variation of k of SDS and CPC with concentration is shown in Fig 6.3. Based on Fig 6.3 the values of cmc of SDS and CPC in acetamide melt were estimated and these values are given in Table 6.2. C_{max} values given in Table 6.2 refer to the maximum concentration of the surfactant which was taken into account for estimating the cmc value. From Table 6.2 it may be seen that with decrease in temperature the values of cmc of both SDS and CPC tend to increase. cmc is known to exhibit such a temperature dependence in water below 25°C.[17] Moreover, the cmc values obtained for CPC in acetamide melt are lower than the cmc values for SDS and this is similar to the trend observed in aqueous medium.[18] The cmc value of SDS in acetamide melt at 90°C is reported[8] to be 0.016 mol dm^{-3} which was estimated from the conductance data with $C_{max} \approx 0.042$ mol dm^{-3}. Since this reported cmc value of SDS is almost half of the value obtained by us (Table 6.2), the cmc value of SDS in acetamide melt at 89°C was reestimated by

considering the conductance data of SDS up to ~ 0.042 mol kg^{-1} only, i.e.,$C_{max} \approx$ 0.042 mol kg^{-1}. Such an analysis also provided from our data cmc value = 0.016 $\pm$ 0.001 mol kg^{-1} for SDS. This is also illustrated in Fig 6.3. The above observation thus envisages that cmc value of surfactants in acetamide melt depends upon the value of C_{max} used for cmc determination. Same observation was also made by Binana - Limbele and Zana[16] in polar nonaqueous solvents, viz., ethyleneglycol, formic acid and formamide, and they suggested an empirical relation of the type, cmc $\approx C_{max} / 3$. In our present study, this particular empirical relation seems to hold good for SDS and CPC at 89°C, but at 84°C it appears that the cmc values of SDS and CPC are more close to the relation cmc $\approx C_{max} / 2$. When cmc value of a surfactant in any solvent shows dependence on the extent of concentration range covered in the conductance measurement, both interionic interactions and interactions responsible for micelle formation are considered to be playing decisive roles in governing the concentration dependence of electrical conductance of the surfactant.[16] Under such a situation, the visual cmc value determined from the plot of k versus concentration of surfactant may not correspond to the true cmc value and the visual cmc might be caused predominantly by the interionic interactions. Binana - Limbele and Zana[16] named such visual cmc's as operational cmc's (cmc_{op}). It is therefore necessary to ascertain that the cmc values which we obtained for SDS and CPC in acetamide melt from the conductance data are not due to interionic interactions. For this purpose, we also measured the specific conductance of $NaNO_3$ in acetamide melt at 89°C and the data are given in Table 6.5. The solution of $NaNO_3$ in molten acetamide would behave like a normal

electrolytic solution as interactions responsible for micellization are not operative in this $NaNO_3$ solution. The variation of k of $NaNO_3$ solution in molten acetamide with concentration up to ~0.072 mol kg^{-1} is shown in Fig 6.3 and from this plot it is apparent that all the data points fall on a single straight line without any significant deviation from linearity due to ion-ion interactions. In Figs 6.4 and 6.5 we have also plotted k of SDS, CPC and $NaNO_3$ solutions in acetamide melt at 89°C against concentration covering the higher concentration ranges of the present conductance measurement. At higher concentrations above ~0.01 mol kg^{-1} the nature of the k versus concentration plots for all the three systems appears to be similar as can be seen from Figs 6.4 and 6.5. In fact, at high concentrations even conductance maxima were observed for the solutions of SDS (at ~1.0 mol kg^{-1}), CPC (at ~1.4 mol kg^{-1}) and $NaNO_3$ (at ~2.6 mol kg^{-1}) in acetamide melt. Although occurrence of conductance maxima is a common feature of normal electrolytic solutions, for surfactants such conductance maxima have not reported in any solvent. Normally, conductance maxima occur when mobility of ionic species starts controlling the dependence of k on concentrations. The above results thus indicate that in acetamide melt the conduct-ance behaviour of SDS and CPC above ~0.1 mol kg^{-1} concentration is almost similar to that of a normal electrolytic solution thereby envisaging the dominance of ion-ion interactions. Therefore, it may be concluded that the changes in the slopes of the linear plots of k versus concentration observed in the case of SDS and CPC below ~0.1 mol kg^{-1} are due to micellization of these surfactants in acetamide melt. It may be pointed out that a similar approach as above, viz., comparison of conductance behaviour of surfactant solutions with that

of a solution in the same solvent of a normal salt having cation and anion same as or similar to the counterions and ionic head groups of the surfactants, was adopted by Binana - Limbele and Zana[16] for ascertaining the micelle formation of cationic surfactants in ethyleneglycol, formic acid and formamide. It may however be predicted that in acetamide melt the aggregates or micelles formed are of small size with small aggregation numbers. As suggested by Binana - Limbele and Zana,[16] if the value of α, which is the ratio of the slopes of the linear plots of k versus concentration above and below the cmc, is considered as an indication of the size of the aggregate or micelle formed, then the aggregation number in acetamide melt is relatively less than in water because for SDS in water $\alpha \approx 0.45$ whereas in acetamide melt $\alpha \approx 0.81$. Same argument holds good in the case of CPC also. In water surfactant aggregates or micelles are formed as a result of two opposite forces, viz., electrostatic repulsion between head groups and attractive hydrophobic interactions between water and hydrocarbon chains of the surfactant molecules. When these two opposing forces are balanced aggregates or micelles of fairly large aggregation number are formed in water. In acetamide melt (dielectric constant = 61.9 at 89°C),[19] the electrostatic repulsions can be considered to be comparable to those in water, but the solvophobic interactions are considerably reduced because acetamide is more lipophilic than water. As a result, repulsions may be expected to be predominant and formation of micelles of large size may not be favoured.

The ability of a solvent to force surfactants to form micelles is quantified sometimes in terms of its cohesive energy density reported by the term $D_e = \gamma / V^{1/3}$ where γ is the surface tension of the solvent and V its molar volume.[16,20] For micellization to occur in a particular solvent it was reported that the value of D_e for the solvent is required to be above 1.0-1.1 J m^{-3}. Binana-Limbele and Zana[16] further commented that for D_e = 1.0 to 1.1 J m^{-3} aggregation of ionic surfactants may take place, but for micelle formation with large aggregation number D_e is required to have values above 1.7 J m^{-3}. Hydrogen bonding capability of a solvent has not been shown to be a necessary condition for micellization.[16] In view of the above, it therefore appears that in acetamide melt, for which $D_e \approx 1.0$ J m^{-3} at 89°C which is comparable to the value of formic acid at 25°C, ionic surfactants do form micelles but of smaller aggregation number compared to the size of micelles in water (D_e = 2.75 J m^{-3} at 25°C).

In the light of the above discussion the following conclusions may be made regarding the behaviour of CNTH+acetamide melt. (1) In this melt if k increases with solute concentration then acetamide controls the conductance behaviour of the added solute and this happens when the amount of acetamide in the melt is > ~73 weight %. (2) When k decreases with increase in solute concentration the conductance behaviour of the solute in the binary molten mixture is governed by CNTH. (3) Micellization of ionic surfactants takes place in this melt but the aggregation number of the micelles seems to be small. The cmc of SDS at 38°C seems to decrease with increase in the amount of CNTH up to ~30 weight % in the

melt. Thus the effect of addition of CNTH on the cmc of SDS in acetamide-rich melt is similar to the effect of added electrolyte on cmc in aqueous medium.[27] Such an effect on cmc is explained in terms of the reduction being caused by the added counter ions in the interaction between the ionic heads residing on the micellar surface. The cmc of SDS appears to exhibit an increase on further addition of CNTH above ~30 weight %. (4) When both CNTH and acetamide control the conductance behaviour of the added ionic surfactant, a minimum occurs in the k versus concentration plot below cmc. This happens when the amount of acetamide in the binary melt is in the range from ~70 to 68 weight %. (5) Above cmc, k either increases (acetamide dominating region), remains almost constant, or decreases (CNTH dominating region) with increase in surfactant concentration.

Table 6.1 : Speccific Conductance (k) of SDS in CNTH + Acetamide Melts at 38°C

Conc. of SDS (mol kg^{-1})	k ($S\ m^{-1}$)	Conc.of SDS (mol kg^{-1})	k ($S\ m^{-1}$)
78.30 weight % acetamide (Melt+A)			
0.0	0.4809	0.0019	0.4844
0.0044	0.4858	0.0074	0.4907
0.0132	0.4959	0.0168	0.4986
0.0239	0.4982	0.0316	0.4992
0.0407	0.5068	0.0467	0.5069
0.0658	0.5112	0.0841	0.5188
73.47 weight % acetamide (Melt B)			
0.0	0.4924	0.0031	0.4954
0.0068	0.4988	0.0108	0.5005
0.0145	0.5061	0.0181	0.5054
0.0233	0.5077	0.0278	0.5090
0.0315	0.5133	0.0383	0.5127
0.0436	0.5174	0.0500	0.5178
0.0553	0.5214		

Table 6.1 Continued

Conc. of SDS (mol kg^{-1})	k ($S\ m^{-1}$)	Conc.of SDS (mol kg^{-1})	k ($S\ m^{-1}$)
70.18 weight % acetamide (Melt C)			
0.0	0.5017	0.0019	0.4995
0.0044	0.4957	0.0071	0.4994
0.0107	0.5011	0.0141	0.5044
0.0186	0.5036	0.0255	0.5037
0.0271	0.5057	0.0325	0.5054
68.38 weight % acetamide (Melt D)			
0.0	0.4951	0.0045	0.4927
0.0089	0.4876	0.0133	0.4840
0.0197	0.4853	0.0262	0.4768
0.0321	0.4765	0.0411	0.4603
0.0521	0.4512		

Table 6.1 Continued

Conc. of SDS (mol kg^{-1})	k (S m^{-1})	Conc.of SDS (mol kg^{-1})	k (S m^{-1})
34.68 weight % acetamide (Melt E)			
0.0	0.5593	0.0048	0.5355
0.0102	0.5144	0.0159	0.5009
0.0212	0.4743	0.0273	0.4581
0.0349	0.4405	0.0413	0.4170

Table 6.2 : Values of CMC of SDS in CNTH+Acetamide Melts and of SDS and CPC in Acetamide Melt

Molten Medium	Temperature (°C)	cmc (mol kg^{-1})	Cmax (mol kg^{-1})
	Surfactant = SDS		
Melt A	38	0.017	0.0841
Melt B	38	0.014	0.0553
Melt C	38	0.014	0.0325
Melt D	38	0.020	0.0521
Melt E	38	0.021	0.0413
Acetamide	89	0.031	0.0800
Acetamide	84	0.038	0.0802
Acetamide	89	0.016	0.0416
	Surfactant = CPC		
Acetamide	89	0.019	0.0667
Acetamide	84	0.024	0.0445

Table 6.3 : Specific Conductance (k) of SDS in Acetamide Melt at 89 and 84°C

Conc. of SDS (mol kg^{-1})	k ($S\ m^{-1}$)	Conc. of SDS (mol kg^{-1})	k ($S\ m^{-1}$)
Temperature = 89°C			
0.0011	0.0026	0.0022	0.0051
0.0027	0.0065	0.0033	0.0116
0.0040	0.0094	0.0049	0.0116
0.0058	0.0136	0.0064	0.0151
0.0073	0.0171	0.0082	0.0192
0.0092	0.0215	0.0103	0.0241
0.0110	0.0252	0.0119	0.0274
0.0138	0.0319	0.0150	0.0340
0.0158	0.0363	0.0180	0.0401
0.0233	0.0513	0.0266	0.0577
0.0376	0.0790	0.0416	0.0883
0.0497	0.1031	0.0554	0.1127
0.0626	0.1251	0.0799	0.1421
0.2090	0.3197	0.3333	0.4156
0.5744	0.5304	0.5844	0.5362
0.5931	0.5375	0.5993	0.5408

Table 6.3 Continued

Conc. of SDS (mol kg^{-1})	k ($S\ m^{-1}$)	Conc. of SDS (mol kg^{-1})	k ($S\ m^{-1}$)
Temperature = 89°C			
0.6039	0.5432	0.6396	0.5533
0.7334	0.5746	1.0219	0.5892
1.2326	0.5828	1.3006	0.5788
1.3278	0.5656	1.3778	0.5565
1.5134	0.5404	1.7714	0.5095
2.0665	0.4699		

Table 6.3 Continued

Conc. of SDS (mol kg^{-1})	k (S m^{-1})	Conc. of SDS (mol kg^{-1})	k (S m^{-1})
Temperature = 84°C			
0.0035	0.0074	0.0060	0.0129
0.0093	0.0200	0.0134	0.0282
0.0183	0.0380	0.0242	0.0497
0.0308	0.0625	0.0423	0.0840
0.0530	0.1023	0.0655	0.1234
0.0802	0.1458	0.0950	0.1689
0.1282	0.2139	0.1525	0.2439
0.1883	0.2824	0.2319	0.3231
0.3177	0.3887	0.4050	0.4366
0.4800	0.4653	0.5800	0.4859
0.6689	0.5010	0.7637	0.5087
0.8682	0.5097	0.9208	0.5150
0.9609	0.5129	1.0110	0.5087
1.0737	0.5034	1.1051	0.5019
1.1328	0.5003		

Table 6.4 : Specific Conductance (k) of CPC in Acetamide Melt at 89 and 84°C

Conc. of CPC (mol kg^{-1})	k (S m^{-1})	Conc. of CPC (mol kg^{-1})	k (S m^{-1})
	Temperature 89°C		
0.0012	0.0035	0.0019	0.0056
0.0024	0.0071	0.0031	0.0093
0.0045	0.0131	0.0056	0.0162
0.0065	0.0189	0.0080	0.0229
0.0112	0.0319	0.0124	0.0351
0.0157	0.0442	0.0233	0.0637
0.0347	0.0863	0.0518	0.1239
0.0667	0.1545	0.0899	0.2001
0.1122	0.2405	0.1298	0.2711
0.1501	0.3032	0.1794	0.3472
0.2005	0.3805	0.2129	0.3979
0.2315	0.4222	0.2812	0.4790
0.3254	0.5203	0.3803	0.5747
0.4390	0.6201	0.5019	0.6716
0.5450	0.6947	0.5959	0.7299

Table 6.4 Continued

Conc. of CPC (mol kg^{-1})	k ($S\ m^{-1}$)	Conc. of CPC (mol kg^{-1})	k ($S\ m^{-1}$)
	Temperature 89°C		
0.6414	0.7644	0.7091	0.7910
0.7587	0.8062	0.8081	0.8281
0.8597	0.8446	1.0046	0.8716
1.1582	0.9012	1.2994	0.9158
1.4063	0.9166	1.5676	0.9132
1.5992	0.9085		

Table 6.4 Continued

Conc. of CPC (mol kg^{-1})	k (S m^{-1})	Conc. of CPC (mol kg^{-1})	k (S m^{-1})
	Temperature 84°C		
0.0021	0.0077	0.0042	0.0141
0.0070	0.0241	0.0112	0.0375
0.0137	0.0463	0.0165	0.0544
0.0195	0.0642	0.0226	0.0726
0.0260	0.0842	0.0311	0.0980
0.0347	0.1089	0.0383	0.1193
0.0445	0.1363		

Table 6.5 : Specific Conductance (k) of $NaNO_3$ in Acetamide Melt at 89°C

Conc. of $NaNO_3$ (mol kg^{-1})	k (S m^{-1})	Conc. of $NaNO_3$ (mol kg^{-1})	k (S m^{-1})
0.0092	0.0309	0.0130	0.0442
0.0168	0.0546	0.0310	0.0964
0.0461	0.1395	0.0618	0.1838
0.0723	0.2103	0.1268	0.3401
0.1997	0.4903	0. 3395	0.7209
0.4631	0.8830	0.6005	1.0207
0.8619	1.2141	1.1623	1.3604
1.4292	1.4142	2.0386	1.4984
2.2440	1.5035	2.5297	1.5153
3.2870	1.4862	3.7055	1.4267

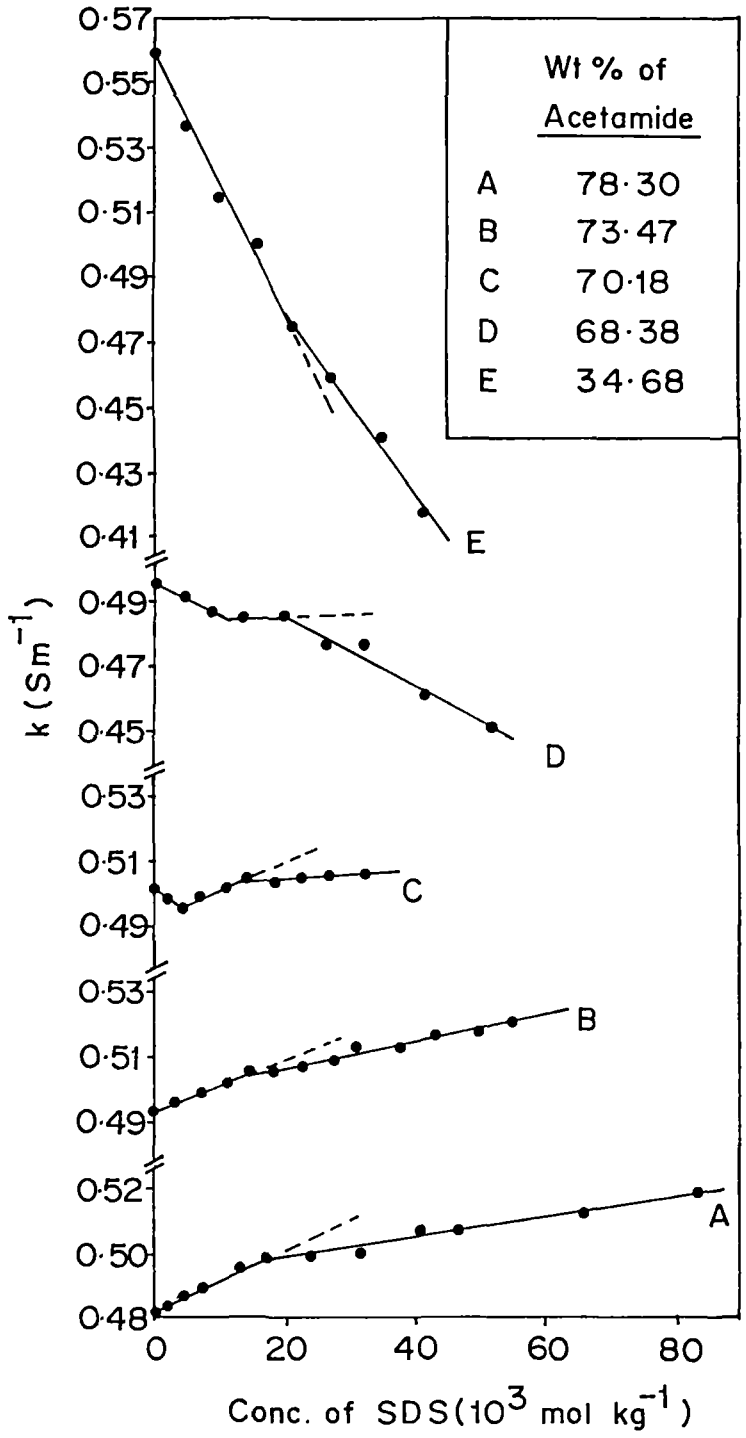

Fig. 6.1: Plot of k versus concentration of SDS in CNTH + Acetamide molten mixtures of different composition at 38°C.

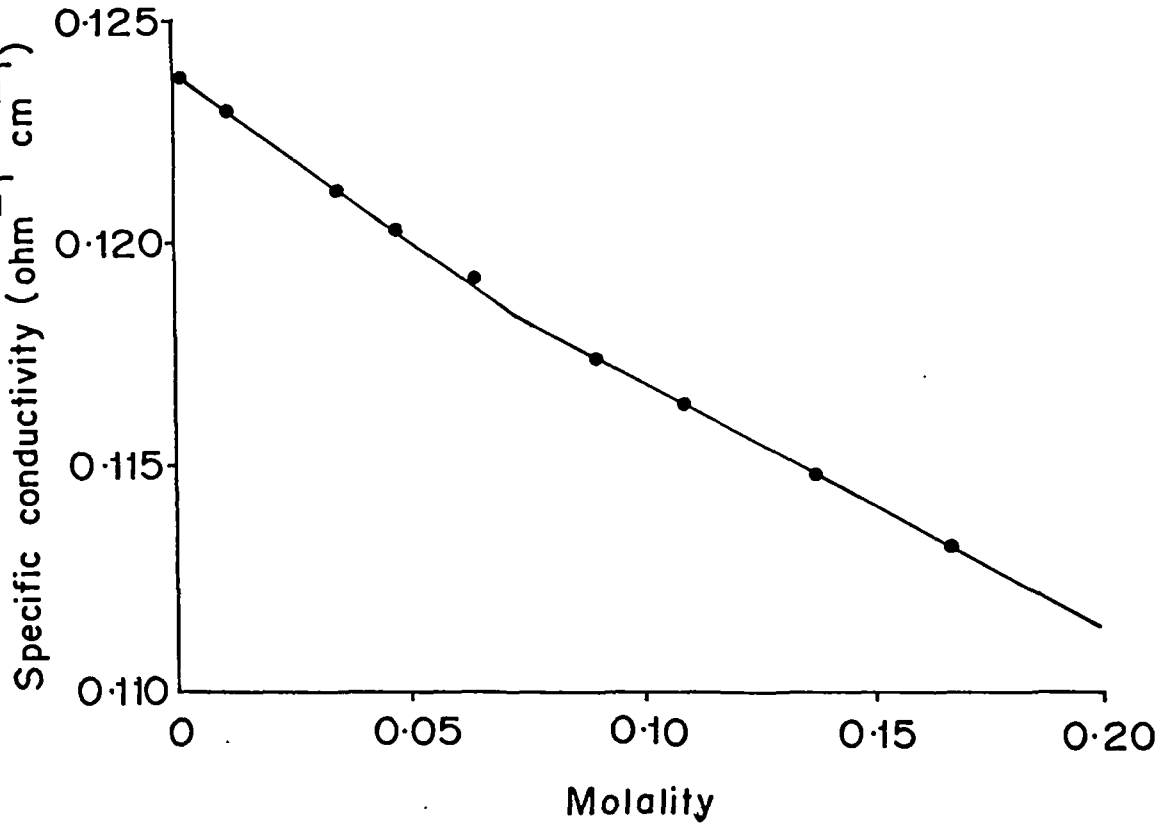

Fig. 6.2: Plot of Specific Conductance of Cetyldimethylbenzylammonium chloride in molten pyridinium chloride at 155^{0}C[Taken from Ref. 4].

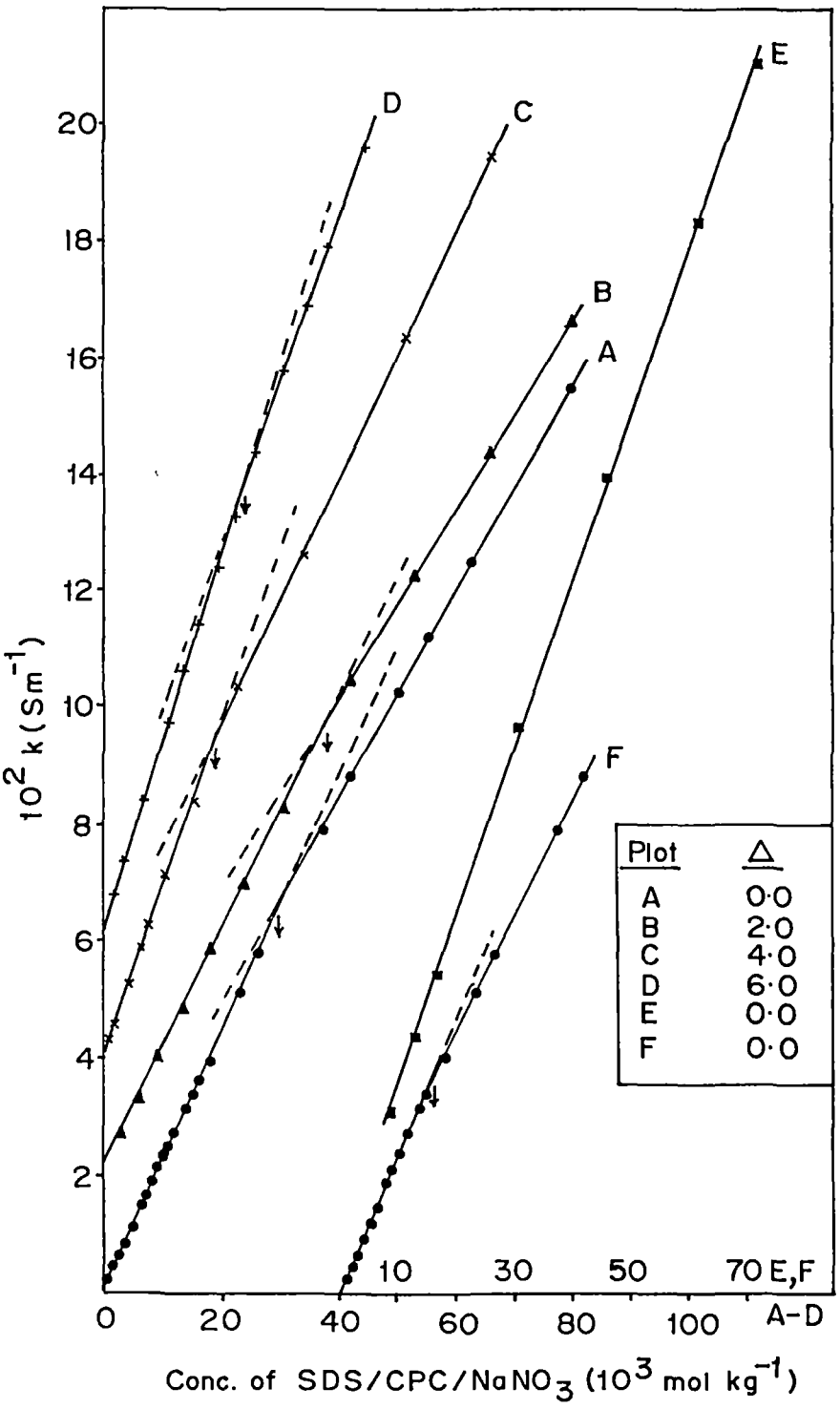

Fig. 6.3: Plot of k versus concentration of added solute in acetamide melt .

(A) SDS at 89°C ,(B) SDS at 84°C , (C) CPC at 89°C, (D) CPC at 84°C,

(E) $NaNO_3$ at 89°C (F) SDS at 89°C with C_{max} = 0.0416 mol kg^{-1} .

Δ indicates upward shift of ordinate scale for the different plots.

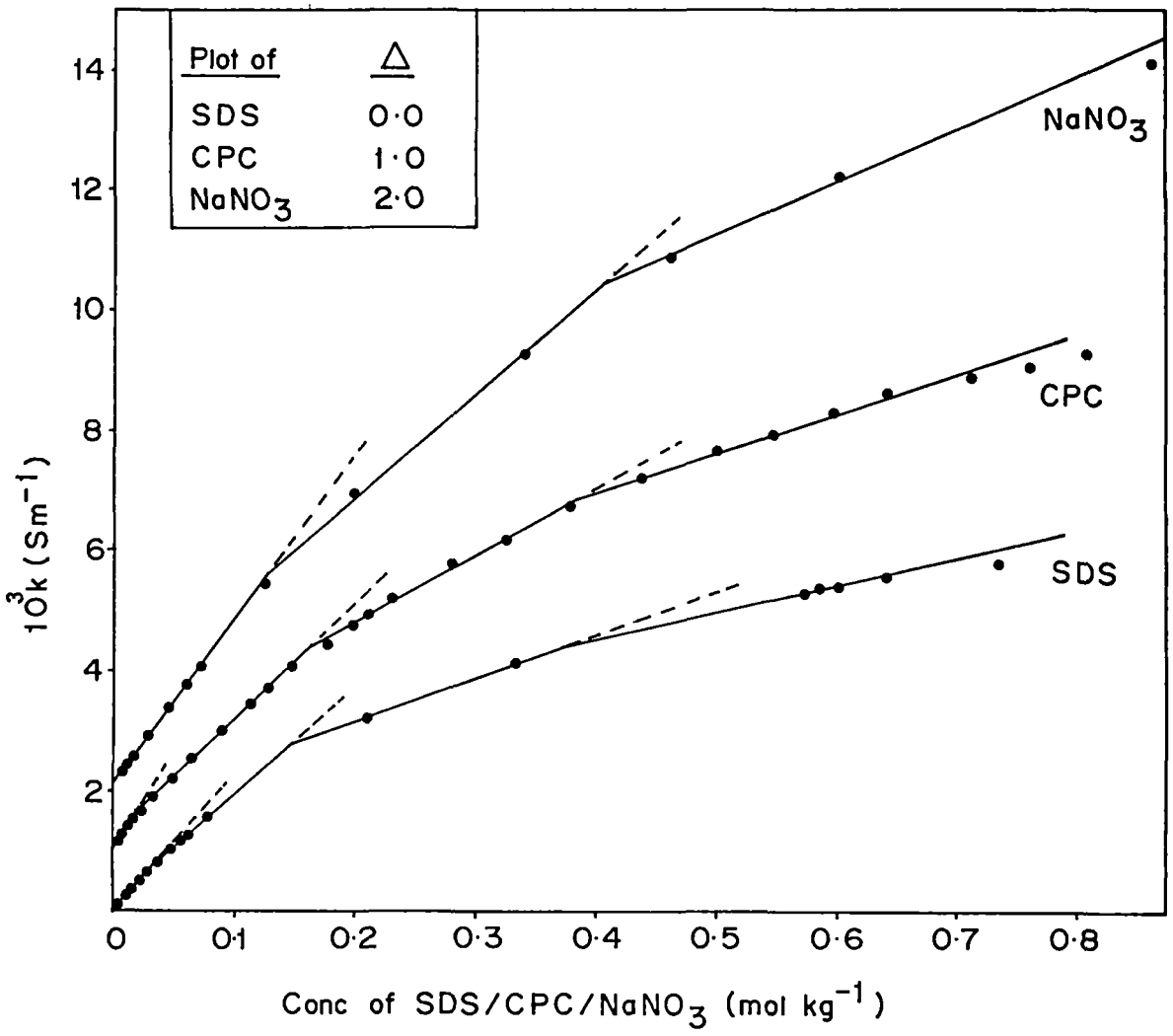

Fig. 6.4: Plot of k versus concentration of added solute in acetamide melt at 89°C covering extended range of concentration. Δ indicates upward shift of ordinate scale for the different plots.

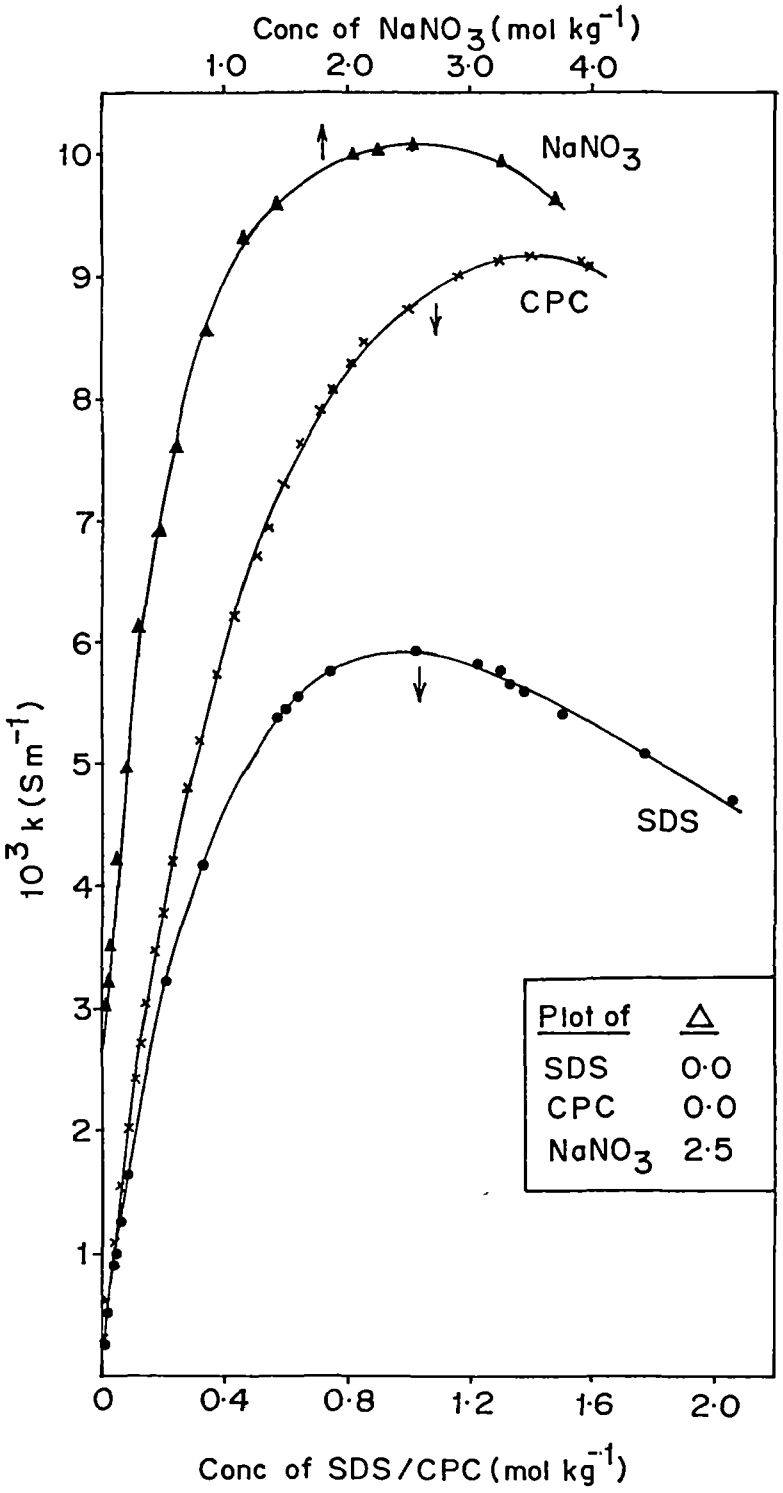

Fig. 6.5: Plot of k versus concentration of added solute in acetamide melt at 89^{0}C covering entire range of concentration studied. Δ indicates upward shift of ordinate scale for the different plots.

References

1. H. Bloom and V. C. Reinsborough, Aust. J. Chem., **1967**, 20, 2583.
2. H. Bloom and V. C. Reinsborough, Aust. J. Chem., **1968**, 21, 1525.
3. V. C. Reinsborough and J. P. Valleau, Aust. J. Chem., **1968**, 21, 2905.
4. H. Bloom and V. C. Reinsborough, Aust.J. Chem., **1969**, 22, 519.
5. V. C. Reinsborough, Aust. J. Chem., **1970**, 23, 1473.
6. D. F. Evans, A. Yamauchi, R. Roman, and E. Z. Casassa, J. Colliod Interface Sci., **1982**, 88, 89.
7. D. F. Evans, A. Yamauchi, G. J. Wei, and V. A. Bloomfield, J. Phys. Chem., **1983**, 87, 3537.
8. M. S. Akhter, Colloids Surf. A, **1995**, 99, 255.
9. S. K. Chettri, S. Dev, and K. Ismail, J. Chem. Eng. Data, **1995**, 40, 12.
10. J. Tripkovic, R. Nikolic, and D. H. Kerridge, J. Serb. Chem. Soc., **1989**, 54, 527.
11. C. T. Moynihan, J. Phys. Chem., **1966**, 70, 3399.
12. E. I. Franses, H. T. Davis, W. G. Miller, and L. E. Scriven, J. Phys. Chem., **1980**, 84, 2413.
13. I. Rico and A. Lattes, J. Phys. Chem., **1986**, 90, 5870.

14. M. Almgren, S. Swarup, and J. E. Löforth, J. Phys. Chem., **1985**, 89, 4621.

15. A. Belmajdoub, K. ElBayed, J. Brondeau, D. Canet, I. Rico, and A. Lattes, J. Phys. Chem., **1988**, 92, 3569.

16. W. Binana - Limbele and R. Zana, Colloid Polymer Sci., **1989**, 267, 440.

17. B. C. Paul and K. Ismail, Bull. Chem. Soc. Jpn., **1993**, 66, 703.

18. J. H. Fendler and E. J. Fendler, ' Catalysis in Micellar and Macromolecular Systems,' Academic Press, 1975.

19. R. A. Wallace, J. Phys. Chem., **1971**, 75, 2687.

20. M. Ramadan, D. F. Evans, R. Lumry, and S. Philson, J. Phys. Chem., **1985**, 89, 3405.

CHAPTER 7

ELECTRICAL CONDUCTANCE BEHAVIOUR OF CALCIUM NITRATE TETRAHYDRATE + METHANOL/ETHANOL/PROPANOL BINARY SYSTEMS FROM PURE MELT TO INFINITE DILUTION IN THE TEMPERATURE RANGE FROM 45 TO - 75°C

7.1 Introduction

The electrical conductance behaviour of dilute aqueous and non-aqueous electrolytic solutions is explainable by the Debye-Hückel-Onsager (DHO),[1] Falkenhagen-Leist-Kelbg (FLK),[2] and the Fuoss-Onsager (FO)[3,4] theoretical equations. All these theoretical equations based on DHO, FLK and FO models become inadequate when the concentration of electrolytic solutions becomes of the order of about 0.01 mol dm^{-3}. Modifications to the FLK equation have been made to extend its applicability to higher concentrations.[5-10] However, when the concentration becomes very high an altogether different approach is required for describing the conductance behaviour of binary systems owing to the following reasons : (1) At high concentrations, when comparable amounts of the two components of a binary system are present the concept of solute and solvent disappears. The primitive model which treats solvent as a continuum is therefore not applicable.[11] (2) At infinitely concentrated region the system becomes a molten electrolyte.[12] Thus at ultra high concentrations expressions obtained by modifying the FLK or the other theoretical equations, which are valid in the dilute region, are not conceptually acceptable. Consequently, an alternative approach is adopted in which theoretical equations employed to describe the conductance behaviour of molten salt systems are modified.[11-15] Expressions obtained in this fashion are reported[12-15] to be useful to describe the conductance behaviour of electrolytic solutions in the dilute as well as concentrated regions. However, the validity and applicability of these isothermal equations are not tested rigorously mainly because of nonavailability of conductance data of electrolytic solutions in the entire

concentration region. Thus experimental data of binary systems in the entire concentration region ranging from infinte dilution to pure melt are necessary to understand their transport behaviours properly and the importance of such data has been highlighted from time to time.[16-21]

Binary electrolytic systems may be prepared by mixing (1) two liquids, (2) a liquid and a salt, or (3) two molten salts. For binary electrolytic systems of types 1 (e.g., $H_2O + H_2SO_4$) and 3 (e.g., $ZnCl_2 + KCl$) the entire concentration region may be scanned during an experimental measurement. However, not many binary systems of the type 2 have been studied in the entire region of concentration owing to practical difficulties involved in making isothermal measurements. Isothermal measurements of thermodynamic and transport properties of aqueous and non-aqueous solutions of inorganic salts from infinite dilution to pure melt have been hindered due to high melting points and low solubility of inorganic salts. Therefore, some of the systems whose transport properties were studied in the entire concentration region consist of a low melting organic salt and a non-aqueous liquid.[16-18,22]

Another type of binary electrolytic systems whose transport or thermodynamic properties can be measured from infinite dilution to molten salt is that consisting of a hydrated inorganic salt and an organic compound. Hydrated inorganic salts like $Ca(NO_3)_2.4H_2O$, $Cd(NO_3)_2.4H_2O$, $Zn(NO_3)_2.6H_2O$, $Mg(NO_3)_2.6H_2O$, $Na_2S_2O_3.5H_2O$, etc., have low melting points and form a separate category of interesting room-temperature molten salts as described in the preceding chapters. These hydrate

melts behave like anhydrous molten salts with hydrated metal ions as the cations.[24] In recent years structure and dynamics of hydrated metal ions have drawn the attention of both theoretical and experimental chemists.[25-30] In this chapter we have made an attempt to measure the electrical conductances of binary mixtures of calcium nitrate tetrahydrate (CNTH) melt with methanol, ethanol and propanol covering the entire concentration range and temperature range from 45 to -75°C. The reasons for choosing the second component of binary mixture as methanol / ethanol / propanol are (1) these alcohols readily dissolve CNTH, (2) addition of these alcohols renders low temperature measurements more feasible, and (3) currently there has been a renewed interest on the hydrogen bonding tendency of these alcohols.[31-35]

7.2 Experimental Section

CNTH (SD, AR grade) and methanol (Spectrochem) were used without further purification. Ethanol (Bengal Chemicals) and n-propanol (Loba) were purified first by simple distillation. The distilled alcohols were then refluxed with CaO for ~ 6 hours and distilled again after keeping for overnight. Ethanol and propanol purified thus are further dehydrated by reacting the alcohols with magnesium turnings (~ 5 g) and iodine (~ 0.5 g) and by finally distilling off.

Weighed amount of CNTH was taken in a sample tube. Transfer of CNTH into the weighing bottle and from the weighing bottle into the sample tube was done in an atmosbag (Aldrich) under dry argon atmosphere. A dip-type conductivity cell

of cell constant 113.41 m^{-1} was immersed into the sample tube containing CNTH. The sample was melted at ~ 45°C in a water thermostat (INSREF-IRI 015). The electical conductances of the supercooled melt below 45°C were measured at 1 kHz using Wayne Kerr B905 automatic precision bridge. Below ambient temperature the conductance measurements were made in an ultra-low-temperature thermostat (INSREF) whose description is given in chapter 2. Throughout the conductance measurement an inert atmosphere was maintained above the sample by passing dry argon gas into the sample tube. After finishing the conductance measurement each day the sample tube was closed and kept in a vacuum desiccator until starting of the next measurement. Different volumes of alcohol were added to the CNTH melt in the sample tube using a calibrated graduated pipette (A grade) and after each addition of alcohol the conductance of the binary mixture was measured as a function of temperature as described above. The weight of the added alcohol was determined by weighing separately known volumes of alcohol as well as from the reported density values of the alcohols.[36] For each sample conductance measurements were made in the temperature range from 45 to -75°C or from 45°C till solidification of the sample in case the mixture tends to solidify above -75°C.

7.3 Results and Discussion

The experimental specific conductance (k) data as a function of temperature and mole fraction of alcohol (x) for CNTH + methanol, CNTH + ethanol and CNTH + propanol mixtures are given in Tables 7.1, 7.2 and 7.3, respectively.

Conductance data obtained by making duplicate measurements agreed within ± 3% or less which is found to be attributable mainly to the difference in the water content of the CNTH samples. About 2% change in the electrical conductance value of a hydrate melt for every 0.01 change in the water/salt molar ratio (this is equivalent to 0.2% change in the molality scale) has been reported[37] to occur. By comparing the specific conductance values of the CNTH samples used in the present study with the reported data,[38,39] it was estimated that the water/salt molar ratio of CNTH used in the CNTH + methanol binary mixture is about 4.30 whereas that of CNTH used in CNTH + ethanol and CNTH + propanol binary mixtures is about 4.18.

Temperature Dependence of Specific Conductance : The variation of k with temperature for the three binary mixtures, viz., (1-x)CNTH + x Methanol, (1-x)CNTH + x Ethanol, and (1-x)CNTH + x Propanol, are shown in Figs 7.1a - 7.3 b. From these plots it is apparent that the temperature dependance of k is non-Arrhenius. Therefore, the conductance data were fitted to the VTF equation of the form

$$k = A \exp[-B / (T-T_{01})] \qquad (7.1)$$

using an iterative least-squares method. This equation is the same as Eq (1.7) and the significance of the parameters are explained in chapter 1. The values of the best-fit parameters of eq (7.1) are listed in Tables 7.4 - 7.6 for the CNTH + x Methanol, CNTH + x Ethanol, and CNTH + x Propanol mixtures. In all the three mixtures although there is an overall decrease in the values of A, B and T_{01} with increasing amount of alcohol, no regular trend in the variation of A, B, T_{01} with x has been noticed. For CNTH + water system also a decrease in the values of A, B, T_{01} with increasing amount of water is noticeable from the reported[11] values of VTF parameters for the equivalent conductance of $Ca(NO_3)$+ H_2O system. The best-fit values of T_{01} for CNTH are however found to be much lower than its reported ideal glass transition temperature.[11,37,40,41] On the other hand, the extrapolated values of T_{01} of methanol, ethanol, and propanol (Fig. 7.4) are found to be higher than the expected values. The reported values of calorimetric glass transition temperatures, T_g, of methanol, ethanol, and propanol are 103K, 95-97K, and 96-100K, respectively.[42-45] Since the ideal glass transition temperature, T_{01} in eq (7.1), has a value generally lower than T_g ($T_g/T_0 \approx 1.1$, cf. chapter 1), the expected values of T_{01} for methanol, ethanol, and propanol must therefore lie below the respective T_g values. In supercooled water also the value of ideal glass transition temperature (170K) computed from VTF equation is reported to be higher than the calorimetric glass transition temperature, T_g, of pure water (135K).[46] Furthermore, in the light of the relative values of T_g for the three alcohols it is expected that T_{01} (methanol) > T_{01} (propanol) ≥ T_{01} (ethanol). On the contrary, from the above data analysis it has

been observed (Tables 7.4 - 7.6) that T_{01} (propanol) > T_{01} (ethanol) > T_{01} (methanol).

The least-squares fits of the specific conductance data to the VTF eq (7.1) are found to be very sensitive to the value of T_{01} supplied initially. For small variations in T_{01} value larger variations were produced in A and B such that different A-B- T_{01} sets were obtained which adequately describe the conductance data. Similar observations were reported by others[37,40,41] also and an alternative method was therefore suggested for least-squares fitting of transport property data to the VTF equation by keeping the value of B parameter almost constant (cf. chapter 5). Using this alternative method of data fitting, the specific conductance data of the three binary mixtures were again least-squares fitted to the VTF eq (7.1) keeping B $\approx$ 508. The results of such a data fitting are given in Tables 7.7 -7.9. The ideal glass transition temperature obtained thus is termed as T_{02}. The constant value of B was chosen to be ~ 508 (cf. chapter 5) so that the value of T_{02} for CNTH becomes comparable with the reported value.[11,37,40,41] From Tables 7.7-7.9 it is apparent that the CNTH used in the binary mixture containing methanol has a T_{02} value about 5K less than the value for CNTH used in the other two binary mixtures containing ethanol and propanol which is attributable to the higher water/salt ratio in the former case.[11] The values of ideal glass transition temperatures obatined for methanol, ethanol and propanol (Fig 7.4) from the alternative method of data analysis are also found to be in the order T_{02} (propanol) > T_{02} (ethanol) > T_{02} (methanol) as is the case with T_{01}. Furthermore, although T_{02} of methanol is

comparable with the expected value of its ideal glass transition temperature, T_{02} values of ethanol and propanol are still more than their T_g values which is again contrary to the correlation between ideal glass transition temperature and T_g. The values of A parameter computed with constant value of B exhibit a monotonous decrease with increase in x value of the alcohol.

An attempt was also made to describe the temperature dependence of specific conductance of the three binary mixtures under investigation in terms of the Adam- Gibbs (AG) equation of the form

$$k = A_3 \exp[-B_3/T\ln(T/T_{03})] \qquad (7.2)$$

The theoretical basis of eq (7.2) is given in chapter 1 and this equation is the same as eq (1.13). The values of the best-fit parameters of eq (7.2) obtained by using an iterative least-squares fitting method are given in Tables 7.10-7.12. Comparing the best-fit parameters of VTF and AG equations, it is apparent that the values of B_3 are larger than the corresponding values of B whereas the values of A_3 and T_{03} are less than the corresponding values of A and T_{01}. The ideal glass transition temperatures of methanol, ethanol, and propanol obtained on the basis of AG eq (7.2) also follow the trend T_{03} (propanol) > T_{03} (ethanol) > T_{03} (methanol).

Finally, the temperature dependence of k was also analyzed in terms of the power-law (PL) equation of the form

$$k = k_0[(T/T_{04})-1]^{\beta} \qquad (7.3)$$

Eq (7.3) is the same as eq (1.14) and its theoretical basis has been given in chapter 1. The results of an iterative least-squares fitting of k data to eq (7.3) are given in Tables 7.13-7.15. In the case of eq (7.3) the least-squares fits of conductance data were found to be very sensitive to the value of β parameter. For some of the compositions of the binary mixture good fits were not obtained if the entire experimental range of temperature was used for data fitting. In such cases the temperature range of data fitting was curtailed so as to obtain a best-fit. For e.g., in the case of 0.3 CNTH + 0.7 Methanol mixture a best-fit was obtained using k data in the temperature range from 45 to -50°C whereas the experimental temperature range of conductance measurements extends up to -71°C. As in the case of VTF equation , an overall decrease occurs in the values of k_0, β, T_{04} with increase in x value. The values of T_{04} for methanol, ethanol, and propanol follow the same trend as exhibited by T_{01}, T_{02}, and T_{03}. However, the values of T_{04} are found to be higher than the corresponding values of T_{01}, T_{02} and T_{03}. In fact, the value of T_{04} is reported to be nearly 1.2 times more than T_g.[47] In the case of supercooled water, T_{04} has been reported to be nearly 1.7 times more than the T_g of water.[46] In the present study it has been observed that for CNTH $T_{04} \approx 1.1T_g$, for methanol $T_{04} \approx 1.7T_g$, and for ethanol and propanol $T_{04} \approx 1.9\ T_g$. It has been reported[44] that the applicability of the PL eq (7.3) is limited to the temperature range lying below the critical temp[erature, T_c . This critical temperature T_c is identified as a temperature of liquid-liquid transition where the α- and β- types of relaxations merge .[44,47] It has

been demonstrated that when relevant data of glass - forming substances were fitted to eq (7.3) in the temperature range $T \leq T_c$, the computed value of T_{04} becomes lower than the T_g value.[44] Thus the T_{04} values obtained in the present study may not correspond to the ideal glass transiton temperatures of the binary mixtures under investigation and may refer , on the other hand, to some other type of critical temperature which may presumably be the temperature of the merger of α- and β- relaxations.

Concentration Dependence of Specific Conductance : The nature of the concentration dependence exhibited by specific conductance of the three binary mixtures under investigation is illustrated in Figs 7.5-7.7. In these figures k is plotted against mole fraction of alcohol at some selected experimental temperatures. At temperatures $\leq 20^0$C , the shape of the k vs. concentration (mole fraction of alcohol) isotherms looks to be similar in the case of all the binary mixtures and all these isotherms tend to pass through a maximum. The concentration of alcohol (c_{max}) at which k becomes maximum shifts towards higher concentration of alcohol as the temperature is decreased. In fact, below - 65^{0}C no conductance maximum was observed in CNTH + methanol and CNTH + ethanol mixtures. The above observations on the appearance of specific conductance maximum and the dependence of c_{max} on temperature are in accordance with the similar trends observed in aqueous electrolytic solutions.[11,15,48] Specific conductance maximum is known to occur in electrolytic solutions due to the opposing effects of ionic concentration and viscosity on specific conductance. At a given temperature,

the values of c_{max} of the three binary mixtures follow the order, c_{max} (CNTH + propanol) < c_{max} (CNTH + ethanol)< c_{max} (CNTH + methanol). In this context it may also be worthwhile to note that the specific conductance values of the three binary mixtures at a particular temperature and alcohol concentration are in the order, k(CNTH + propanol) < k (CNTH + ethanol) < k (CNTH + methanol).

In the range 25 to 45^{0}C, k increases on addition of methanol to CNTH as is the case at $\leq$ 20^{0}C, whereas on adding ethanol or propanol to CNTH k decreases initially and then starts increasing unlike the case at $\leq$ 20^{0}C (Tables 7.1- 7.3). At 45^{0}C, on adding propanol to CNTH the specific conductance decreases monotonically without even exhibiting any maximum. The initial decrease in k caused by addition of ethanol or propanol to CNTH above 20^{0}C is simillar to the conductance behaviour observed by the addition of acetamide to CNTH (cf. Chapter 6). Methanol, ethanol, and propanol molecules on addition to CNTH may undergo hydrogen bonding with $Ca(H_2O)_4^{2+}$ ions[33] causing a decrease in the mobility of the hydrated calcium ions. In view of the steric factor, the decrease in mobility is expected to be maximum on addition of propanol and the least on addition of methanol. This ion-alcohol interaction resulting in the decrease in the mobility of hydrated calcium ions may be the reason for the initial decrease of k observed above 20°C on adding propanol and ethanol to CNTH. Since no initial decrease of k was observed by the addition of methanol to CNTH, the decrease in mobility of hydrated calcium ions in this case is however negligible. The conductance behaviour of CNTH + methanol system appears to be similar to the conductance

behaviour of CNTH + H_2O or $Ca(NO_3)_2$ + H_2O system.[11,15] At 35^{0}C, in CNTH + H_2O system c_{max} occurs at ~ 0.96 mole fraction of water[15] whereas in CNTH + methanol mixture c_{max} occurs at ~0.88 mole fraction of methanol. Thus c_{max} for CNTH + H_2O system is the highest and occurs at lowest salt (CNTH) concentration compared to that of CNTH + methanol / ethanol / propanol systems. The values of c_{max} of binary mixtures containing CNTH and methanol / ethanol / propanol/ water seem to have a correlation with the dielectric constant and viscosity of the liquid component, i.e., alcohol/water, since dielectric constant controls the ionic concentration and viscosity controls the mobility of ions. The dielectric constant (ε) and viscosity (η) of the liquids under consideration are in the order,[36,49] ε (water) > ε (methanol > ε (ethanol) > ε propanol and η (propanol) > η(ethanol) > η (methanol) > η(water).

By accounting for the concentration dependance of the parameters of VTF eq (7.1), a semiempirical equation of the form

$$y = a_y \exp[b_y x + c_y x^2] \qquad (7.4)$$

was developed by us earlier[15,50] to describe the concentration dependance of molar conductance or viscosity of aqueous electrolytic solutions from low to very high concentrations. In eq (7.4), y refers to either molar conductance or viscosity, the parameters a_y, b_y and c_y are emphirical constants, and x is the concentration in molal or mole fraction units. Recently an extended form of Eq (7.4) of the type

$$y = a_y \exp[b_y x + c_y x^2 + d_y x^3] \qquad (7.5)$$

was employed by Kumar[22] to describe the concentration dependance of viscosity of a non-aqueous system containing anisole and tetra-n-butylammonium picrate in the entire concentration range. We made an attempt to describe the concentration dependence of specific conductance of the binary mixtures under investigation by least-squares fitting the k data to eqs (7.4) and (7.5). We failed to obtain a satisfactory fit of the specific conductance data to eq (7.4) or (7.5) which is attributable to the fact that specific conductance, unlike molar conductance or viscosity, exhibits conductance maximum at intermediate concentration as discussed above. In the absence of density data of the binary mixtures their molar conductance could not however be evaluated.

From the above discussion it may therefore be concluded that (1) the temperature dependence of CNTH + methanol/ethanol/propanol systems is explainable satisfactorily by the VTF, AG, and PL equations, (2) the ideal glass transition temperatures obtained for the alcohols from the VTF and AG equations are however found to be greater than their respective T_g values and do not also follow the same order as that shown by T_g, (3) conceptually therefore the VTF and AG equations do not seem to be applicable to these binary systems, (4) the temperature T_{04} obtained from PL equation does not appear to correspond to the ideal glass transition temperature and probably refers, on the other hand, to some other critical temperature, (5) the concentration dependence of specific conductance of the three binary mixtures seems to have a correlation with the

dielectric constant and viscosity of the alcohol, and (6) analytical expressions of the form (7.4) and (7.5) are not adequate to explain the concentration dependence of specific conductance of the binary mixtures.

Table 7.1 Specific Conductance Data of CNTH+Methanol system

Temp. (°C)	k/S m^{-1}					
	0.0	**0.099**	**0.204**	**0.305**	**0.398**	**0.502**
45	1.7182	1.7255	1.7494	1.8191	1.8625	1.9355
40	1.4251	1.4346	1.4532	1.5196	1.5673	1.6467
35	1.1055	1.1325	1.1676	1.2333	1.2815	1.3723
30	0.8901	0.9013	0.9276	0.9838	1.0230	1.1140
25	0.6346	0.6729	0.6924	0.7712	0.8215	0.8985
20	0.5190	0.5248	0.5517	0.6012	0.6467	0.6758
15	0.3789	0.3897	0.4150	0.4538	0.4954	0.5408
10	0.2852	0.2900	0.3095	0.3449	0.3770	0.4203
5	0.1932	0.2042	0.2231	0.2487	0.2833	0.3133
0	0.1400	0.1443	0.1539	0.1754	0.1996	0.2350
-5	0.0855	0.0856	0.0960	0.1162	0.1326	0.1640
-10			0.0606	0.0721	0.0888	0.1111
-15				0.0450	0.0553	0.0687
-17					0.0437	-
-20						0.0405
-22						0.0331
-25						0.0232
-27						0.0182

Table 7.1 Continued

Temp. (°C)	k/S m^{-1}			
	0.601	0.700	0.800	0.900
45	1.9981	2.1638	2.3069	2.3079
40	1.7119	1.8727	2.0322	2.0847
35	1.4414	1.5955	1.7651	1.8723
30	1.1883	1.3422	1.5143	1.65651
25	0.9761	1.1140	1.2930	1.4806
20	0.7614	0.8906	1.0751	1.3097
15	0.6041	0.7200	0.9094	1.1383
10	0.4759	0.5760	0.7491	0.9990
5	0.3648	0.4500	0.6179	0.8583
0	0.2767	0.3614	0.5115	0.7389

Table 7.1 Continued

Temp. (°C)	k/S m^{-1}			
	0.601	**0.700**	**0.800**	**0.900**
-5	0.2008	0.2663	0.3914	0.6209
-10	0.1387	0.2013	0.2949	0.5113
-15	0.0890	0.1394	0.2177	0.4252
-20	0.0613	0.0928	0.1621	0.3331
-25	0.0338	0.0600	0.1094	0.2611
-30	0.0182	0.0354	0.0745	0.2039
-35	$9.15x10^{-3}$	0.0201	0.0474	0.1526
-40	$4.65x10^{-3}$	0.0103	0.0282	0.1093
-45	$1.94x10^{-3}$	$5.06x10^{-3}$	0.0165	0.0799
-50	$6.17x10^{-4}$	$2.55x10^{-3}$	$9.21x10^{-3}$	0.0502
-55	$1.87x10^{-4}$	$1.04x10^{-3}$	$7.23x10^{-3}$	0.0324
-60	$3.94x10^{-5}$	$2.76x10^{-4}$	$3.40x10^{-3}$	$5.97x10^{-3}$
-65	$1.08x10^{-5}$	$6.73x10^{-5}$	$2.09x10^{-3}$	-
-70	-	$2.39x10^{-5}$	$6.49x10^{-4}$	-
-75	-	$1.21x10^{-5}$	-	-

Table 7.1 Continued

Temp. (°C)	k/S m^{-1}					
	0.925	0.943	0.962	0.971	0.977	0.990
45	2.1131	2.0497	1.7982	1.5643	1.3065	0.6950
40	1.9407	1.8715	1.6924	1.4624	1.2251	0.6589
35	1.7686	1.7099	1.5618	1.3461	1.1371	0.6213
30	1.6038	1.5596	1.4499	1.2628	1.0581	0.5866
25	1.4335	1.4266	1.3218	1.1799	1.0057	0.5750
20	1.2964	1.3017	1.2139	1.0688	0.9474	0.5477
15	1.1600	1.1849	1.1191	0.9910	0.8705	0.5164
10	1.0344	1.0634	1.0237	0.9275	0.8086	0.4884
5	0.9082	0.9444	0.9249	0.8517	0.7502	0.4571
0	0.7958	0.8318	0.8356	0.7728	0.6902	0.4282
-5	0.6852	0.7350	0.7416	0.6975	0.6255	0.3973
-10	0.5914	0.6328	0.6551	0.6260	0.5685	0.3692
-15	0.4978	0.5362	0.5783	0.5557	0.5133	0.3404
-20	0.4085	0.4481	0.4991	0.4891	0.4598	0.3161
-25	0.3338	0.3777	0.4270	0.4279	0.4109	0.2888
-30	0.2668	0.3010	0.3619	0.3682	0.3591	0.2614

Table 7.1 Continued

Temp. (°C)	k/S m^{-1}					
	0.925	**0.943**	**0.962**	**0.971**	**0.977**	**0.990**
-35	0.2116	0.2437	0.3029	0.3163	0.3145	0.2367
-40	0.1587	0.1895	0.2486	0.2652	0.2681	0.2103
-45	0.1205	0.1423	0.2029	0.2186	0.2292	0.1866
-50	0.0852	0.1073	0.1597	0.1780	0.1912	0.1624
-55	0.0597	0.0770	0.1224	0.1499	0.1589	0.1467
-60	0.0403	0.0568	0.0970	0.1095	0.1247	0.1208
-65	0.0249	0.0364	0.0803	0.0831	0.1013	0.1025
-70	0.0154	0.0263	-	0.0625	0.0799	0.0871
-72	-	-	-	-	0.0729	0.0821
-74	-	-	-	-	-	0.0742
-75	9.19×10^{-3}	0.0189	-	0.0462	-	-

Table 7.2 Specific Conductance Data of CNTH+Ethanol system

Temp (°C)	k/S m^{-1}						
	0.0	**0.10**	**0.267**	**0.398**	**0.500**	**0.614**	**0.701**
45	1.3365	1.3064	1.2919	1.3485	1.3157	1.2855	1.2441
40	1.0729	1.0552	1.0568	1.0938	1.1101	1.0889	1.0621
35	0.8449	0.8272	0.8375	0.8807	0.8968	0.9056	0.8948
30	0.6413	0.6311	0.6436	0.6975	0.7174	0.7366	0.7483
25	0.4806	0.4732	0.4982	0.5409	0.5663	0.5892	0.6033
20	0.3515	0.3554	0.3649	0.4099	0.4286	0.4686	0.4954
15	0.2509	0.2534	0.2755	0.3233	0.3394	0.3768	0.3915
10	0.1766	0.1820	0.1929	0.2384	0.2524	0.2825	0.3210
5	0.1255	0.1437	0.1479	0.1723	0.1861	0.2124	0.2477
0	0.0765	0.0949	0.1107	0.1183	0.1335	0.1588	0.1873
-5	0.0467	0.0642	0.0796	0.0765	0.0898	0.1143	0.1341

Table 7.2 Continued

Temp (°C)	k/S m^{-1}						
	0.0	**0.10**	**0.267**	**0.398**	**0.500**	**0.614**	**0.701**
-10				0.0473	0.0580	0.0775	0.0967
-15				0.0279	0.0357	0.0504	0.0661
-20					0.0198	0.0322	0.0438
-25						0.0198	0.0291
-30						0.0104	0.0170
-35						5.62×10^{-3}	9.26×10^{-3}
-40							4.62×10^{-3}
-45							2.51×10^{-3}
-50							1.03×10^{-3}
-55							3.91×10^{-4}
-60							9.20×10^{-5}
-65							2.39×10^{-5}
-70							4.53×10^{-6}

Table 7.2 Continued

Temp (°C)	k/S m^{-1}						
	0.762	0.801	0.900	0.920	0.932	0.961	0.980
45	1.2352	1.1902	0.8942	0.7853	0.7197	0.4963	0.2826
40	1.0707	1.0388	0.8027	0.7151	0.6562	0.4600	0.2651
35	0.9119	0.8920	0.7134	0.6408	0.5934	0.4227	0.2474
30	0.7661	0.7596	0.6310	0.5733	0.5321	0.3855	0.2296
25	0.6368	0.6374	0.5565	0.5082	0.4760	0.3506	0.2124
20	0.5288	0.5343	0.4879	0.4514	0.4248	0.3185	0.1957
15	0.4269	0.4452	0.4187	0.3897	0.3777	0.2845	0.1783
10	0.3472	0.3615	0.3640	0.3478	0.3337	0.2599	0.1640
5	0.2774	0.2934	0.3117	0.3034	0.2888	0.2302	0.1496
0	0.2160	0.2359	0.2654	0.2612	0.2534	0.2053	0.1349
-5	0.1677	0.1867	0.2191	0.2221	0.2189	0.1801	0.1200
-10	0.1253	0.1402	0.1823	0.2185	0.1869	0.1576	0.1083
-15	0.0895	0.1002	0.1471	0.1530	0.1552	0.1367	0.0960
-20	0.0618	0.0726	0.1149	0.1223	0.1276	0.1156	0.0833
-25	0.0403	0.0495	0.0895	0.0965	0.1047	0.0967	0.0720
-30	0.0259	0.0326	0.0684	0.0761	0.0828	0.0808	0.0611

Table 7.2 Continued

Temp °C	k/S m^{-1}						
	0.762	**0.801**	**0.900**	**0.920**	**0.932**	**0.961**	**0.980**
-35	0.0154	0.0207	0.0510	0.0583	0.0645	0.0662	0.0527
-40	8.61×10^{-3}	0.0125	0.0381	0.0434	0.0487	0.0527	0.0437
-45	5.11×10^{-3}	7.79×10^{-3}	0.0257	0.0316	0.0362	0.0427	0.0364
-50	2.26×10^{-3}	4.19×10^{-3}	0.0165	0.0223	0.02 69	0.0330	0.0295
-55	9.04×10^{-4}	2.19×10^{-3}	0. 0115	0.0150	0.0191	0.0249	0.0236
-60	3.29×10^{-4}	9.65×10^{-4}	$7 .22 \times 10^{-3}$	9.92×10^{-3}	0.0131	0.0184	0.0184
-65	1.08×10^{-4}	5.58×10^{-4}	3.97×10^{-3}	6.35×10^{-3}	9.44×10^{-3}	0.0139	0.0146
-70	3.61×10^{-4}	1.69×10^{-4}	2.28×10^{-3}	3.84×10^{-3}	5.88×10^{-3}	9.87×10^{-3}	0.0116
-75	-	6.53×10^{-5}	1.19×10^{-3}	2.35×10^{-3}	3.68×10^{-3}	7.03×10^{-3}	9.80×10^{-3}

Table 7.3 Specific Conductance Data of CNTH+Propanol system

Temp. (°C)	k/S m^{-1}						
	0.00	0.107	0.226	0.333	0.430	0.524	0.618
45	1.3365	1.2889	1.2719	1.1891	1.1097	1.0042	0.8880
40	1.0729	1.0388	1.0400	0.9827	0.9195	0.8387	0.7494
35	0.8449	0.8211	0.8251	0.7916	0.7445	0.6941	0.6181
30	0.6413	0.6255	0.6430	0.6187	0.5926	0.5563	0.5007
25	0.4806	0.4780	0.4941	0.4820	0.4655	0.4344	0.4083
20	0.3515	0.3524	0.3688	0.3720	0.3588	0.3453	0.3211
15	0.2509	0.2513	0.2812	0.2731	0.2703	0.2639	0.2507
10	0.1766	0.1893	0.2039	0.2030	0.2059	0.1986	0.1995
5	0.1255	0.1257	0.1390	0.1488	0.1513	0.1522	0.1521
0	0.0765	0.0850	0.0948	0.1033	0.1062	0.1044	0.1107
-5	0.0467	0.0493	0.0597	0.0658	0.0697	0.075€	0.0779
-10		0.0292	0.0374	0.0399	0.0456	0.0491	0.0532
-15		0.0168	0.0213	0.0245	0.0297	0.031€	0.0350
-20		0.0078	0.0114	0.0137	0.0189	0.018ᵓ	0.0220
-25			$5.77x10^{-3}$	0.0071			

Table 7.3 Continued

Temp. (°C)	k/S m^{-1}					
	0.684	**0.804**	**0.904**	**0.932**	**0.963**	**0.979**
45	0.7834	0.5488	0.3241	0.2390	0.1261	0.0649
40	0.6657	0.4790	0.2898	0.2166	0.1175	0.0614
35	0.5578	0.4087	0.2559	0.1962	0.1084	0.0579
30	0.4552	0.3498	0.2240	0.1749	0.0989	0.0536
25	0.3690	0.2931	0.1965	0.1557	0.0905	0.0493
20	0.2977	0.2453	0.1718	0.1370	0.0815	0.0452
15	0.2321	0.2016	0.1473	0.1201	0.0728	0.0411
10	0.1934	0.1744	0.1273	0.1058	0.0640	0.0367
5	0.1512	0.1355	0.1076	0.0888	0.0569	0.0332
0	0.1123	0.1078	0.0902	0.0779	0.0505	0.0295
-5	0.0798	0.0831	0.0734	0.0661	0.0441	0.0266
-10	0.0563	0.0636	0.0601	0.0548	0.0376	0.0232
-15	0.0386	0.0464	0.0483	0.0471	0.0322	0.0202
-20	0.0247	0.0332	0.0370	0.0374	0.0267	0.0172
-25	0.0163	0.0236	0.0287	0.0298	0.0222	0.0145
-30	0.0098	0.0159	0.0233	0.0231	0.0183	0.0120

Table 7.3 Continued

Temp. (°C)	k/S m^{-1}				
	0.684	**0.804**	**0.904**	**0.932**	**0.963**	**0.979**
-35	0.0105	0.0165	0.0177	0.0143	0.0100
-40	$6.25X10^{-3}$	0.0122	0.0135	0.0113	$8.06X10^{-3}$
-45	$3.83X10^{-3}$	$8.53X10^{-3}$	0.0104	$9.13X10^{-3}$	$6.20X10^{-3}$
-50	$2.19X10^{-3}$	$5.90X10^{-3}$	$7.28X10^{-3}$	$6.82X10^{-3}$	$5.20X10^{-3}$
-55	$1.10X10^{-3}$	$3.98X10^{-3}$	$4.79X10^{-3}$	$5.01X10^{-3}$	$3.78X10^{-3}$
-60	$4.82X10^{-4}$	$2.52X10^{-3}$	$3.25X10^{-3}$	$3.59X10^{-3}$	$2.83X10^{-3}$
-65	$1.84X10^{-4}$	$1.44X10^{-3}$	$2.14X10^{-3}$	$2.50X10^{-3}$	$2.07X10^{-3}$
-70	$6.26X10^{-5}$	$7.83X10^{-4}$	$1.46X10^{-3}$	$1.69X10^{-3}$	$1.45X10^{-3}$
-75	$2.27X10^{-5}$	$4.46X10^{-4}$	$8.29X10^{-4}$	$1.20X10^{-3}$	$1.09X10^{-3}$

Table 7.4 Best-Fit Parameters of VTF Equation for Specific Conductance of CNTH + Methanol System

Mole fraction of Methanol (x)	A	B	T_{01} (K)	Std. Dev in k (S m^{-1})
0.0	1115.6	1026.5	159.6	0.0191
0.099	823.11	949.2	164.1	0.0104
0.204	759.68	945.3	162.4	0.0103
0.305	513.47	858.7	165.9	0.0053
0.398	485.27	867.0	162.2	0.0060
0.502	359.41	801.5	164.5	0.0106
0.601	291.45	778.6	161.7	0.0066
0.700	328.32	845.0	149.7	0.0073
0.800	202.50	781.0	143.6	0.0072
0.900	92.766	701.1	128.5	0.0056
0.925	50.641	606.6	127.4	0.0058
0.943	35.065	537.6	129.7	0.0095
0.962	27.459	552.8	115.3	0.0060
0.971	19.732	529.9	110.1	0.0090
0.977	13.704	503.8	105.0	0.0066
0.990	4.1248	384.1	103.8	0.0041

Table 7.5 Best-Fit Parameters of VTF Equation for Specific Conductance of CNTH + Ethanol System

Mole fraction of ethanol (x)	A	B	T_{01} (K)	Std. Dev in k (S m^{-1})
0.0	708.04	897.3	175.0	0.0043
0.1	4307.8	1463.7	137.3	0.0076
0.267	3303.4	1433.3	135.3	0.0088
0.398	553.78	945.8	161.5	0.0056
0.500	430.13	906.1	161.5	0.0063
0.614	310.51	888.3	156.1	0.0038
0.701	255.17	904.6	148.2	0.0035
0.762	236.24	942.6	138.6	0.0027
0.801	179.20	915.2	135.6	0.0033
0.900	57.260	821.7	120.7	0.0019
0.920	33.730	747.5	119.5	0.0075
0.932	29.523	759.7	113.8	0.0020
0.961	12.873	682.9	108.4	0.0012
0.980	4.4940	585.6	106.3	0.0007

Table 7.6 Best-Fit Parameters of VTF Equation for Specific Conductance of CNTH + Propanol System

Mole fraction of Propanol (x)	A	B	T_{01} (K)	Std. Dev in k (S m^{-1})
0.0	708.04	897.3	175.0	0.0043
0.107	825.14	969.5	168.1	0.0041
0.226	668.47	957.4	165.2	0.0035
0.333	479.94	919.6	164.8	0.0038
0.430	537.81	1003.4	155.8	0.0026
0.524	315.09	915.9	158.7	0.0036
0.618	346.61	1030.0	145.5	0.0029
0.684	327.86	1099.0	136.0	0.0038
0.809	87.001	932.2	134.1	0.0019
0.904	28.337	898.7	117.2	0.0007
0.932	12.102	791.3	116.4	0.0006
0.963	2.5755	575.3	126.9	0.0005
0.979	0.7675	453.2	133.6	0.0004

Table 7.7 Least-Squares-Fitted Values of the Parameters of VTF Equation for Specific Conductance of CNTH + Methanol System Selected to Give Almost Constant Value for B parameter

Mole fraction of Methanol (x)	A	B	T_{02} (K)	Std. Dev in k (S m^{-1})
0.0	108.63	508.5	197.5	0.0437
0.099	110.16	508.2	197.3	0.0354
0.204	103.63	508.2	195.3	0.0379
0.305	98.454	508.5	192.7	0.0390
0.398	92.763	508.3	190.1	0.0390
0.502	85.041	508.0	186.5	0.0498
0.601	68.904	508.5	180.3	0.0872
0.700	65.018	508.3	174.5	0.0887
0.800	60.299	509.0	166.4	0.0636
0.900	41.205	508.6	146.5	0.0528
0.925	33.606	509.0	137.2	0.0289
0.943	29.665	508.7	131.3	0.0281
0.962	23.069	508.5	120.2	0.0126
0.971	18.558	508.0	113.7	0.0093
0.977	14.057	509.0	104.7	0.0069
0.990	6.1653	508.8	83.19	0.0081

Table 7.8 Least-Squares-Fitted Values of the Parameters of VTF Equation for Specific Conductance of CNTH + Ethanol System Selected to Give Almost Constant Value for B parameter

Mole fraction of Ethanol (x)	A	B	T_{02} (K)	Std. Dev in k ($S\ m^{-1}$)
0.0	101.94	508.4	202.6	0.0310
0.1	81.452	508.3	198.2	0.0502
0.267	72.970	508.2	195.4	0.0515
0.398	74.747	508.7	194.2	0.0299
0.500	66.460	508.5	191.0	0.0351
0.614	49.169	508.7	183.2	0.0496
0.701	35.480	509.6	174.9	0.0732
0.762	29.802	508.8	169.0	0.0751
0.801	28.843	509.4	166.3	0.0565
0.900	14.531	507.8	146.1	0.0415
0.920	12.280	508.0	141.0	0.0279
0.932	10.504	509.0	136.2	0.0247
0.961	6.4950	509.0	125.6	0.0113
0.980	3.2626	508.5	113.7	0.0042

Table 7.9 Least-Squares-Fitted Values of the Parameters of VTF Equation for Specific Conductance of CNTH + Propanol System Selected to Give Almost Constant Value for B parameter

Mole fraction of Propanol (x)	A	B	T_{02} (K)	Std. Dev in k (S m^{-1})
0.0	101.94	508.4	202.6	0.0310
0.107	81.356	508.1	198.8	0.0451
0.226	69.413	508.5	195.1	0.0511
0.333	61.628	508.3	193.1	0.0430
0.430	53.592	508.8	190.6	0.0395
0.524	47.558	508.9	189.0	0.0280
0.618	38.222	508.7	185.7	0.0226
0.684	25.808	508.0	178.7	0.0347
0.809	10.151	508.4	161.3	0.0466
0.904	4.9887	507.9	146.1	0.0197
0.932	3.5624	508.8	139.5	0.0105
0.963	1.7908	508.3	130.8	0.0030
0.979	0.8924	508.0	124.3	0.0006

Table 7.10 Best-Fit Parameters of AG Equation for Specific Conductance of CNTH + Methanol System

Mole fraction of Methanol (x)	A_3	B_3	T_{03} (K)	Std. Dev in k (S m^{-1})
0.0	454.28	1338.2	149.7	0.0191
0.099	352.22	1215.2	155.0	0.0104
0.204	326.67	1215.2	153.1	0.0103
0.305	233.89	1085.4	157.5	0.0052
0.398	221.38	1109.1	153.3	0.0060
0.502	170.45	1009.5	156.5	0.0105
0.601	141.95	988.99	153.3	0.0065
0.700	154.63	1116.8	139.5	0.0083
0.800	102.96	1061.8	132.1	0.0075
0.900	51.722	1010.3	114.7	0.0062
0.925	30.246	869.36	114.1	0.0064
0.943	21.921	755.89	117.4	0.0099
0.962	17.548	842.10	99.55	0.0061
0.971	12.908	826.74	93.57	0.0095
0.977	9.2317	809.73	87.35	0.0069
0.990	3.0209	610.41	87.15	0.0041

Table 7.11 Best-Fit Parameters of AG Equation for Specific Conductance of CNTH + Ethanol System

Mole fraction of Ethanol (x)	A_3	B_3	T_{03} (K)	Std. Dev in k (S m^{-1})
0.0	304.99	1104.4	167.8	0.0042
0.1	1378.6	2114.8	122.3	0.0075
0.267	1083.1	2087.5	119.9	0.0088
0.398	237.94	1218.0	152.2	0.0056
0.500	190.08	1162.8	152.4	0.0063
0.614	140.72	1158.4	146.4	0.0038
0.701	117.01	1218.1	137.0	0.0035
0.762	107.85	1320.6	125.6	0.0028
0.801	84.412	1299.2	122.0	0.0034
0.900	29.956	1244.2	104.6	0.0021
0.920	18.665	1134.2	103.4	0.0076
0.932	16.403	1189.0	96.38	0.0022
0.961	7.6129	1093.2	90.41	0.0013
0.980	2.8436	937.73	88.69	0.0007

Table 7.12 Best-Fit Parameters of AG Equation for Specific Conductance of CNTH + Propanol System

Mole fraction of Propanol (x)	A_3	B_3	T_{03} (K)	Std. Dev in k (S m^{-1})
0.0	304.99	1104.4	167.8	0.0042
0.107	338.75	1218.8	159.9	0.0041
0.226	279.42	1214.0	156.7	0.0035
0.333	207.20	1166.1	156.3	0.0037
0.430	223.83	1319.7	145.5	0.0026
0.524	139.32	1187.5	149.2	0.0036
0.618	147.03	1416.7	133.0	0.0029
0.684	135.76	1575.7	121.7	0.0038
0.809	40.640	1333.1	120.2	0.0020
0.904	14.216	1394.8	99.83	0.0007
0.932	6.5218	1221.1	99.61	0.0006
0.963	1.5698	821.03	113.9	0.0004
0.979	0.5068	617.46	122.9	0.0003

Table 7.13 Best-Fit Parameters of PL Equation for Specific Conductance of CNTH + Methanol System

Mole fraction of Methanol (x)	k_0	β	T_{04} (K)	Std. Dev in k (S m^{-1})
0.0	54.155	3.7690	227.2	0.0195
0.099	53.255	3.5996	229.5	0.0111
0.204	48.269	3.5682	228.0	0.0107
0.305	43.648	3.3709	228.9	0.0060
0.398	38.120	3.3351	226.4	0.0061
0.502	34.599	3.2352	225.4	0.0118
0.601	28.138	3.1610	221.8	0.0087
0.700	22.894	3.1177	216.4	0.0095
0.800	16.077	2.8084	211.9	0.0072
0.900	8.0667	2.4170	199.3	0.0047
0.925	5.8358	2.1496	195.9	0.0061
0.943	5.0968	1.9817	195.2	0.0106
0.962	3.5353	1.8627	187.3	0.0080
0.971	2.6223	1.7744	182.3	0.0083
0.977	1.9601	1.6504	178.8	0.0065
0.990	0.8960	1.3029	174.7	0.0051

Table 7.14 Best-Fit Parameters of PL Equation for Specific Conductance of CNTH + Ethanol System

Mole fraction of Ethanol (x)	k_0	β	T_{04} (K)	Std. Dev in k (S m^{-1})
0.0	63.018	3.6903	235.3	0.0052
0.1	41.958	4.6315	215.9	0.0082
0.267	34.108	4.5050	214.3	0.0095
0.398	34.250	3.6011	226.4	0.0062
0.500	29.795	3.4728	225.9	0.0069
0.614	20.847	3.3449	221.6	0.0044
0.701	14.867	3.2356	217.2	0.0037
0.762	10.889	3.2191	210.8	0.0029
0.801	8.7722	3.0769	208.9	0.0026
0.900	3.1979	2.6590	196.4	0.0017
0.920	2.3823	2.4318	194.7	0.0071
0.932	1.8884	2.4264	190.2	0.0018
0.961	1.0050	2.1873	184.3	0.0017
0.980	0.4760	1.9178	180.2	0.0015

Table 7.15 Best-Fit Parameters of PL Equation for Specific Conductance of CNTH + Propanol System

Mole fraction of Propanol (x)	k_0	β	T_{04} (K)	Std. Dev in k (S m^{-1})
0.0	63.018	3.6903	235.3	0.0052
0.107	53.033	3.8326	230.6	0.0045
0.226	42.369	3.7328	228.6	0.0039
0.333	33.533	3.6019	227.8	0.0043
0.430	26.006	3.6724	223.4	0.0032
0.524	20.433	3.4494	224.3	0.0042
0.618	13.742	3.5165	218.0	0.0028
0.684	9.2952	3.5904	211.7	0.0037
0.809	3.9568	3.1173	207.8	0.0019
0.904	1.1974	2.8308	195.1	0.0008
0.932	0.7089	2.5485	192.3	0.0008
0.963	0.3201	2.0886	193.4	0.0008
0.979	0.1475	1.7989	193.7	0.0006

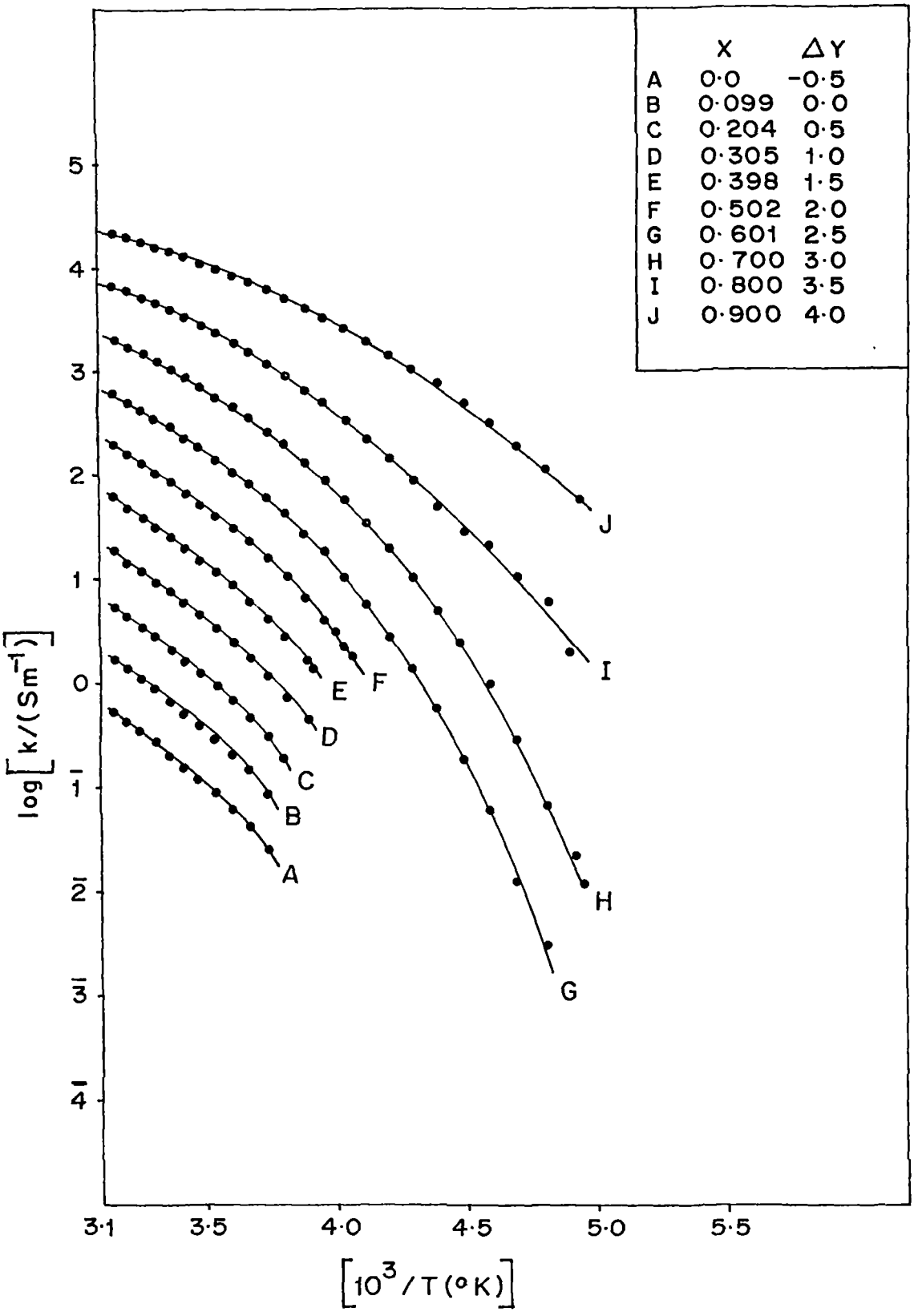

Fig 7.1a. Plot of logk versus 1/T for (1-x)CNTH+x Methanol systems. ΔY indicates the upward shift of ordinate scale for the different plots

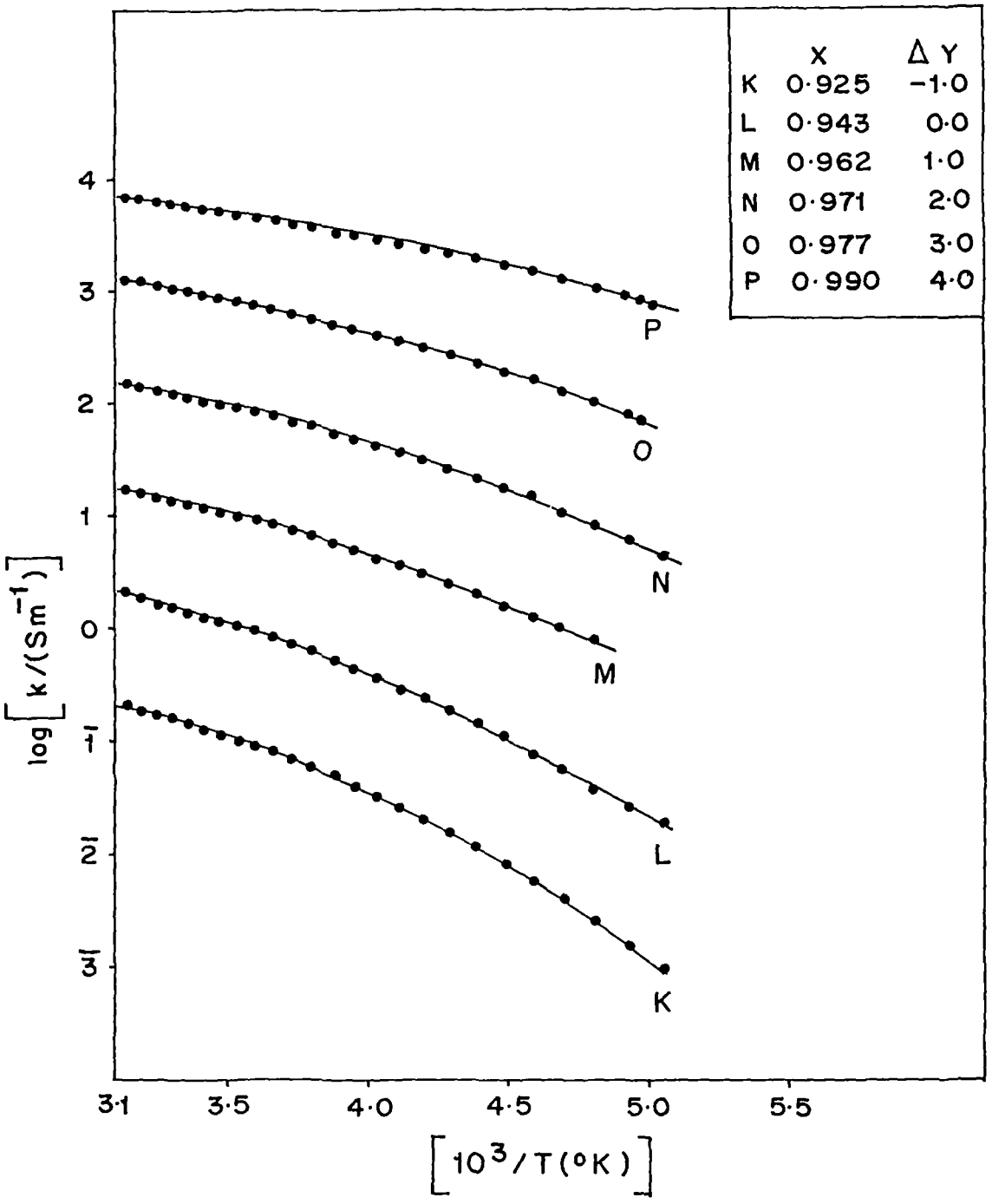

Fig 7.1b. Plot of logk versus 1/T for (1-x)CNTH +x Methanol systems. ΔY indicates the upward shift of ordinate scale for the different plots

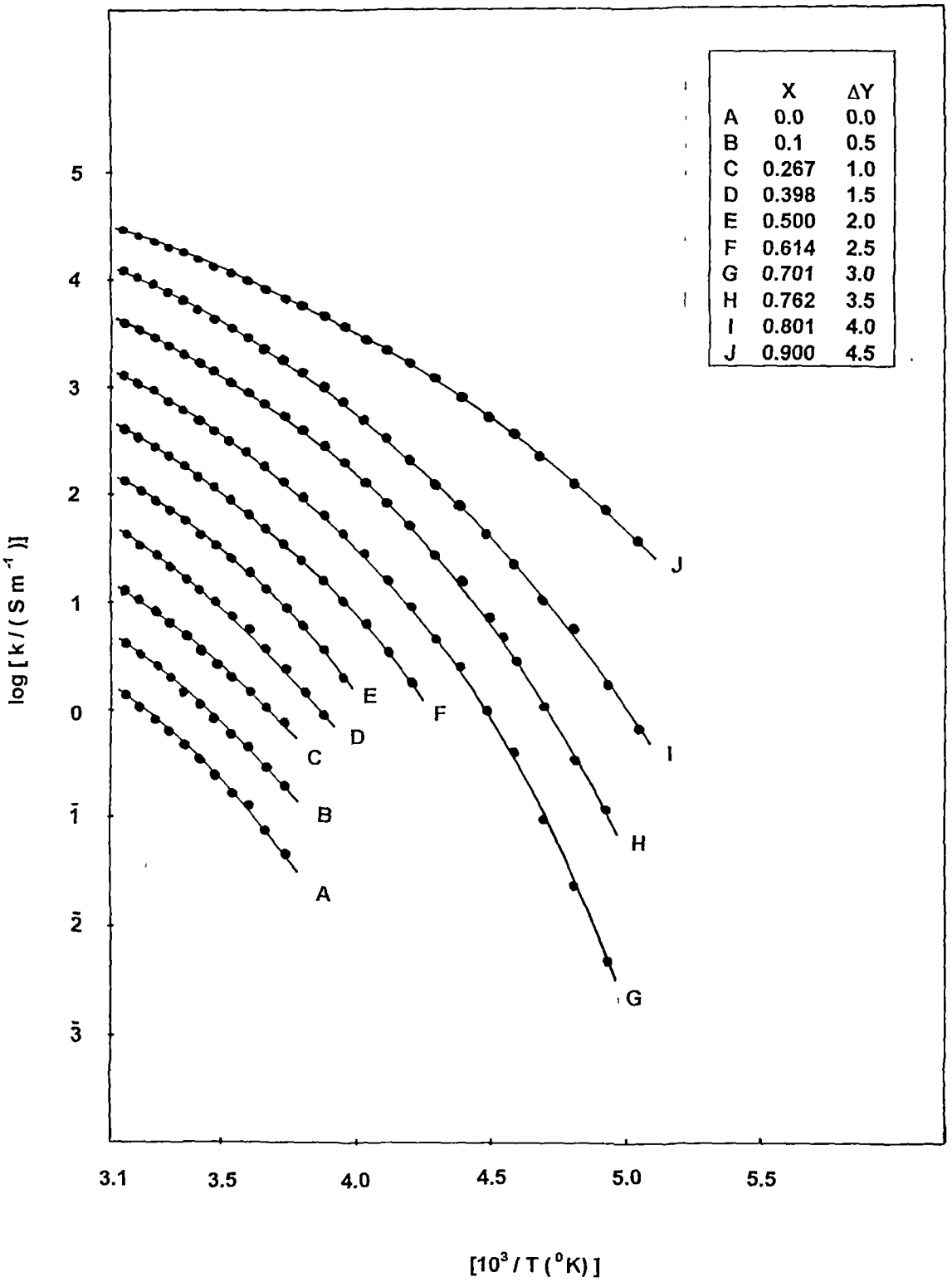

Fig 7.2a. Plot of logk versus 1/T for (1-x)CNTH +x Ethanol systems. ΔY indicates the upward shift of ordinate scale for the different plots

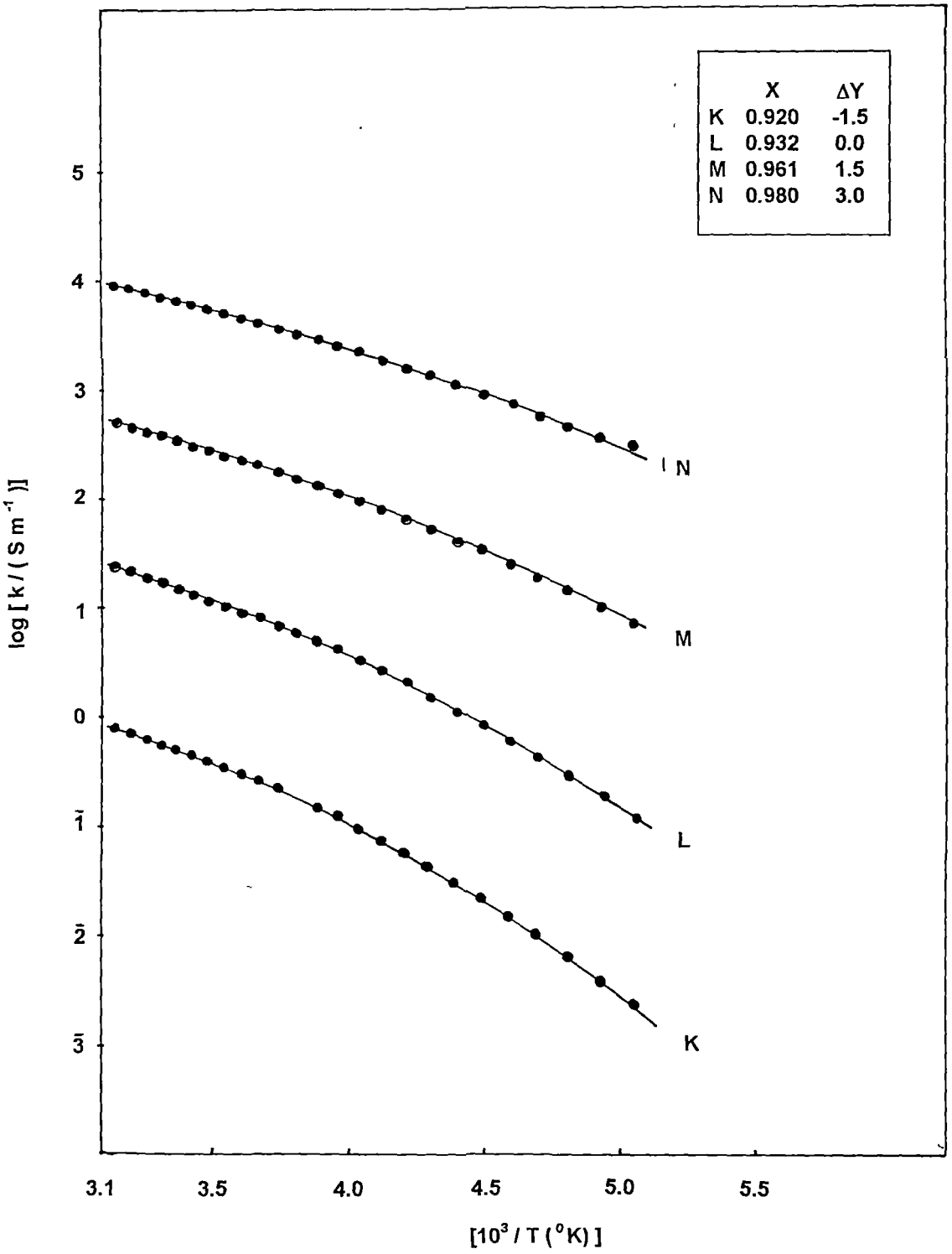

Fig 7.2b. Plot of logk versus 1/T for (1-x)CNTH + x Ethanol systems. ΔY indicates the upward shift of ordinate scale for the different plots

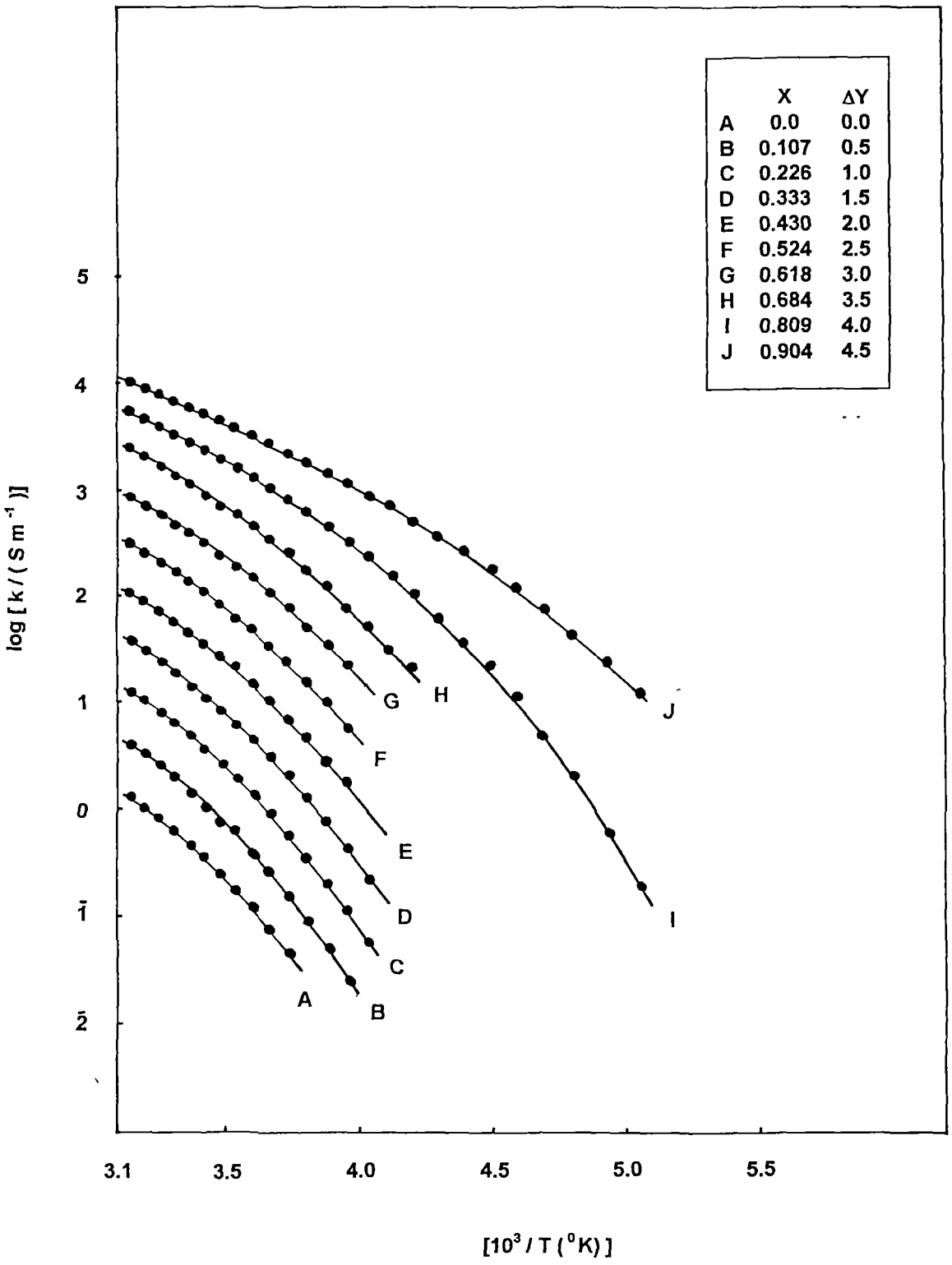

Fig 7.3a. Plot of logk versus 1/T for (1-x)CNTH + x Propanol systems. ΔY indicates the upward shift of ordinate scale for the different plots

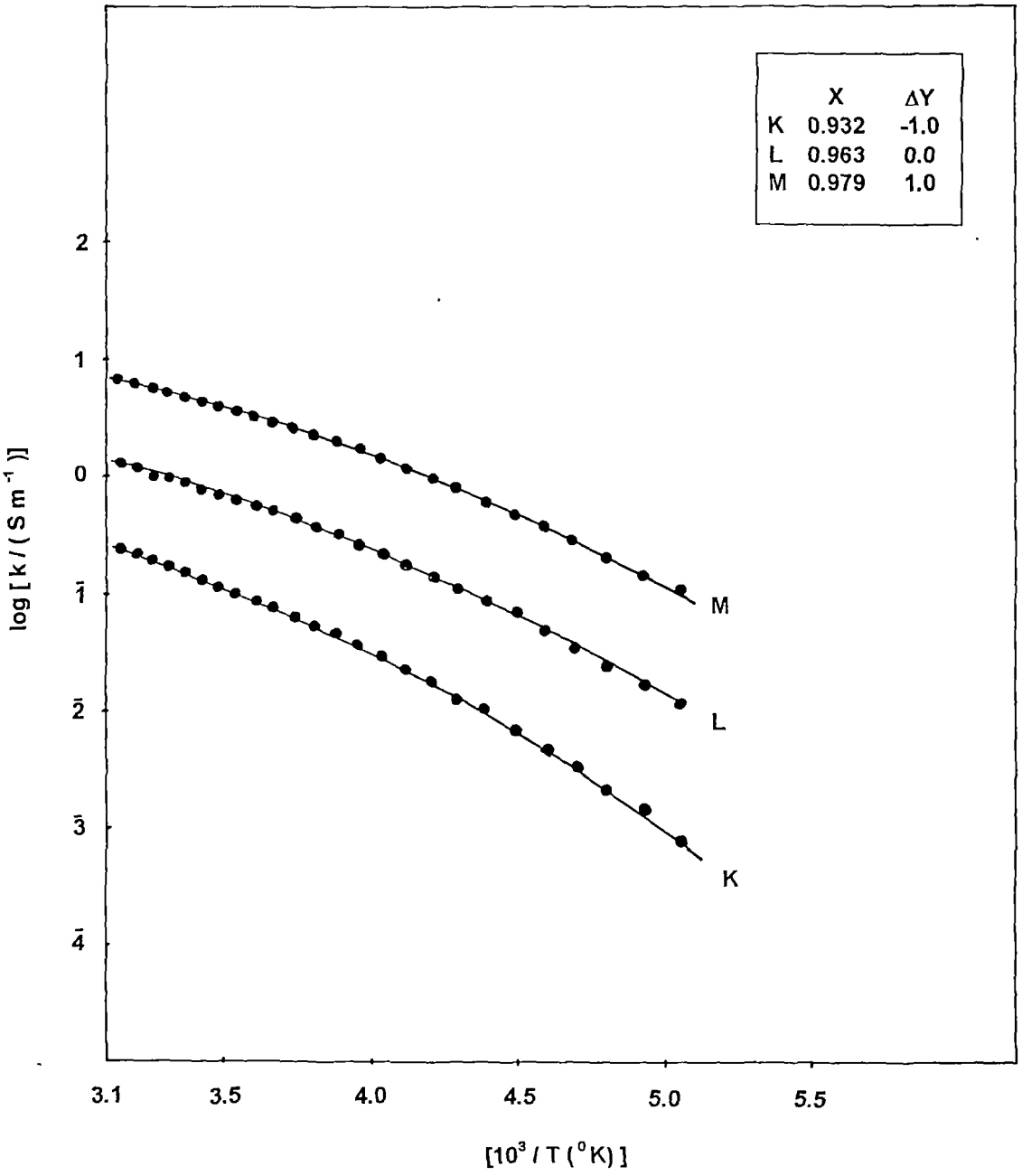

Fig 7.3b. Plot of logk versus 1/T for (1-x)CNTH + x Propanol systems. ΔY indicates the upward shift of ordinate scale for the different plots

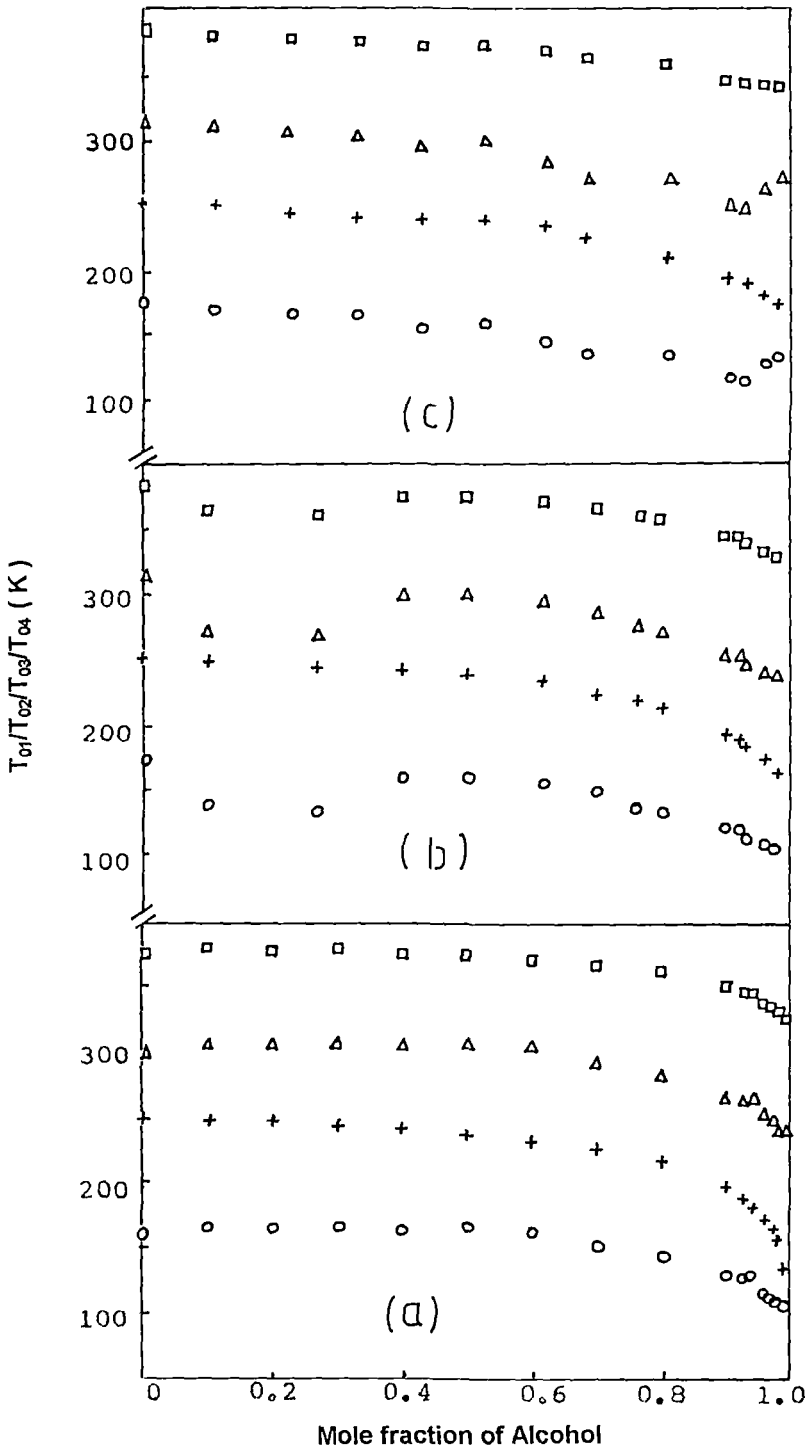

Fig 7.4 Plot of T_{01} (o), T_{02} (+), T_{03} (Δ) and T_{04} ($\square$) of (a) CNTH+Methanol, (b) CNTH+Ethanol, and (c) CNTH+Propanol binary mixtures versus mole fraction of alcohol. Ordinate scale is shifted by 50K for T_{02} and 150K for T_{03} and T_{04}

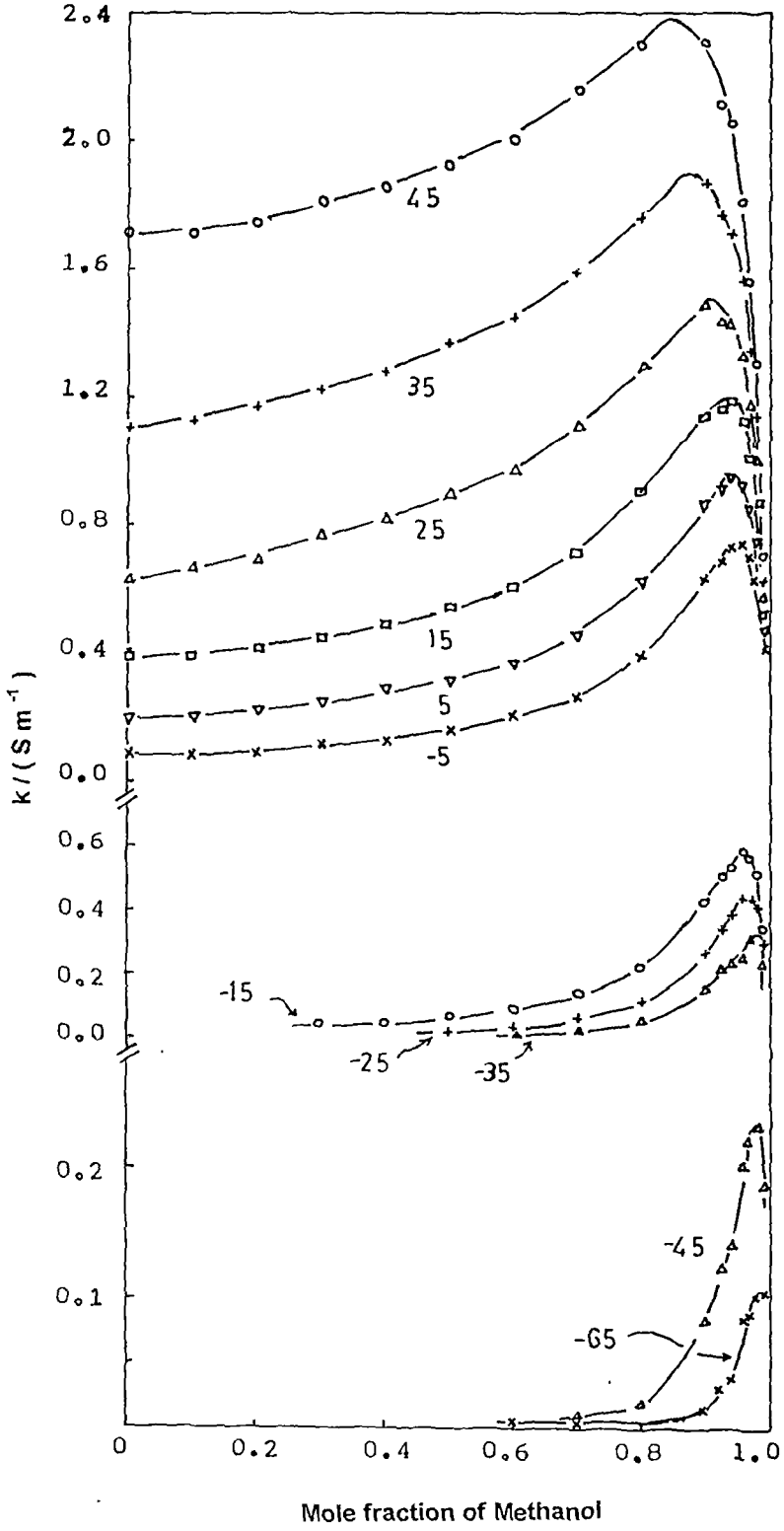

Fig. 7.5 Specific Conductance versus mole fraction of methanol isotherms at different temperatures for CNTH + Methanol system. Numbers on the isotherms indicate temperature in °C

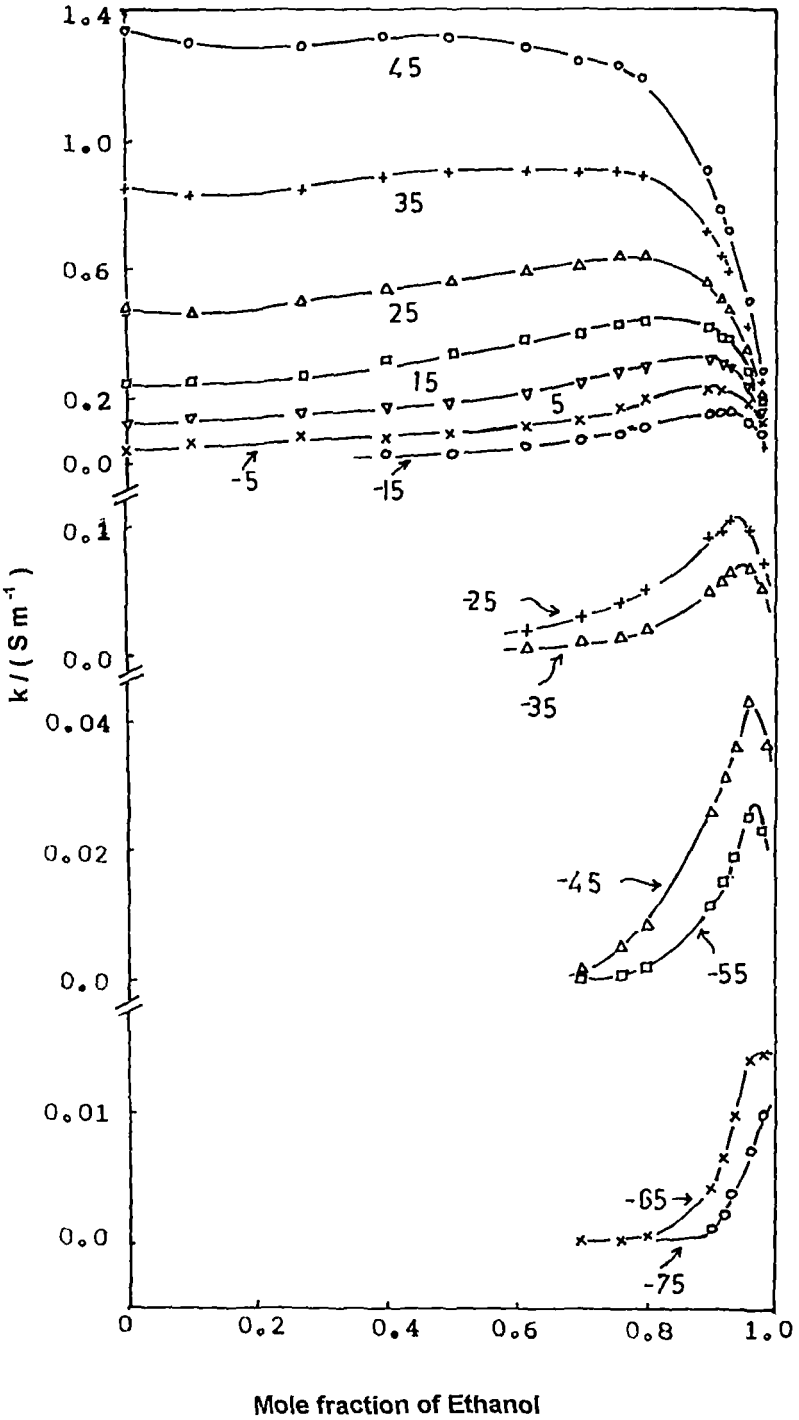

Fig. 7.6 Specific Conductance versus mole fraction of ethanol isotherms at different temperatures for CNTH + Ethanol system. Numbers on the isotherms indicate temperature in °C

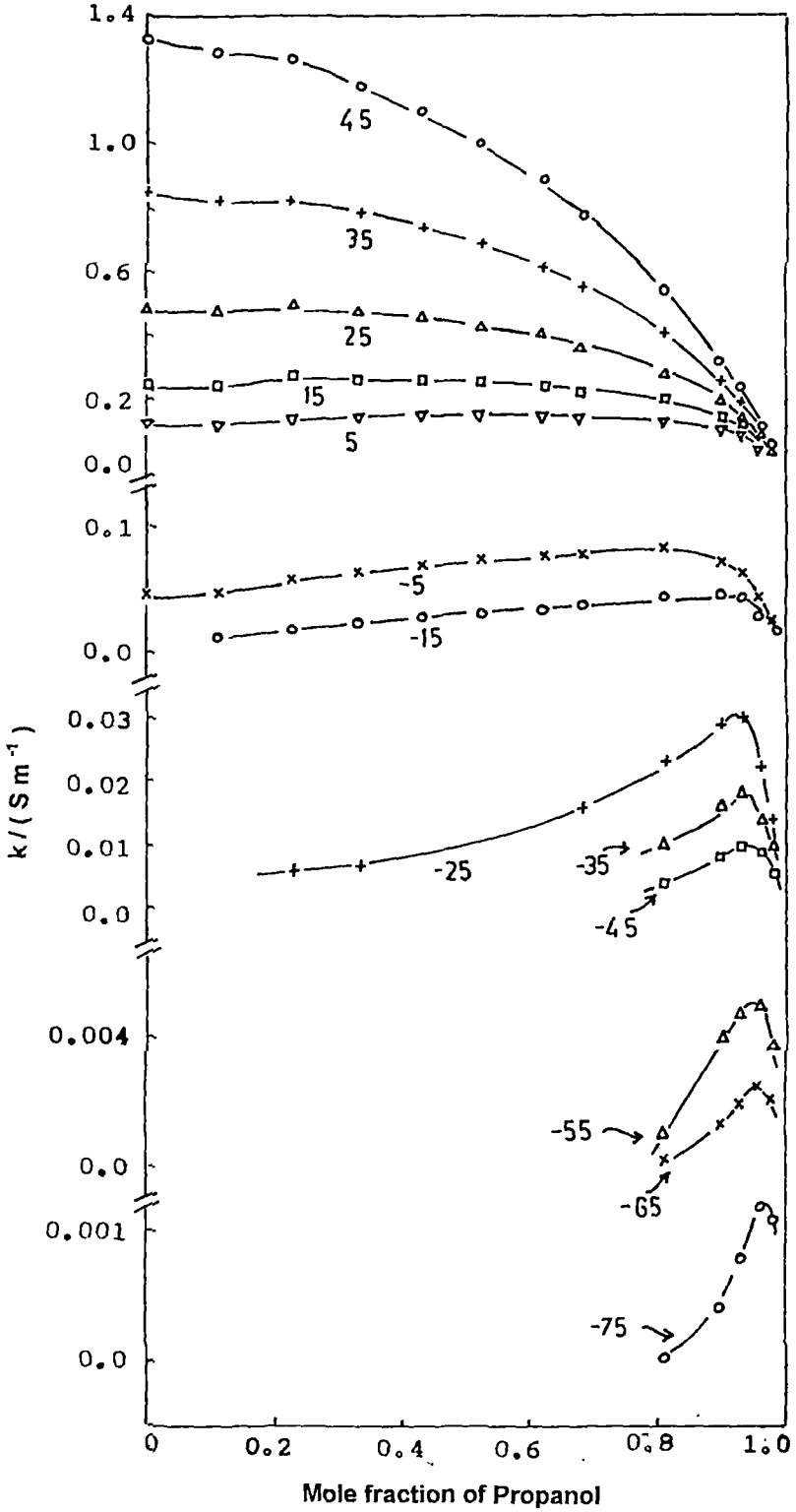

Fig. 7.7 Specific Conductance versus mole fraction of propanol isotherms at different temperatures for CNTH + Propanol system. Numbers on the isotherms indicate temperature in °C

References

1. J. O' M. Bockris andd A.K.N.Reddy, ' Modern Electrochemistry', Plenum Press, New York, Vol. 1, **1970.**
2. H. Falkenhagen, M. Leist, and G. Kelbg, Ann. Phys., **1952**, 6, 51.
3. R. M. Fuoss and L. Onsager, J. Phys. Chem., **1957**, 61, 668; **1958**, 62, 1339.
4. R. M. Fuoss and F. Accascina,' Electrolytic Conductance,' Interscience, New York,**1959**
5. B.F. Wishaw and R.H. Stokes, J. Am. Chem. Soc., **1954**, 76, 2065.
6. M. D. Monica, Electrochim. Acta, **1984**, 29, 159
7. M.D. Monica, A. Ceglie, and A. Agostiano, Electrochim. Acta, **1984**, 29, 933.
8. M.D. Monica, A. Ceglie, and A. Agostiano, Electrochim. Acta, **1984**, 88, 2124.
9. D.E. Goldsack, R. Franchetto, and A. Franchetto, Can. J. Chem., **1976**, 54, 2953.
10. S. S. Islam, R. L. Gupta, and K. Ismail, J. Chem. Eng. Data, **1991**, 36, 102.
11. C. A. Angell and R. D. Bressel, J. Phys. Chem., **1972**, 76, 3244.
12. C. A. Angell , J. Phys. Chem., **1966**, 70, 3988.
13. J. Barthel, Pure Appl. Chem., **1985**, 57, 355.
14. J. Barthel, H. -J. Gores, P. Carlier, F. Feuerlein , and M. Utz, Ber

Bunsenges. Phys. Chem., **1983**, 87, 443.

15. S. Mahiuddin and K. Ismail, J. Phys. Chem., **1984**, 88, 1027.
16. R. P. Seward, J. Phys. Chem., **1951**, 73, 515.
17. R. P. Sewardd, J. Am. Chem. Soc., **1958**, 62,758.
18. N. - P. Yao and D. N. Bennion, J. Phys. Chem., **1971**, 75, 3586.
19. K. S. Pitzer, J. Am. Chem. Soc., **1980**, 102, 2902.
20. M. Abraham and M. -C. Abraham, Electrochim. Acta, **1986**, 31, 821.
21. M. Abraham M. -C. Abraham, and I. Ziogas, J. Am. Chem. Soc., **1991**,113, 8583.
22. A. Kumar, J. Am. Chem. Soc., **1993**, 115, 9243.
23. A. Das, S. Dev, H. Shangpliang, K. L. Nonglait, and K. Ismail, J. Phys. Chem. B, **1997**, 101, 4166.
24. C. A. Angell, J. Electrochem. Soc., **1965**, 112, 1224.
25. H. Ohtaki and T. Radnai, Chem. Rev., **1993**, 93, 1157.
26. M. Sanekata, F. Misaizu, K. Fuke, S. Iwata, and K. Hashimoto, J. Am. Chem. Soc., **1995**, 117, 747.
27. H. Watanabe, S. Iwata, K. Hasimoto, F. Misaizu, and k. Fuke, J. Am. Chem. Soc., **1995**, 117, 755.
28. J. Blixt, J. Glaser, J. Mink, I. Persson, P. Persson, and M. Sandström, J. Am. Chem. Soc.,**1995**, 117, 5089.
29. E. D. Glendening and D. Feller, J. Phys. Chem., **1996**, 100, 4790.
30. H. Watanabe and S. Iwata, J. Phys. Chem. A, **1997**, 101, 487.

31. S. W. Benson, J. Am. Chem. Soc., **1996**, 118, 10645.

32. S. S. N. Murthy, J. Phys. Chem. B, **1997**, 101, 6043.

33. M. M. Hoffmann and M. S. Conradi, J. Phys. Chem. B, **1998**, 102, 263.

34. W. Lu and S. Yang, J. Phys. Chem. A, **1998**, 102, 825.

35. T. Kabeya, Y. Tamai, and H. Tanaka, J. Phys. Chem. B, **1998**, 102, 899.

36. J. Timmermans, ' Physico-Chemical Constants of Pure Organic Compounds', Elsevier, Amsterdam, Vol. 2, **1965.**

37. C. T. Moynihan, J. Phys. Chem. , **1966**, 70, 3399.

38. S. K. Chetri, S. Dev, and K. Ismail, J. Chem. Eng. Data , **1995**, 40, 12.

39. S. Mahiuddin, J. Chem. Eng. Data., **1996**, 41, 231.